Current Medicinal Chemistry, 2008, *15*, 2933-2983

New Inhibitors of Glycogen Phosphorylase as Potential Antidiabetic Agents

L. Somsák*,[1], K. Czifrák[1], M. Tóth[1], É. Bokor[1], E.D. Chrysina[2], K.-M. Alexacou[2], J.M. Hayes[2], C. Tiraidis[2], E. Lazoura[2], D.D. Leonidas[2], S.E. Zographos[2] and N.G. Oikonomakos*,#,[2]

[1]*Department of Organic Chemistry, University of Debrecen, POB 20, H-4010 Debrecen, Hungary*

[2]*Institute of Organic & Pharmaceutical Chemistry, The National Hellenic Research Foundation, 48 Vassileos Constantinou Avenue, GR-116 35, Athens, Greece*

Abstract: The protein glycogen phosphorylase has been linked to type 2 diabetes, indicating the importance of this target to human health. Hence, the search for potent and selective inhibitors of this enzyme, which may lead to antihyperglycaemic drugs, has received particular attention. Glycogen phosphorylase is a typical allosteric protein with five different ligand binding sites, thus offering multiple opportunities for modulation of enzyme activity. The present survey is focused on recent new molecules, potential inhibitors of the enzyme. The biological activity can be modified by these molecules through direct binding, allosteric effects or other structural changes. Progress in our understanding of the mechanism of action of these inhibitors has been made by the determination of high-resolution enzyme inhibitor structures (both muscle and liver). The knowledge of the three-dimensional structures of protein-ligand complexes allows analysis of how the ligands interact with the target and has the potential to facilitate structure-based drug design. In this review, the synthesis, structure determination and computational studies of the most recent inhibitors of glycogen phosphorylase at the different binding sites are presented and analyzed.

Keywords: Glycogen phosphorylase, inhibitor, type 2 diabetes, structure-based drug design, antidiabetic agent.

INTRODUCTION

General Background – Diabetes, Glycogen Metabolism

The end of the 20th century has witnessed a dramatic increase in the number of patients diagnosed with diabetes worldwide. Diabetes mellitus is characterized by chronically elevated blood glucose levels, and afflicts approximately 6 % of the adult population in Western society [1]. There is a rapidly increasing incidence of type 2 diabetes which is predicted to reach 220 million by 2010 [2]. This represents a 46% increase over ten years, which could even be an underestimate due to methodological uncertainties as well as undiagnosed cases [3]. The highest increases are expected in the developing countries of Africa, Asia, and South America, while European populations seem to be less affected [4]. Especially due to its long term complications like retinopathy, neuropathy, and nephropathy, but particularly cardiovascular diseases, diabetes has become one of the largest contributors to mortality.

Diabetes mellitus is divided into two main forms: type 1 (T1DM) is an autoimmune disease characterized by a complete insulin deficiency, and can be treated by exogenous insulin; type 2 (T2DM) involves abnormal insulin secretion and/or insulin resistance, and blood glucose levels of patients are controlled mainly by diet, exercise, and oral hypoglycemic agents [5]. While the ratio of T1DM and T2DM was estimated to be ~ 25: 75 in the early nineties [6], the frequency of the latter has increased to more than 90 % for today [1, 2]. The epidemic of T2DM is in conjunction with genetic susceptibility: evidence for a genetic component to the disease are accumulating, and the potential of these factors in the treatment and prevention of diabetes has been reviewed [7, 8]. A similarly high contribution to this epidemic may originate from behavioral factors such as sedentary lifestyle, overly rich nutrition diets, and obesity. Recent years have seen the appearance and spreading of the disease among young people including children and this forecasts severe economic and health service burdens in the coming decades [9-11].

Although several pathomechanisms [12-14] are under investigation, in the absence of a firm understanding of the molecular origins of the disease several types of oral hypoglycemic drugs (sulfonylureas, biguanides, thiazolidinediones) are in use as symptomatic treatments for T2DM [15-22]. α-Glucosidase inhibitors (acarbose, miglitol, voglibose) are also widely used [23]. These treatments aim to more or less approach the normal physiological regulation of blood glucose levels, however, there are several adverse side effects as well as the danger of causing hypoglycemia [24]. Furthermore, these drugs are inadequate for 30-40 % of patients [25]. Therefore, other therapeutic possibilities (among these novel insulin secretagogues, insulin sensitizers, glucagon receptor antagonists, inhibitors of hepatic glucose output, combination therapies) have been intensively investigated [1, 26-32], with a therapy solely based on nutrition also proposed [33].

Inhibition of Liver Glycogen Phosphorylase as an Investigational Concept in Fighting T2DM

The liver is the predominant source of blood glucose. Numerous studies have shown that hepatic glucose production is increased in type 2 diabetes in the post-absorptive state, and it is directly correlated to fasting hyperglycemia [1, 27, 29, 34, 35]. Hepatic glucose is produced from two pathways: glycogenolysis (the breakdown of glycogen) and glu-

---

*Address correspondence to these authors at the Department of Organic Chemistry, University of Debrecen, POB 20, H-4010 Debrecen, Hungary; E-mail: somsak@tigris.unideb.hu

Institute of Organic & Pharmaceutical Chemistry, The National Hellenic Research Foundation, 48 Vassileos Constantinou Avenue, GR-116 35, Athens, Greece; E-mail: echrysina@eie.gr

[#]Passed away on August 31st, 2008. His memory is enshrined in our hearts.

0929-8673/08 $55.00+.00 © 2008 Bentham Science Publishers Ltd.

coneogenesis (*de novo* synthesis of glucose). Glycogenolysis may account for more than 70 % of the hepatic glucose production, furthermore, a substantial portion of glucose formed by gluconeogenesis [36] is cycled through the glycogen pool prior to efflux from the liver cells (for references, see [37]).

Hepatic glucose output is regulated by a complex system of enzymes. The main regulatory enzyme of this system is glycogen phosphorylase (GP), and only the phosphorylated form (GPa) has significant activity. GPa releases glucose 1-phosphate from glycogen suggesting an important role for glycogenolysis in hepatic glucose production. Gluconeogenesis from lactate and other precursor molecules can also contribute to the elevated blood glucose levels, however, it was clearly demonstrated that glucose arising from gluconeogenesis has cycled through glycogen. Therefore the inhibition of hepatic GP could suppress glucose production arising from both glycogenolysis and gluconeogenesis [27, 38, 39].

Brief Description of GP (Isoforms, Binding Sites)

There are three mammalian GP isoenzymes termed as "muscle", "brain", or "liver" GP depending on the tissue in which they are preferentially expressed and each encoded by different genes located on human chromosomes 11, 20, and 14, respectively (for details see [39]). GP-s are dimers of two identical subunits (MW about 97500 Da) and all isoenzymes can be converted from the inactive form (GPb) into the active GPa form through the phosphorylation of Ser-14 by phosphorylase kinase. In addition, muscle and brain specific GP-s are also allosteric enzymes: the b form can be found predominantly in T state and the a form in R state, respectively. Allosteric activators (e.g. AMP) promote degradation of glycogen, while allosteric inhibitors (e.g. glucose, glucose 6-phosphate, ATP) retard degradation by altering the equilibrium between a less active T state and a more active R state (for references see [38]). The liver specific GP, on the other hand, is much more tightly controlled by phosphorylation rather than by allosteric regulation. Allosteric effectors such as AMP and glucose 6-phosphate have little effect on the activity of the hepatic isoenzyme [34].

It is known that the activity of liver glycogen synthase (GS) is also controlled by reversible phosphorylation of multiple serine residues. The dephosphorylated form of GS is the catalytically active (GSa) form. Phosphorylation is associated with an inactivation of GS and conversion to the b form. The dephosphorylation of GP and GS is interrelated and catalyzed by the glycogen-associated protein phosphatase-1. GPa, but not GPb, is a potent inhibitor of the phosphatase action on GS and it is only when GPa has been dephosphorylated that the phosphatase is free to activate GS, the rate limiting enzyme of glycogen synthesis [34].

The existence of isoforms raises the question of the selectivity of inhibition: for decreasing blood sugar levels the liver isoenzyme needs to be targeted without affecting the

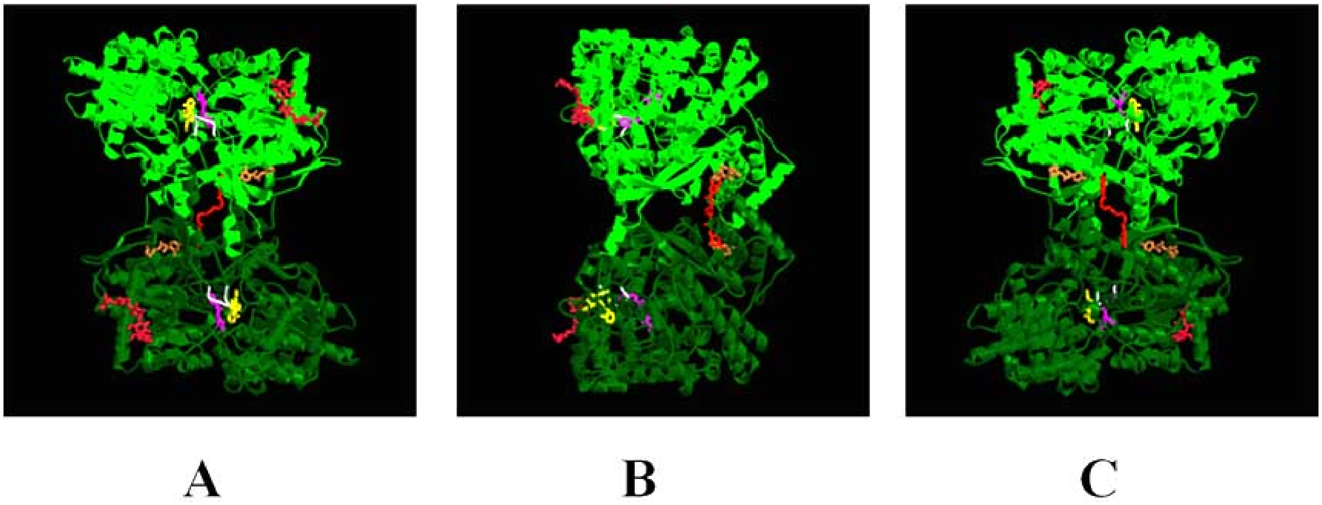

Fig. (1). A schematic diagram of muscle glycogen phosphorylase b dimer with bound ligands shown in ball-and-stick representation. One subunit (monomer) is coloured green and the other dark-green. (**a**) A view down the molecular dyad showing the positions of the catalytic site, inhibitor site, allosteric site, glycogen storage site and the new allosteric site. The catalytic site, which includes the essential cofactor pyridoxal-5'-phosphate (not shown), is buried at the center of the subunit accessible to the bulk solvent through a 15 Å long channel. 2-Naphthoyl urea (Entry 6 in Table **4**, shown in magenta) upon binding to the catalytic site induces a significant rearrangement of the 280s loop (shown in white) within the catalytic site. The allosteric site, which binds to an acyl urea derivative (Entry 3 in Table **13**, shown in brownish), is situated at the subunit–subunit interface approximately 30 Å from the catalytic site. The inhibitor site, which binds flavopiridol (Entry 1 in Table **12**, shown in yellow) is located on the surface of the enzyme approximately 12 Å from the catalytic site and, in the T state, obstructs the entrance to the catalytic site tunnel. The new allosteric inhibitor site, which binds Pfizer compound CP-526423 (**73a** shown in red), is located inside the central cavity formed on association of the two subunits. The glycogen storage site (with bound maltopentaose, shown in redish) is on the surface of the molecule approximately 30 Å from the catalytic site, 40 Å from the original allosteric site, and 50 Å from the new allosteric site. (**b**) A view rotated 90° with respect to (**a**) and normal to the 2-fold axis. (**c**) A view rotated 180° with respect to (a).

other two. This problem has been addressed recently indicating that the extent of glycogen phosphorylase inhibition that occurred during muscle contraction was not of a magnitude sufficient to measurably influence the glycogen metabolism; therefore, glycogen phosphorylase inhibition aimed at attenuating hyperglycaemia is unlikely to negatively impact muscle metabolic and functional capacity [40]. Another study demonstrated that a glycogen phosphorylase inhibitor might favour glycogen recovery after exercise by activating glycogen synthase in glycogen deprived muscle cells [41]. On the other hand, carbohydrate utilization in muscle was impaired during prolonged low-intensity contraction contrary to high-intensity contraction [42]. These sporadic data underline the need for further studies on tissue selectivity as well as for a more intensive search for liver-specific glycogen phosphorylase inhibitors [43, 44].

The aim of the present article is to highlight new molecules which have been investigated as inhibitors of glycogen phosphorylase, and therefore may have the capacity for diminishing glucose production in the liver. Special emphasis is laid on new inhibitors and informations about older molecules which have been discovered since the appearance of the last review articles [38, 45-47]. The compounds are discussed according to binding sites.

INHIBITORS ACCORDING TO BINDING SITES

Five different binding sites (Fig. **1**) have been the targets for compounds that might prevent unwanted glycogenolysis under high glucose concentrations, thus offering multiple opportunities for GP modulation.

Catalytic Site

The catalytic site is buried at the centre of the monomer, where domains 1 (residues 1-484) and 2 (residues 485-842) come together, accessible to the bulk solvent through a 15 Å long channel; the site has been extensively investigated with glucose analogue inhibitors that bind at this site and promote the less active T state through stabilisation of the closed position of the 280s loop (residues 282 to 287), between helices α7 (residues 261-274) and α8 (residues 289-314), and blocks access of the substrate (glycogen) to the catalytic site. This position prevents the crucial conformational changes that take place on activation of the enzyme that are critical for catalytic activity and create the phosphate recognition site. Residues that contribute to the catalytic site come from α6 (134-150), β13 (371-376), and β18 (478-484) in domain 1 and from β19 (562-570), the loop (571-574) between β19 (562-570) and α18 (575-593), and the loop (666-675) between β22 (661-665) and α21 (676-684) in domain 2 [48-50]. On transition from T state to R state (activation of the enzyme), the 280s loop becomes disordered and displaced, opening a channel that allows a crucial residue, Arg569, to enter the catalytic site in place of Asp283 and create the recognition site for the substrate phosphate; that also allows access of the glycogen substrate to reach the catalytic site and promotes a favourable electrostatic environment for the 5'-phosphate of the essential cofactor pyridoxal-5'-phosphate (PLP); the substrate phosphate site is within hydrogen-bonding distance of the 5'-phosphate group of PLP [51-54]. A further significant conformational change observed in the non-allosteric active maltodextrin phosphorylase (MalP) structure on binding oligosaccharide in-

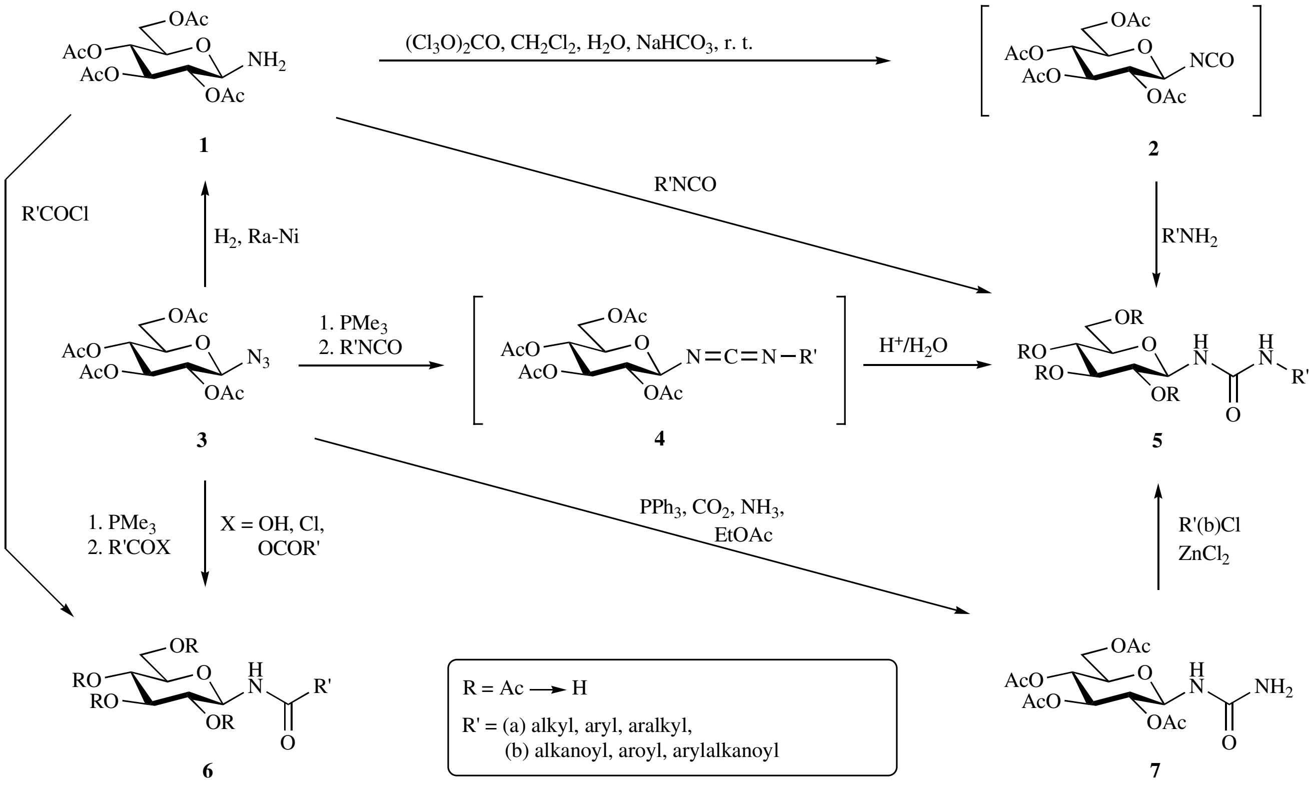

Scheme 1.

volves movement of the 380s loop (377-384) which results in closure of the catalytic site and creation of the recognition site for oligosaccharide [55].

N-Glucosidic Derivatives

N-Acetyl-β-D-glucopyranosylamine [56] (Table **1**, Entry 1) was among the first efficient glucose analogue inhibitors

Table 1. Inhibitory Efficiency of *N*-Acyl-β-D-glucopyranosylamines Towards RMGPb [63]

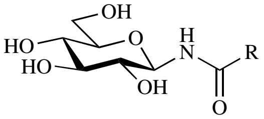

Entry	R	K_i [µM]	IC_{50} [µM]	Entry	R	K_i [µM]	IC_{50} [µM]
1.	$-CH_3$ (**NAG**)	32 [56]		9.	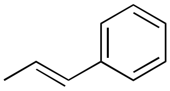	18	
2.	$-CF_3$	81 [64] 75 [59]		10.	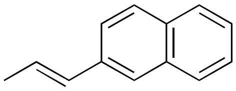	3.5	
3.	$-CH_2N_3$	49 [65]		11.	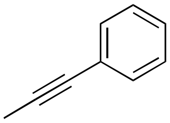	61	
4.	$-C(CH_3)_3$		7500	12.	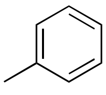 (**NBzG**)	81 [56] 144 [64]	
5.	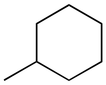	289		13.	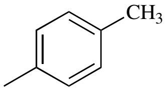		4500
6.	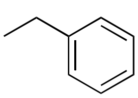		1100	14.	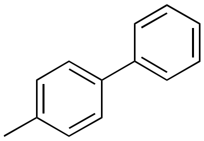	281	
7.	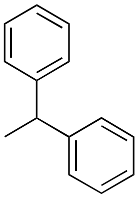	no inhibition		15.	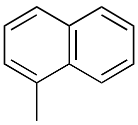	444	
8.	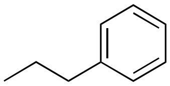	85		16.	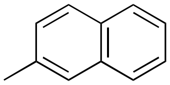 (**N2NG**)	4 (10)	
17.	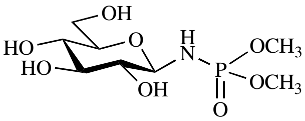 OH HO HO O H N P OCH_3 OCH_3 OH O				K_i = 5900 µM [61]		
18.	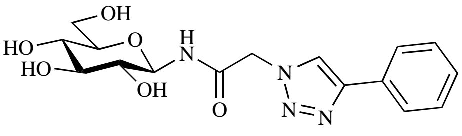				K_i = 180 µM [62]		

of GP. A large array of compounds with the *N*-acyl-β-D-glucopyranosylamine structure was synthesized, tested, and also reviewed earlier (see [38, 45] and refs. cited therein). A widely applied general method for the preparation of such compounds uses per-*O*-acetylated β-D-glucopyranosyl azide **3** in a Staudinger reaction to give an intermediate phosphinimine which, without being isolated, is then reacted with a carboxylic acid or acid chloride or anhydride to get protected compounds of type **6** (Scheme **1**, for an exhaustive review see [57]). Alternative synthetic routes (e. g. **6** (R = Ac) can also be obtained by acylation of per-*O*-acetylated β-D-glucopyranosylamine **1**) have been critically surveyed [58]. Subsequent deprotection yields test compounds of type **6** (R = H), and several recent examples as inhibitors of rabbit muscle glycogen phosphorylase b (RMGPb) are collected in Table **1**.

Substitution in the methyl group of *N*-acetyl-β-D-glucopyranosylamine makes the inhibition weaker (compare Entries 1 and 2-8). Very recently structural details of the binding of the *N*-acetyl- and *N*-trifluoroacetyl derivatives (Entries 1 and 2) to RMGPb were studied explaining the differences resulting in the weaker binding of the latter [59]. Longer aliphatic chains with an aromatic endgroup (Entries 8-11) render the inhibitors into the low micromolar range while the flexibility and orientation of the chain as well as the size of the aromatic moiety are important factors. Replacement of the methyl group by an aromatic ring (Entries 12-16) does not improve the binding although the 2-naphthoyl derivative has a slightly better effect than the acetamide (compare Entries 1 and 16). This, together with the properties of the cinnamoyl and 2-naphthylacryloyl derivatives (Entries 9 and 10), reveals the importance of interactions of inhibitors in the β-channel of the catalytic site.

Reaction of protected glucopyranosyl azide **3** with trimethyl phosphite (a modification of the Staudinger methodology) resulted in the corresponding *N*-β-D-glucopyranosyl phosphoramidate which, after deprotection, gave the test compound shown in Entry 17 [60]. Changing the acyl residue of *N*-acyl-β-D-glucopyranosylamines to a phosphoryl group resulted in a significant loss of inhibition [61].

N-(β-D-glucopyranosyl)-(4-phenyl-1,2,3-triazol-1-yl) acetamide (Entry 18) obtained by azide–terminal acetylene „click" chemistry from the corresponding azido-acetamide (cf. Entry 3) proved a modest inhibitor [62].

The binding modes of some of the N-acyl-β-D-glucopyranosylamines collected in Table **1** were studied by X-ray crystallography, and comparisons gave deeper insights into the effects of some particular substituents. Common features of these compounds are that they bind at the catalytic site and promote the T state (less active) through stabilisation of the closed position of 280s loop (residues 282–287), which blocks access of the substrate glycogen to the catalytic site. Also, an interaction that is conserved in each compound of this class is the hydrogen bond from the amide nitrogen (N1) to the carbonyl O of His377. E.g. NAG (Table **1**, Entry 1) binds to the protein [59] without significant structural changes within the catalytic site. Residues of the 280s loop are in the same position where they are found in the RMGPb-α-D-glucose complex. NAG, by making a hydrogen bond (through its O2 hydroxyl) and 10 van der Waals contacts to Asn284, stabilizes the geometry of the 280s loop. The hydrogen-bonding distance of N1 to the main-chain O of His377 is 2.9 Å. There are, in total, 15 hydrogen bonds and 61 van der Waals interactions (6 nonpolar/nonpolar, 10 polar/polar and 45 nonpolar/polar) in the RMGPb-NAG complex [59].

The non-polar substitution, made by replacing the methyl group of NAG by a phenyl group (NBzG, Table **1**, Entry 12), resulted in an inhibitor with a K_i value of 81 μM. The structure of the RMGPb-NBzG complex, now determined at 2.1 Å resolution (100 mM soak for 4 hrs) showed that the hydrogen bond between the amide N1 with CO of His377 is maintained (the hydrogen-bonding distance is 3.1 Å), and the O7 is hydrogen-bonded to Asp283 OD1 through a water

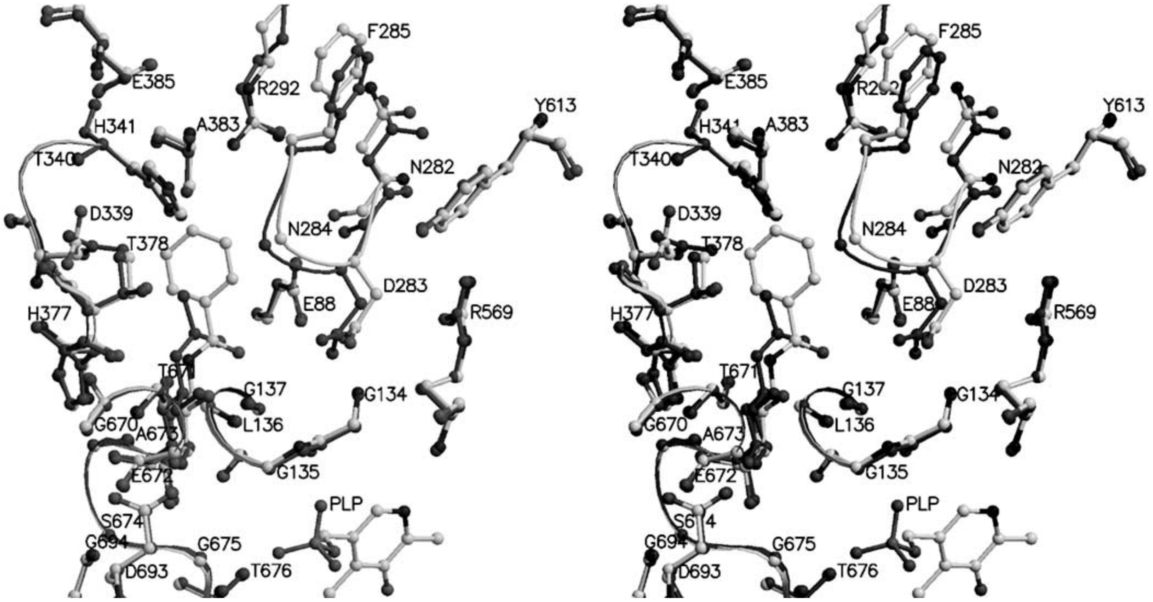

Fig. (2). Comparison between the RMGPb–NBzG complex (for NBzG, shown in light grey, see Entry 12 in Table **1**) and the RMGPb-NAG complex (for NAG, shown in dark grey, see Entry 1 in Table **1**), in the vicinity of the catalytic site.

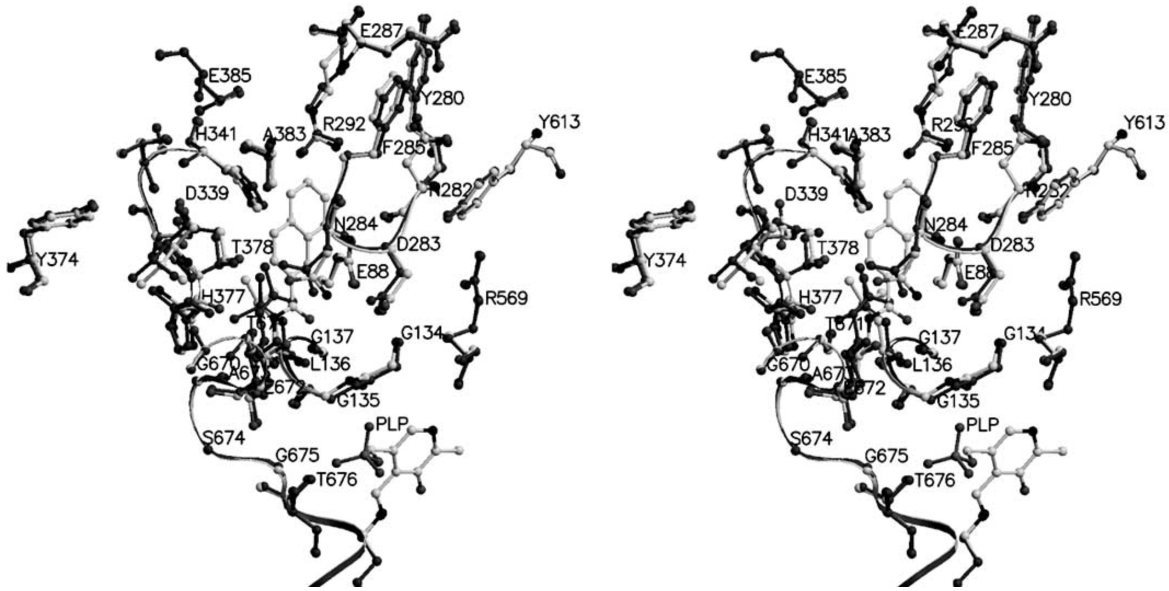

Fig. (3). Comparison between the RMGPb−N2NG complex (for N2NG, shown in light grey, see Entry 16 in Table **1**) and the RMGPb−NAG complex (for NAG, shown in dark grey, see Entry 1 in Table **1**), in the vicinity of the catalytic site.

molecule (Wat164), which in turn is hydrogen bonded to Glu88 OE2 and Gly134 N through another water molecule (Wat67). The atomic positions of C1, N1, C7, and O7 are changed in the RMGPb–NBzG structure (compared to those of NAG) and exhibit shifts of 0.5, 0.6, 0.8, and 0.9 Å, respectively. NBzG can be accommodated in the catalytic site with some changes in water structure and shifts of residues in the vicinity. Briefly, in order to avoid a clash, the Asp339 side chain moves away from the ring but does not flip; in order to minimise steric clash with Asn284, this residue shifts away from the ligand, with concomitant shifts of the other residues of the 280s loop. The most remarkable shifts of the Cα atoms are observed for residues Asn282 (0.6 Å), Asp283 (0.6 Å), Asn284 (0.8 Å), Phe285 (0.6 Å), Phe286 (0.7 Å), Glu187 (0.9 Å), and Gly288 (0.7 Å). NBzG, on binding to the enzyme makes a total of 12 hydrogen bonds, and 75 van der Waals interactions (11 nonpolar/nonpolar, 14 polar/polar, 50 nonpolar/polar) with protein. The result of restructuring of the 280s loop, other residues in the vicinity (e.g. Asp339), the small adjustments of the glucopyranose moiety and water structure needed to accommodate the ligand may explain the increase in K_i value. The structural comparison of RMGPb-NBzG complex with the RMGPb-NAG complex is shown in Fig. (**2**).

The replacement of the methyl of NAG by a 2-naphthyl group resulted in an inhibitor (N2NG, Table **1**, Entry 16) with a K_i value of 4 μM. N2NG can be accommodated within the catalytic site with the naphthyl moiety inclined ~50 degrees with respect to the phenyl ring of NBzG, with only small shifts of the residues of the 280s (0.2-0.3 Å) and the 380s (0.3-0.5 Å) loops, and changes in water structure in order to optimize contacts. O7 makes a direct hydrogen bonding interaction to Leu136 N and indirect interactions to Asp283 OD1 (through Wat185) and Wat71; Wat71 is in turn hydrogen bonded to Glu88 OE2, Gly134 N, and Gly137 N. These contacts promote the closed geometries and give rise to increased rigidity of the 280s and 380s loops. The hydrogen-bonding distance of N1 to the main-chain O of His377 is 3.3 Å, and the atomic positions of C1, N1, C7, and O7 are changed in the RMGPb–N2NG structure (compared to those of NAG) and exhibit shifts of 0.6, 0.9, 1.2, and 1.3 Å, respectively. Also, the side-chain of Asp339 moves away from the naphthyl group to avoid bad contacts. There are in total 15 hydrogen bonds, and 106 van der Waals interactions (15 nonpolar/nonpolar, 15 polar/polar, 76 nonpolar/polar). These extensive contacts might provide an explanation for the increased affinity of N2NG compared to that of the lead compound NAG. The structural comparison of RMGPb-N2NG complex with the RMGPb-NAG complex is shown in Fig. (**3**).

In order to further test the interactions in the β-channel, a series of *N*-β-D-glucopyranosyl monoamides of dicarboxylic acids were prepared [66] from **3** by using variants of the Staudinger methodology. The idea was to place a strongly polar group (COOH) at various distances from the sugar moiety also offering easy modification of the polar character by a simple esterification (to COOMe). These compounds (Table **2**) showed weaker affinity to the enzyme, and the best inhibitor of the series was the succinic acid derivative in Entry 2. This compound with a polar endgroup has a rather flexible linker, and this is in sharp contrast to the compounds having apolar groups attached to an aliphatic chain (Table **1**, Entries 8-11) where the rigidity of the linker appeared to be important for the strong binding.

AS further representatives of *N*-acyl-β-D-glucopyranosyl-amines, oxamic acid and oxamide derivatives[*] [67] were synthesized from **1** (Scheme **1**) by treatment with oxalyl chloride followed by a second amine. In each of these transformations *N*,*N*'-bis-(2,3,4,6-tetra-*O*-acetyl-β-D-glucopyranosyl)oxamide was formed as a by-product. The deprotected derivatives are shown in Table **3**. While *N*-β-D-glucopyranosyl oxamic acid and its simple esters (Entries 1-

---

[*] Czifrák, K.; Felföldi, N.; Docsa, T.; Gergely, P.; Chrysina, E.D.; Kiritsi, C.; Siafaka-Kapadai, A.; Leonidas, D.D.; Zographos, S.E.; Oikonomakos, N.G.; Somsák, L. *in preparation*.

Table 2. ***N*-β-D-Glucopyranosyl Monoamides of Dicarboxylic Acids as Inhibitors of RMGPb [66]**

Entry	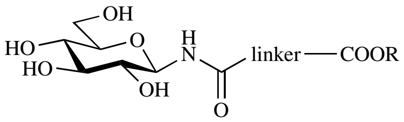			
	–linker–	**R**	**K_i [μM]**	**IC_{50} [μM]**
1.	$–(CH_2)_2–$	CH_3	170	
2.	$–(CH_2)_2–$	H	20	
3.	$–(CH_2)_3–$	CH_3	83	
4.	$–(CH_2)_3–$	H	no effect in 625 μM	
5.	$–(CH_2)_4–$	H		7900
6.	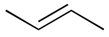	CH_3		1000
7.	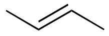	H	no effect in 625 μM	
8.	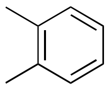	H	no effect in 625 μM	
9.	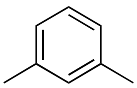	CH_3	580	
10.	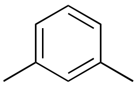	H		4000
11.	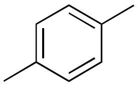	CH_3	329	
12.	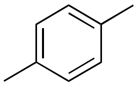	H	no effect in 625 μM	

3) proved weak inhibitors, binding of oxamides (Entries 4-9) was stronger depending on the substituent of the second nitrogen. In the presence of aliphatic moieties (Entries 4 and 5) the inhibition was worse than that of the oxamic acid derivatives. For aromatic oxamides the inhibitor constants were in the low micromolar range, and size and orientation of the ring(s) proved to be a decisive factor (Entries 6-9) rendering the 2-naphthyl derivative (Entry 9) the best inhibitor of the series. The bis-glucopyranosyl compound (Entry 10) showed no significant inhibition.

N-Acetyl- and *N*-benzoyl-*N*'-β-D-glucopyranosyl ureas* (Table **4**, Entries 1 and 9, resp.) were tested and revealed the latter as a very efficient inhibitor [68]. Several analogous structures were prepared by extensively investigated synthetic pathways. Thus, glucosyl azide **3** (Scheme **1**) was transformed by a modified Staudinger protocol [69] into per-*O*-acetylated *N*-β-D-glucopyranosyl urea (**7**) which was then acylated to **5** (R' = acyl) by an acid chloride in the presence of catalytic $ZnCl_2$*#. In another route glucosylamine **1** was transformed into the corresponding isocyanate **2** which was reacted at high temperature with carboxamides to give **5** (R' = acyl)#. Reaction of **1** with acyl-isocyanates also furnished the target compounds of type **5** (R' = acyl)*. Very recently, synthesis of *N*-substituted-*N'*-β-D-glucopyranosyl ureas inclusive *N*-acyl derivatives was described from the unprotected β-D-glucopyranosylammonium carbamate [70].

Kinetic results for these derivatives are shown in Table **4**. Replacement of the methyl group of the acetyl urea by cyclohexyl (Entry 2) or aralkyl substituents (Entries 3 and 4) resulted in a loss of activity. Substitution at the aromatic position 4 of the benzoyl urea by neutral aliphatic (Entries 10 and 11), aromatic (Entry 13), polar (Entry 14), or halogen (Entry 17) moieties, as well as slightly basic (Entry 15) or acidic (Entry 16) groups did not strengthen the binding compared to the parent compound. However, introduction of a sterically demanding and strongly hydrophobic group (Entry 12) in the same position made an inhibitor stronger by almost an order of magnitude. An increase in the size of the aroyl group (Entries 5-7) revealed the importance of the

---

[*] Nagy, V.; Felföldi, N.; Praly, J.-P.; Docsa, T.; Gergely, P.; Chrysina, E.D.; Tiraidis, C.; Alexacou, K.M.; Leonidas, D.D.; Zographos, S.E.; Oikonomakos, N.G.; Somsák, L. *in preparation*.

[#] Chrysina, E.D.; Nagy, V.; Felföldi, N.; Telepó, K.; Praly, J.-P.; Docsa, T.; Gergely, P.; Alexacou, K.M.; Hayes, J.M.; Leonidas, D.D.; Zographos, S.E.; Oikonomakos, N.G.; Somsák, L. *in preparation*.

Table 3. *N*-β-D-Glucopyranosyl Oxamic Acid and Oxamide Derivatives as Inhibitors of RMGPb

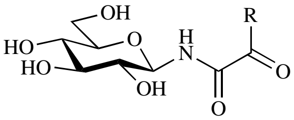

Entry	R	K_i [μM]	Ref.
1.	$-OH$	710	[67]
2.	$-OCH_3$	210	
3.	$-OCH_2CH_3$	920	
4.	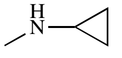	1410	
5.	$-N[CH(CH_3)_2]_2$	no inh.	
6.	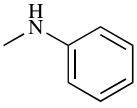	100	*
7.	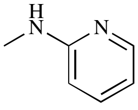	230	
8.	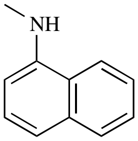	144	
9.	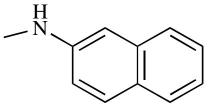	56	
10.	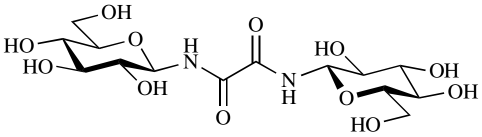 K_i = 1460 μM*		

*Czifrák, K.; Felföldi, N.; Docsa, T.; Gergely, P.; Chrysina, E.D.; Kiritsi, C.; Siafaka-Kapadai, A.; Leonidas, D.D.; Zographos, S.E.; Oikonomakos, N.G.; Somsák, L. *in preparation*.

orientation of the aromatic appendage, and the 2-naphthoyl derivative (Entry 6) exhibited the strongest inhibition among acyl ureas. Entries 6 and 12 represent the first nanomolar glucose analogue inhibitors of GP. Observations with the acyl ureas confirm the significance of contacts between enzyme and inhibitor in the β-channel: the present series of compounds underlines the role of van der Waals and hydrophobic interactions of suitably sized and oriented aromatic moieties properly substituted by hydrophobic groups.

Inhibition by the 2-pyridyl derivative (Entry 8) proved significantly weaker than that by benzoyl urea (Entry 9). A structural comparison between the RMGPb−2-Py-urea complex and RMGPb−Bz-urea complex over well defined residues (24-249, 261-281, 289-313, 326-549, 558-830) shows that the structures superimpose quite well and they closely resemble each other in the vicinity of the catalytic site. The orientation of the 2-pyridyl nitrogen away from Glu88 is predominantly favoured, and is also predicted by docking[#]. The reason for this may be that the lone-pair of N in the pyridine ring can form an intramolecular H-bond with the NH (N2) of the urea in this orientation. In the other orientation it is close to the O of the acyl carbonyl. So this means that the 2-pyridyl ligand has less entropy compared to the benzoyl urea ligand. The kinetics indicate that compound in Entry 8 loses more entropy – and this could be because on going from a polar (H_2O) environment to a non-polar environment (cavity), the intramolecular bond in the 2-

---

[#] Chrysina, E.D.; Nagy, V.; Felföldi, N.; Telepó, K.; Praly, J.-P.; Docsa, T.; Gergely, P.; Alexacou, K.M.; Hayes, J.M.; Leonidas, D.D.; Zographos, S.E.; Oikonomakos, N.G.; Somsák, L. *in preparation*.

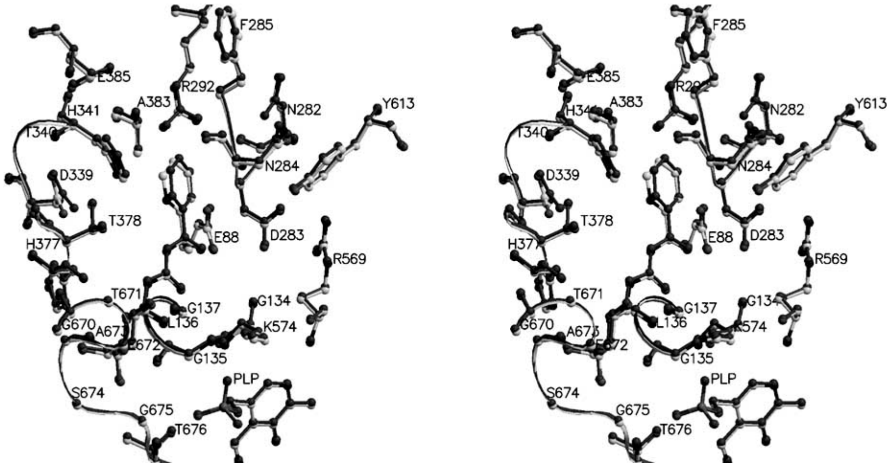
F285
E385
R292
H341
A383
N282
Y613
T340
N284
D339
T378
H377
E88
D283
R569
T671
G137
G134
G670
A673
L136
K574
E672
G135
PLP
S674
G675
T676

Fig. (4). Comparison between the RMGPb−Bz-urea complex (for Bz-urea, shown in dark grey, see Entry 9 in Table **4**) and the RMGPb−Py-urea complex (for Py-urea, shown in light grey, see Entry 8 in Table **4**), in the vicinity of the catalytic site.

Table 4. Inhibitory Efficiency of *N*-Acyl-*N*'-β-D-glucopyranosyl Ureas with RMGPb

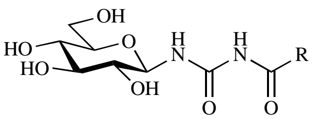				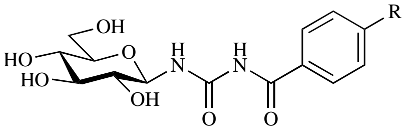		
Entry	**R**	**K$_i$ [μM]**	**IC$_{50}$ [μM]**	**Entry**	**R**	**K$_i$ [μM]**
1.	$-CH_3$	305 [68]		9.	–H (**Bz-urea**)	4.6 [68]
2.	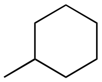		5000 #	10.	$-CH_3$	2.3 *
3.	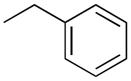		10000 †	11.	$-CF_3$	1.8 #
4.	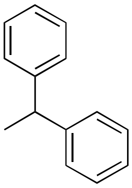		>5000 †	12.	$-C(CH_3)_3$	0.7 #
				13.	$-C_6H_5$	3.7 *
5.	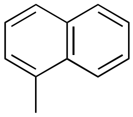	15 #		14.	$-NO_2$	3.3 *
6.	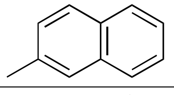	0.35 #		15.	$-NH_2$	6.0 *
7.	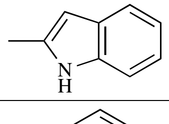	4.0 #		16.	–OH	6.3 *
8.	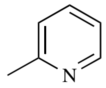 (**Py-urea**)	68 #		17.	–Cl	4.4 *

#Chrysina, E.D.; Nagy, V.; Felföldi, N.; Telepó, K.; Praly, J.-P.; Docsa, T.; Gergely, P.; Alexacou, K.M.; Hayes, J. M.; Leonidas, D.D.; Zographos, S.E.; Oikonomakos, N.G.; Somsák, L. *in preparation*.

*Nagy, V.; Felföldi, N.; Praly, J.-P.; Docsa, T.; Gergely, P.; Chrysina, E.D.; Tiraidis, C.; Alexacou, K.M.; Leonidas, D.D.; Zographos, S.E.; Oikonomakos, N.G.; Somsák, L. *in preparation*.

†Felföldi, N.; Nagy, V.; Docsa, T.; Gergely, P.; Chrysina, E.D.; Alexacou, K.M.; Hayes, J. M.; Leonidas, D.D.; Zographos, S.E.; Oikonomakos, N.G.; Somsák, L. *in preparation*.

Table 5. Comparison of *N*-Acyl-β-D-glucopyranosylamines, *N*-Substituted-*N*'-β-D-glucopyranosyl Ureas and Related Compounds as Inhibitors of RMGPb (K_i [μM])

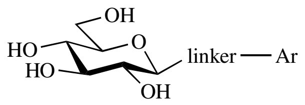 linker — Ar			Ar			
			A	**B**	**C**	**D**
Entry	**linker**		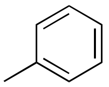	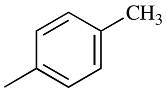	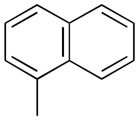	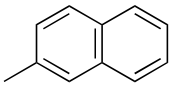
1.	NHCO	2 atoms	81 [56] 144 [64]	4500 (IC_{50}) [63]	444 [63]	4 (10[63]) (**N2NG**)
2.	NHCONH	3 atoms	18 †	-	350 (IC_{50}) †	5.2 †
			(**Ph-urea**)			(**2-Naphthyl- urea**)
3.	NHCOCH$_2$		1100 (IC_{50}) [63]	-	-	-
4.	NHCONHCO	4 atoms	4.6 [68]	2.3 *	10 #	0.35 #
			(**Bz-urea**)			(**2-Naphthoyl- urea**)
5.	NHCONHCH$_2$		42 % (1 mM) †	-	-	-
6.	NHCOOCH$_2$		350 [56]	-	-	-
7.	NHCOCH$_2$CH$_2$		85 [63]	-	-	-
8.	NHCOCH=CH		18 [63]	-	-	3.5 [63]
9.	NHCOC≡C		62 [63]	-	-	-
10.	NHCONHCONH	5 atoms	21 †	-	-	-
11.	NHCONHCOCH$_2$		600 † (**PhAc-urea**)	-	-	-
12.	NHCONHCONHCO	6 atoms	-	-	-	45 % (625 μM) †
13.	NHCONHCOCH=CH		-	16 †	-	-

†Felföldi, N.; Nagy, V.; Docsa, T.; Gergely, P.; Chrysina, E.D.; Alexacou, K.M.; Hayes, J. M.; Leonidas, D.D.; Zographos, S.E.; Oikonomakos, N.G.; Somsák, L. *in preparation*.
*Nagy, V.; Felföldi, N.; Praly, J.-P.; Docsa, T.; Gergely, P.; Chrysina, E.D.; Tiraidis, C.; Alexacou, K.M.; Leonidas, D.D.; Zographos, S.E.; Oikonomakos, N.G.; Somsák, L. *in preparation*.
#Chrysina, E.D.; Nagy, V.; Felföldi, N.; Telepó, K.; Praly, J.-P.; Docsa, T.; Gergely, P.; Alexacou, K.M.; Hayes, J. M.; Leonidas, D.D.; Zographos, S.E.; Oikonomakos, N.G.; Somsák, L. *in preparation*.

pyridyl derivative is more tightly held. Also, a non-polar benzoyl group going from polar H$_2$O to a non-polar region of cavity will have a greater enthalpy contribution to binding. This may provide an explanation for the higher affinity of benzoyl urea compared to the 2-pyridyl derivative. The structural comparison of RMGPb−2-Py-urea complex with the RMGPb−Bz-urea complex is shown in Fig. (**4**).

From the studies with *N*-acyl-β-D-glucopyranosylamines (selected examples in Table **5**, Entries 1A-D, 3A, 7-9A, and 8D) and *N*-acyl-*N*'-β-D-glucopyranosyl ureas (Entries 4A-D, 11A, and 13B) it became clear that the length of the linker chain as well as its atomic composition between the sugar and the aromatic group had strong influence on the inhibition. To have a more systematic picture of the role of the linker additional compounds were synthesized according to the reactions summarized in Scheme **1**. Protected *N*-aryl-*N*'-β-D-glucopyranosyl ureas were prepared either by acid catalyzed hydration of carbodiimide **4** obtained from azide **3** *via* reaction of the Staudinger phosphinimine with the corresponding isocyanate, or by the addition of glucosylamine **1** to the isocyanate[†]. Test compounds obtained by subsequent deprotection are shown in Entries 2A, 2C, 2D, and 5A. *N*-Phenyl-*N*'-β-D-glucopyranosyl biuret was prepared by reacting isocyanate **2** with phenyl urea, and *N*-(2-naphthoyl)-*N*'-β-D-glucopyranosyl biuret was obtained in a reaction of glucopyranosyl urea **7** with 2-naphthoyl-isocyanate both followed by Zemplén deprotection (Entries 10A and 12D, respectively)[†].

Comparing the inhibitors listed in Table **5** clearly indicates that the best ones have a 4 atom linker and within this group the acyl urea structures β-D-Glc$_p$-NHCONHCO-aryl are the most efficient. Although compounds having K_i values in the low micromolar range can be found among aryl-

---

[†] Felföldi, N.; Nagy, V.; Docsa, T.; Gergely, P.; Chrysina, E.D.; Alexacou, K.M.; Hayes, J.M.; Leonidas, D.D.; Zographos, S.E.; Oikonomakos, N.G.; Somsák, L. *in preparation*.

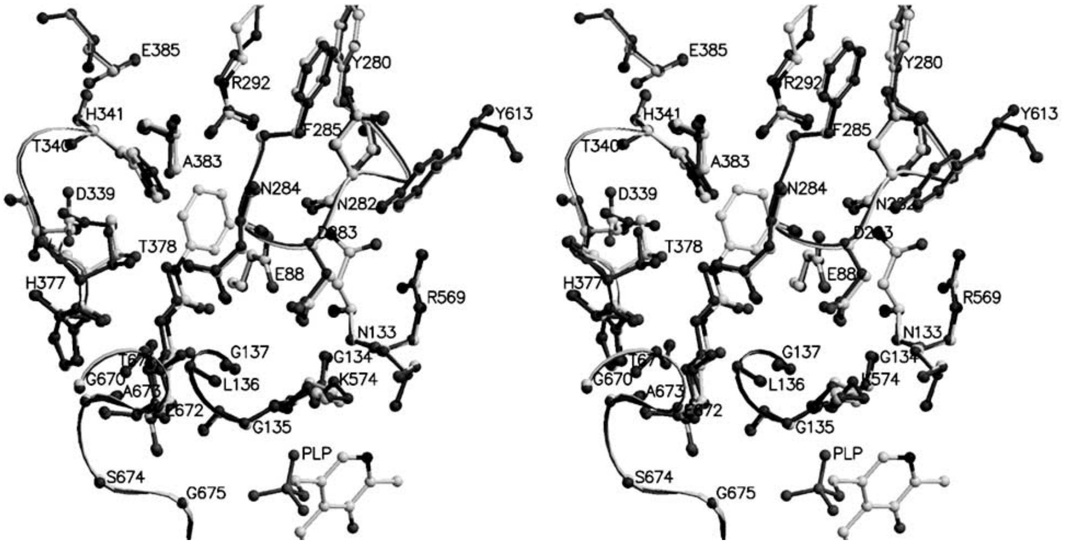

Fig. (5). Comparison between the RMGPb−Ph-urea complex (for Ph-urea, shown in light grey, see Entry 2A in Table **5**) and the RMGPb−NAG complex (for NAG, shown in dark grey, see Entry 1 in Table **1**), in the vicinity of the catalytic site.

amides and -ureas, comparisons of compounds having the same aromatic group (cf. the respective columns A-D in Table **5**) demonstrate the superiority of the acyl ureas. The NHCO, NHCONH, NHCONHCO, and NHCONHCONH linkers are rigid and planar structures. Replacement of the element next to the aromatic part (compare Entries 2A and 3A; 4A, 5A, and 6A; 10A and 11A) and/or elongation of the chain (compare Entries 1A and 3A; 2A and 5A; 4A and 11A) by a methylene group, which breaks the rigidity and makes the endgroup freely rotatable, results in a significant loss of binding strength (cf X-ray comparison below). Exchange of an NHCO moiety in acyl ureas to a two-carbon element (compare Entries 4A to 7-9A and 4D to 8D) makes the inhibition again weaker, however, maintaining the rigidity seems less detrimental (Entries 8A and 8D). Elongation of the NHCONHCO linker by two atomic rigid moieties (Entries 12D and 13B) proved also not beneficial. As a conclusion considering the above one can state that the whole acyl urea part linking the sugar to an aromatic system of suitable size and orientation is necessary for a good inhibitor.

Elongations of the NHCO linkers to NHCONH moieties (compare Entries 1 and 2 in Table **5**) brought about only modest improvement of binding. Some of these compounds were compared crystallographically.

The structure of the RMGPb−Ph-urea (Entry 2A) complex determined at 2.15 Å resolution (100 mM soak for 2 hrs) showed that, on ligand binding, the closed position of the 280s loop is maintained. O7 makes direct hydrogen bonding interactions with Asn284 ND2 and indirect polar contacts to Leu136 N and Asp283 OD1 through a water molecule (Wat40). The hydrogen bonding interaction of amide N1 with CO of His377 (distance=3.0 Å) is maintained, while N2 makes indirect hydrogen bonding interactions to Asp339 OD1 through Wat51. There are some changes in water structure (compared with RMGPb-NAG complex). There are in total 16 hydrogen bonds, and 92 van der Waals interactions (11 nonpolar/nonpolar, 12 polar/polar, 59 nonpolar/polar) in the RMGPb−Ph-urea complex as compared to 15 hydrogen bonds and 61 van der Waals interactions (6 nonpolar/nonpolar, 10 polar/polar and 45 nonpolar/polar) in the RMGPb-NAG complex (Fig. **5**).

The structure of the RMGPb−2-Naphthyl-urea (Entry 2D) complex determined at 1.96 Å resolution (crystal soaked with 4.6 mM for 2.5 hrs) showed the side-chains of Asp339 (CG atom shifts 0.8 Å) and His341 (CE1 atom shifts 0.5 Å) move away from the naphthyl group and side-chain of Leu136 flips to avoid bad contacts. The hydrogen bonding interaction of amide N1 with CO of His377 (distance=2.9 Å) is maintained. N2 makes a rather longer contact with Asn284 OD1 (3.4 Å) and an indirect hydrogen bonding interaction with Asp339 OD1 through a water molecule (Wat107). There are small shifts of the residues of the 280s loop (0.3-0.4 Å) and the 380s loop (0.3-0.5 Å). With the exception of some changes in water structure, the RMGPb−2-Naphthyl-urea and RMGPb-NAG complex structure superimpose quite well in the vicinity of the catalytic site (Fig. **6**). There are in total 14 hydrogen bonds, and 101 van der Waals interactions (11 nonpolar/nonpolar, 12 polar/polar, 78 nonpolar/polar).

Elongation of the -NHCONHCO- by a methylene group, as in compound PhAc-urea (Table **5**, Entry 11A) results in poor affinity (K_i = 600 μM). The conformation of the bound compound is not identical with that described for the Bz-urea for the catalytic site (100 mM soaking of a crystal of RMGPb for 3 hrs, resolution=2.1 Å) (Fig. **7**). In the bound PhAc-urea structure, the torsion angle O7-C7-N2-C8 is 178°, so that the conformation about the C7-N2 bond is in *trans* geometry, significantly different from that of Bz-urea (0°) in the catalytic site. The *trans* geometry directs the phenyl group in a pocket formed by residues Asp283, Asn284, Leu380, His571 and Tyr573. Carbonyl O8, which in the RMGPb−Bz-urea complex forms a hydrogen bonding interaction to Asp283 OD1 and contacts Gly134 N, Leu136 N, Gly137 N, and Glu88 OE2 through a water molecule, is not involved in any hydrogen bonding interactions in the RMGPb−PhAc-urea complex, but it contacts carbonyl O of His377 (3.6 Å) and Thr378 CB (3.6 Å) and CG2 atoms (3.7 Å). There are in total 15 hydrogen bonds and 94 van der Waals interactions (19 nonpolar/nonpolar, 13 polar/polar, 62

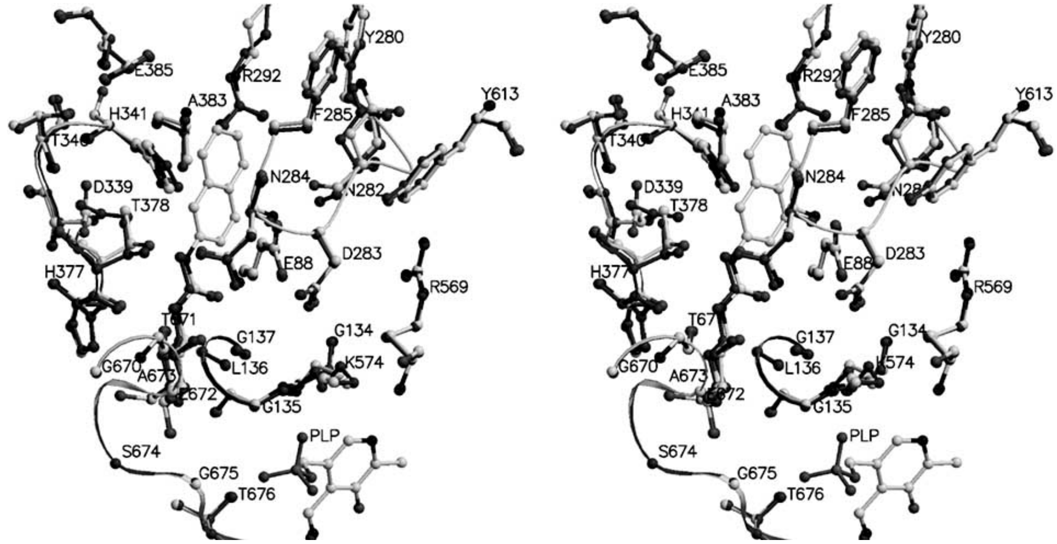

Fig. (6). Comparison between the RMGPb−2-Naphthyl-urea complex (for 2-Naphthyl-urea, shown in light grey, see Entry 2D in Table **5**) and the RMGPb-NAG complex (for NAG, shown in dark grey, see Entry 1 in Table **1**), in the vicinity of the catalytic site.

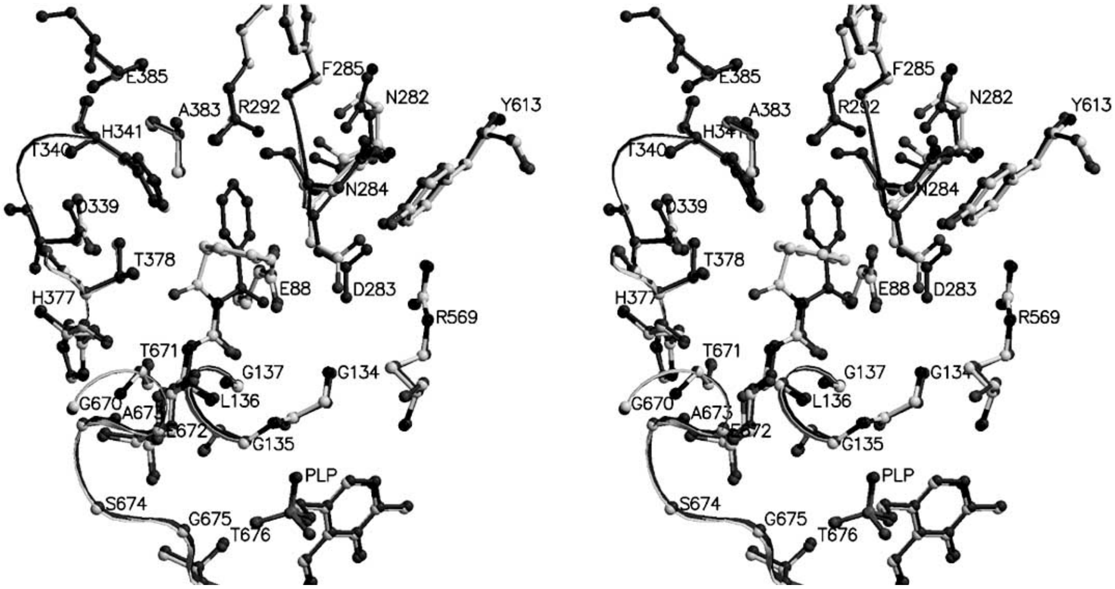

Fig. (7). Comparison between the RMGPb−PhAc-urea complex (for PhAc-urea, shown in light grey, see Entry 11A in Table **5**) and the RMGPb−Bz-urea complex (for Bz-urea, shown in dark grey, see Entry 4A in Table **5**), in the vicinity of the catalytic site.

nonpolar/polar) in the RMGPb−PhAc-urea complex. Jaguar DFT (Jaguar, version 7.0) and Glide docking (Glide, version 4.5) calculations were used to investigate the source of such a large difference in K_is for two ligands differing by only a $-CH_2-$ link. B3LYP optimizations using the 6-31G* basis set on model structures with the β-D-glucose moiety replaced by a methyl group revealed the *trans* form of the ligands with an intra-molecular hydrogen bond to be ~12 kcal/mol and ~ 7 kcal/mol more stable in gas and water (modelled using a Poisson-Boltzmann solver continuum model) phases at this level of theory, respectively. Glide-SP docking calculations replicate experiment in predicting the *cis* form of the Bz-urea ligand as the preferable binding form as it fits better to the shape of the active site – the phenyl ring can be accommodated better and the ligand has greater flexibility. The *trans* form of the PhAc-urea is predicted to be the most favourable binding form by docking also in agreement with experiment, although a *cis* binding pose slightly lower in docking score is also located. Inspection and comparison of the docking poses for Bz-urea and PhAc-urea suggests that the most significant factor regarding the large difference in K_is for binding of the ligands is the entropy cost of freezing the extra rotatable $-CH_2-$ group of PhAc-urea in the active site due to the connected phenyl group being locked between active site residues. Greater steric effects restricting phenyl group flexibility in the the RMGPb−PhAc-urea complex compared to the RMGPb−Bz-urea complex could also be cited[†].

Acyl urea (Table **6**, Entries 1-4) and oxamide (Entries 6-9) derivatives are constitutional isomers. A comparison of the inhibitory efficiencies indicates that binding to the enzyme is significantly stronger for ureas than for oxamides.

[†] Felföldi, N.; Nagy, V.; Docsa, T.; Gergely, P.; Chrysina, E.D.; Alexacou, K.M.; Hayes, J.M.; Leonidas, D.D.; Zographos, S.E.; Oikonomakos, N.G.; Somsák, L. *in preparation*.

Table 6. Permutation of the Elements of the Acyl Urea: Kinetic Data Obtained with RMGPb

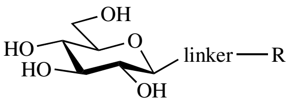

Entry	linker	K_i [μM]	R	Entry	linker	K_i [μM]
1.	NHCONHCO	4.6 [68]	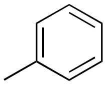	6.	NHCOCONH	100 *
2.		15.2 #	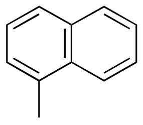	7.		144 *
3.		0.35 # (**2-Naphthoyl-urea**)	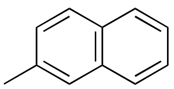	8.		56 * (**2-Nap-oxamide**)
4.		68 #	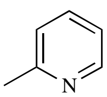	9.		230 *
5.	CONHCONH	no inh. *	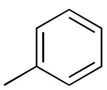	10.	CONHNHCO	22 % at 3.75 mM *

*Czifrák, K.; Felföldi, N.; Docsa, T.; Gergely, P.; Chrysina, E.D.; Kiritsi, C.; Siafaka-Kapadai, A.; Leonidas, D.D.; Zographos, S.E.; Oikonomakos, N.G.; Somsák, L. *in preparation*.
#Chrysina, E.D.; Nagy, V.; Felföldi, N.; Telepó, K.; Praly, J.-P.; Docsa, T.; Gergely, P.; Alexacou, K.M.; Hayes, J. M.; Leonidas, D.D.; Zographos, S.E.; Oikonomakos, N.G.; Somsák, L. *in preparation*.

To see the properties of other possible isomers *C*-glucosyl structures β-D-Glc$_p$-CONHCONH-aryl and β-D-Glc$_p$-CONHNHCO-aryl (Entries 5 and 10, resp.) were prepared (see Section on *C*-glucosyl derivatives), however, these compounds proved inefficient as inhibitors. As a consequence of these findings, the elements of the acyl urea linker are not interchangable and the direction of the chain cannot be reversed.

The binding modes of the most efficient urea and oxamide derivative 2-Naphthoyl-urea and 2-Nap-oxamide (Table **6**, Entries 3 and 8, resp.) were compared based on crystallographic results at a resolution of 1.90 Å. As in the case of Bz-urea, the most prominent changes observed in the RMGPb−2-Naphthoyl-urea complex structure were in the residues of the 280s loop. The structural comparison of RMGPb−2-Naphthoyl-urea with RMGPb−Bz-urea complex structures revealed that the naphthyl moiety was inclined at ~10 degrees with respect to the phenyl ring, while the glucopyranose and the urea moieties superimposed quite well in the two complexes (not shown). 2-Naphthoyl-urea, on binding to RMGPb, makes 19 hydrogen bonding interactions and 117 van der Waals contacts (21 nonpolar/nonpolar, 13 polar/polar, 73 nonpolar/polar) with protein residues in the vicinity of the catalytic site. The strong affinity of 2-Naphthoyl-urea (K_i = 0.35 μM) for RMGPb can be attributed to its extensive interactions with the protein.

Changing the linker functionality from -NHCONHCO- to -NHCOCONH- resulted in an inhibitor, 2-Nap-oxamide (Table **6**, Entry 8), with a K_i value of 56 μM, that indicates a difference in the free energy binding of 3.05 kcal/mol. A structural comparison between 2-Naphthoyl-urea and 2-Nap-oxamide (Fig. **8**) showed that the two ligands display different binding modes: by binding at the catalytic site, 2-Nap-oxamide promotes the closed position of the 280s loop, whereas, on the binding of 2-Naphthoyl-urea, there is a dramatic shift in the 280s loop that results in increased contacts between the inhibitor and the protein. There is no hydrogen bonding interaction between the amide N1 and His377 O in the 2-Nap-oxamide complex as e.g. in the case of the NAG complex [59]. The distance between the amide N1 and main-chain carbonyl oxygen of His377 is 3.5 Å, rather long for a hydrogen bond. Also, the atomic positions of C1, N1, C7, and O7 are changed in the RMGPb−2-Nap-oxamide structure (compared to those of NAG) by 0.7, 0.9, 1.2, and 1.4 Å, respectively, to optimise contacts with protein (see structural comparison between 2-Nap-oxamide and NAG, Fig. **9**). There are also small shifts of the residues of the 280s loop (0.3-0.5 Å) and the 380s loop (0.3-0.4 Å). The 2-naphthyl group makes 13 nonpolar/nonpolar interactions in the RMGPb−2-Naphthoyl-urea complex, compared with 6 in the RMGPb−2-Nap-oxamide complex, indicating that the 2-naphthyl group in 2-Naphthoyl-urea is located in a more nonpolar environment compared to that of 2-Nap-oxamide. The latter, on binding to RMGPb, makes in total 13 hydrogen bonding interactions and 105 van der Waals contacts (12 nonpolar/nonpolar, 22 polar/polar, 71 nonpolar/polar) with the protein.

Contrary to *N*-acetyl-β-D-glucopyranosylamine (Table **7**, Entry 6), where the introduction of the carboxamido function into the α-position (Entry 7) weakened the inhibition, methyl

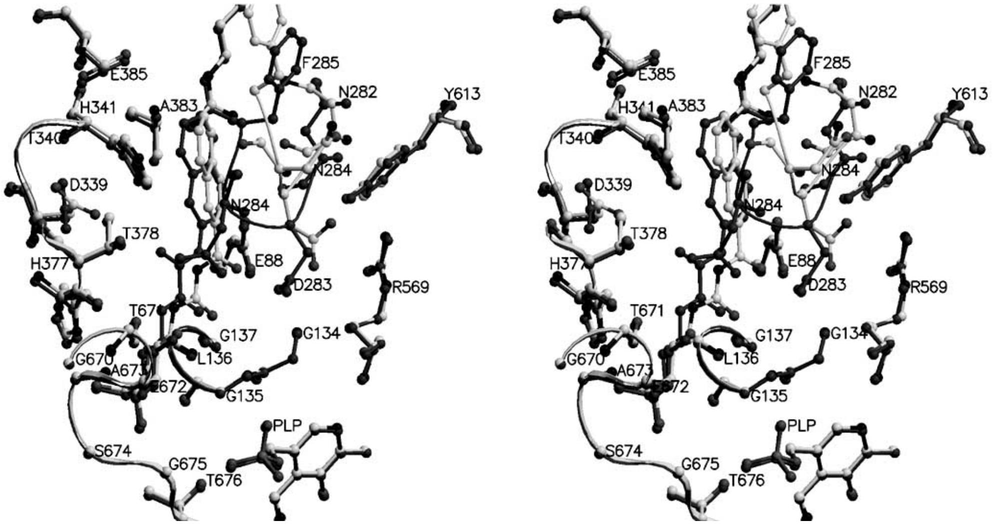
E385
F285
N282
Y613
H341
A383
T340
N284
D339
N284
T378
H377
E88
D283
R569
T671
G137
G134
G670
A673
L136
E672
G135
PLP
S674
G675
T676
E385
F285
N282
Y613
H341
A383
T340
N284
D339
N284
T378
H377
E88
D283
R569
T671
G137
G134
G670
A673
L136
E672
G135
PLP
S674
G675
T676

Fig. (8). Comparison between the RMGPb−2-Nap-oxamide complex (for 2-Nap-oxamide, shown in dark grey, see Entry 8 in Table **6**) and the RMGPb−2-Naphthoyl-urea complex (for 2-Naphthoyl-urea, shown in light grey, see Entry 3 in Table **6**), in the vicinity of the catalytic site.

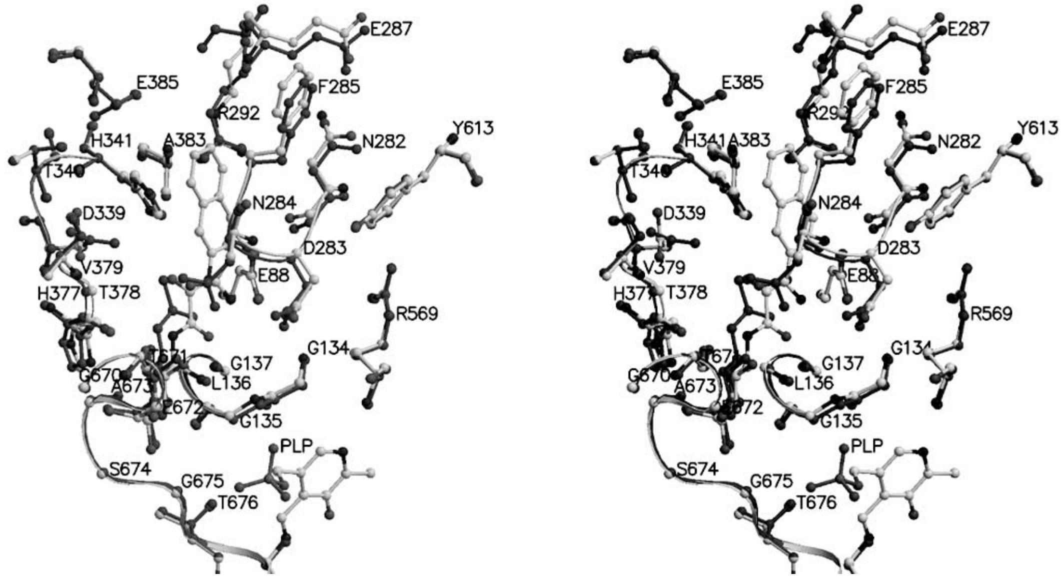
E287
E385
R292
F285
Y613
H341
A383
N282
T340
D339
N284
D283
V379
E88
H377
T378
R569
T671
G137
G134
G670
A673
L136
E672
G135
PLP
S674
G675
T676
E287
E385
R292
F285
Y613
H341
A383
N282
T340
D339
N284
D283
V379
E88
H377
T378
R569
T671
G137
G134
G670
A673
L136
E672
G135
PLP
S674
G675
T676

Fig. (9). Comparison between the RMGPb−2-Nap-oxamide complex (for 2-Nap-oxamide, shown in light grey, see Entry 8 in Table **6**) and the RMGPb-NAG complex (for NAG, shown in dark grey, see Entry 1 in Table **1**), in the vicinity of the catalytic site.

N-(β-D-*gluco*-hept-2-ulopyranosylonamide)carbamate [71] (Entry 9) was shown to be more efficient than its counterpart (Entry 8) without the α-CONH$_2$ group [72]. Therefore, some compounds with similar stuctural features were synthesized and tested (Entries 3-5) [73]. Binding was weakened by the joint presence of the carboxamido and the azide functions at the anomeric centre (Entry 3) in comparison to the anhydro-aldonamide (Entry 1), but strengthened when compared to glucopyranosyl azide (Entry 2). Although this series did not afford new good inhibitors, and even a clearcut conclusion is hard to be drawn based on the limited number of structures, it seems worthwile to synthesize further analogues of this kind especially in the light of some predictions by computational methods [74, 75].

A small library of β-D-glucopyranosyl derivatives (Table **8**) containing nucleobases and analogs was synthesized by a Vorbrüggen-type condensation of per-*O*-acetylated β-D-glucopyranose and silylated pyrimidine or purine derivatives. Tests carried out with the deprotected compounds indicated strong binding for some of the derivatives (Entries 1-3) with K$_i$ values in the low micromolar range [78]. pK$_a$ and quantum chemical calculations, together with docking studies revealed that the most favorable binding form of cytosin derivative in Entry 3 is the higher energy (in gas and water solution phases) imine tautomer, while the compound in Entry 4 with a pK$_a$ close to the pH of experiment (~ 7.0) is significantly ionized with a resulting poor binding affinity compared to the other ligands [78].

The RMGPb-Thym complex (Table **8**, Entry 1) structure was recently determined at 1.90 Å resolution [78]. The β-pocket of the catalytic site provides accommodation of the pyrimidine moiety of the ligand. There are direct hydrogen bonding interactions with Leu136 N, Asn284 N, and also water-mediated hydrogen bonding interactions with Gly135 N, Asp283 OD1, Asp339 OD1 and OD2, His341 NE2, Glu88 OE1, Gly134 N and Gly137 N. Structural comparison

Table 7. Inhibition of RMGPb by *N*-Glycosides of D-*Gluco*-hept-2-ulopyranosonic Acid Derivatives

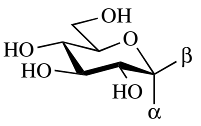

Entry	α	β	K_i [μM]	Ref.
1.	CONH$_2$	H	370	[76]
2.	H	N$_3$	no inh.	[77]
3.	CONH$_2$	N$_3$	1800	[77]
4.	CO$_2$Me	N$_3$	5 % at 10 mM	[73]
5.	CO-NH CH$_2$CO$_2$Me	N$_3$	no inh.	[73]
6.	H	NHCOMe	32	[56]
7.	CONH$_2$	NHCOMe	310	[72, 77]
8.	H	NHCO$_2$Me	86	[72]
9.	CONH$_2$	NHCO$_2$Me	16	[71, 72]

Table 8. β-D-Glucopyranosyl Nucleosides as Inhibitors of RMGPb [78]

Entry	Structure	K_i [μM]
1.	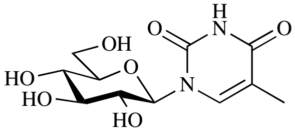 (**Thym**)	6.6
2.	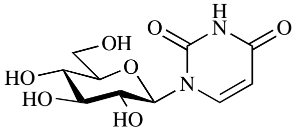	6.1
3.	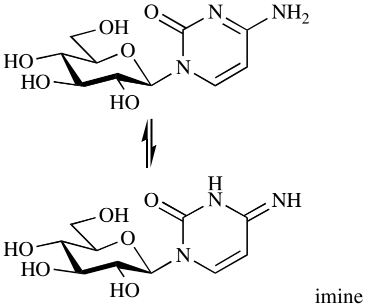	7.7
4.	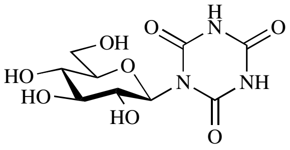	1260
5.	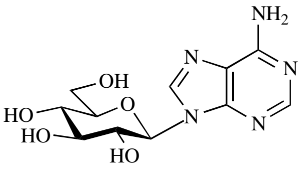	315

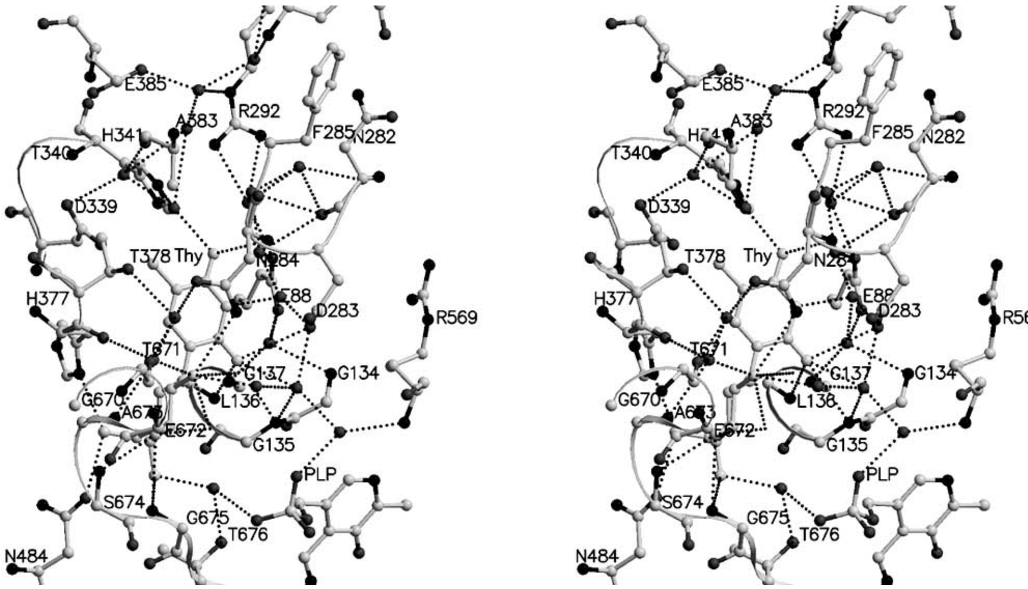
E385
A383
R292
F285
N282
H341
T340
D339
T378
Thy
N284
E88
D283
R569
H377
T671
G137
G134
G670
A673
L136
E672
G135
PLP
S674
G675
T676
N484

Fig. (10). Stereo diagram showing the interactions of compound **Thym** (Table **8**, Entry 1) and protein in the vicinity of the catalytic site. The hydrogen bonding pattern between ligand, protein residues, and water molecules (w) is represented by dotted lines.

Table 9. Glucopyranosylidene-spiro-hydantoins and Related Compounds as Inhibitors of RMGPb with Measured and Predicted Inhibitor Constants

Entry	Structure	K_i [μM]	Ref.
	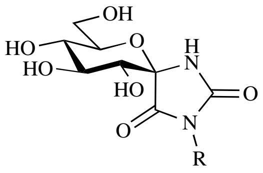 R		
1.	H	3.1* predicted 5.5	[81] [82]
2.	NH_2	146	[72]
3.	OH	39	[72]
4.	CH_3	1200	[72]
5.	$NHCOCH_3$	550	[72]
6.	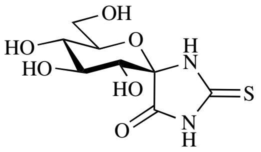	2.3**	[83]
7.	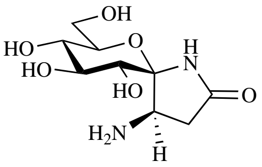 Virtual compound	predicted 0.7	[82]

*Value obtained with respect to Glc-1-P.

**Value obtained with respect to phosphate.

between RMGPb-Thym (Table **8**, Entry 1) and RMGPb-hydantoin (Table **9**, Entry 1) complex structures shows that the pyrimidine ring is almost co-planar with the hydantoin except that the pyrimidine moiety is translated 1.3 to 2.0 Å towards the β-pocket (not shown). Although, there can be no hydrogen bond of pyrimidine nitrogen N1 with His377 O, a H-bond-like interaction with the C-6-H might replace this bond (distance of 3.4 Å).

Glucopyranosylidene-spiro-hydantoin derivatives (Table **9**) were reviewed in details [38, 45, 79]. Recently kinetic and crystallographic studies [72] as well as free energy perturbation analysis [80] have been published explaining the weakening of inhibition on introduction of substituents into the hydantoin ring (Entries 2-5).

A number of recent computational studies have addressed deriving predictive models for receptor-ligand binding properties at the GP catalytic site. Descriptors used to model pharmacokinetic properties (e.g. passive permeability) are the same as those involved in receptor-ligand binding. Integrated use of the VolSurf descriptors [84, 85] based on the GRID [86, 87] interaction fields allowed simultaneous modelling of both protein-ligand binding affinities and ligand pharmacokinetic properties based on the same descriptors for a set of 23 GPb inhibitors [88]. A statistically significant model ($r^2 = 0.94$, $q^2 = 0.89$) for binding affinities was obtained. The authors found that for quality models using this method, information from both the ligand and receptor and/or corresponding ligand-receptor complex are required. Meanwhile, retention of crystallographic cavity waters was found not to be critical for the Volsurf derived models in this work. The disadvantage of the method is that being alignment independent, interpretation of favorable/ unfavorable chemical groups from the models is more complex than with standard 3D-QSAR.

3D-QSAR calculations [89] in the form of flexible molecular comparative molecular field analysis (FCoMFA) using the data for a wide range of 47 structurally dissimilar α and β substituted D-glucose ligands have been also performed. Rather than using fixed and given probe grid positions as in CoMFA, FCoMFA aims to find the optimal probe distribution patterns around ligands at key active site positions. Although the statistical quality ($r^2 = 0.908$; $q^2 = 0.851$) of their model for the training set of 40 ligands was very good, when applied to the test set (7 ligands) r^2 was reduced to 0.679.

In quantitative structure based design (SBD) caution was suggested in neglecting cavity „lining" receptor conformational changes and receptor-ligand induced fit effects at the catalytic site [82, 90]. Following previous computations on inhibitors of GP which used non-flexible (4D-QSAR) [74, 91] and flexible (free energy force field (FEFF) 3D-QSAR [92]) enzyme models, a new method called receptor-dependent (RD-) 4D-QSAR analysis was developed [90]. In an extensive study of the same set of 47 α and β substituted D-glucose ligands used in ref [89], receptor-independent (RI) and receptor-dependent (RD) four-dimensional quantitative structure-activity relationship (RI-4D-QSAR and RD-4D-QSAR, respectively) gave results of similar statistical quality when applied to the training set. However, the binding affinity predictability of RD-4D-QSAR was markedly better when applied to the test set of inhibitors [90]. In particular, the RD-4D-QSAR model could account for important receptor residue conformational effects on ligand binding such as „flip-flopping" of Asn284 so that it can act as a hydrogen bond donor or acceptor depending on inhibitor structure; reorientation of phosphate group of PLP to enhance interactions with certain ligand β-substituents; and reorientations of backbone carbonyl of His377 [90]. Realignments and rearrangements of residues such as the tetrapeptide sequence Ala673-Ser674-Gly676-Thr-676, Leu136, and residues of the 280s and 380s loop have also been included in the RD-4D-QSAR models [82]. A virtual compound with a predicted K_i of 0.7 μM was proposed (Table **9**, Entry 7) for which no experimental data exists. However, the calculated $K_i = 5.5$ μM value for spiro-hydantoin in Entry 1, Table **9** was close to the experimental value of 3.1 μM [82].

Molecular dynamics (MD) in the absence of any explicit water molecules was performed as part of the 12 step process to generate the RD-4D-QSAR models [82, 90]. However, the very recent MD study [62] of receptor-ligand binding at the GP catalytic site for a glucosyltriazolylacetamide (Entry 18, Table **1**) has shown that modelling bulk solvation using the generalized Börn/surface area (GB/SA) continuum model in the absence of any explicit waters can lead to a completely different binding mode than that observed in the crystal. Retaining the ordered crystallographic cavity waters to model local solvation effects in combination with the continuum model for bulk solvation effects was necessary to reproduce the experimental receptor-ligand binding features. The dynamics also revealed that the glucosyltriazolylacetamide had limited flexibility in the β-pocket over the timescale of the simulation. In contrast to the MD calculations, retention of the ordered crystallographic water molecules for accurate redocking (using GOLD [93] and GLIDE [94] 4.0 docking programs) of the ligand into its native rigid protein structure was not necessary.

The receptor structure/conformation dependence on docking results has also been investigated for a set of seven *N*-acyl-*N*'-β-D-glucopyranosyl ureas ligands (Entries 5-9, 11-12 from Table **4**) with a common NHCONHCO core but varying shifts in the 280s loop residues depending on R substituents[#]. A crude way of incorporating to some degree receptor-ligand induced-fit (flexibility) effects in docking calculations is by reduced scaling of van der Waals interactions. However, a more accurate method for probing and measuring these effects is multiple protein structure (MPS) docking. Using receptors derived from each of the co-crystallized complexes, MPS native- and cross-docking calculations of the ligands to their own and the other receptor structures, respectively, was performed using GLIDE [94] 4.5. The calculations revealed that a single rigid receptor approximation derived from any of the co-crystallized complexes was still reasonably valid with respect to reproduction of the inhibitors' crystallographic binding conformations and for correlation between docking scores and experimental binding free energies. However, better results were obtained using receptors prepared from the co-crystallized complexes

---

[#] Chrysina, E.D.; Nagy, V.; Felföldi, N.; Telepó, K.; Praly, J.-P.; Docsa, T.; Gergely, P.; Alexacou, K.M.; Hayes, J.M.; Leonidas, D.D.; Zographos, S.E.; Oikonomakos, N.G.; Somsák, L. *in preparation*.

with bulkier substituents opening up the cavity in regions complementary to binding of the other ligands. The receptor prepared from the co-crystallized RMGPb-indoloyl urea complex (Entry 7, Table **4**) performed best in this regard (for example, docking score – experimental binding free energy correlation *r* ~ 0.9), with the receptor from RMGPb-1-naphthoyl urea (Entry 5) consistently yielding the worst, but still reasonable results (r ~ 0.7). Retaining ordered crystallographic water molecules common to all ligands in the docking calculations helped to orientate the NHCONHCO moieties in their correct crystallographic positions and therefore yielded better results compared to docking without these waters. Considering the results of this study and the RD-4D-QSAR results of Hopfinger *et al.* [82, 90] therefore suggests that the importance of inclusion of receptor-ligand induced fit effects in computational models may be dependent on the degree and type of receptor conformational changes involved, and also the similarity of ligands such as whether they have a common core or scaffold (e.g. acyl ureas). Further studies should reveal more conclusive information in this regard.

In another computational study [78], the importance of consideration of all relevant ligand ionization/tautomeric states of β-D-glucopyranosyl nucleosides (Table **8**) as potential binding forms of the ligands has been highlighted (as mentioned above) by docking calculations using GLIDE [94] 4.5.

C-*Glucosyl Derivatives*

The first *C*-glucopyranosyl heterocyclic derivatives prepared [95] and tested as inhibitors of GP [96] were the com-

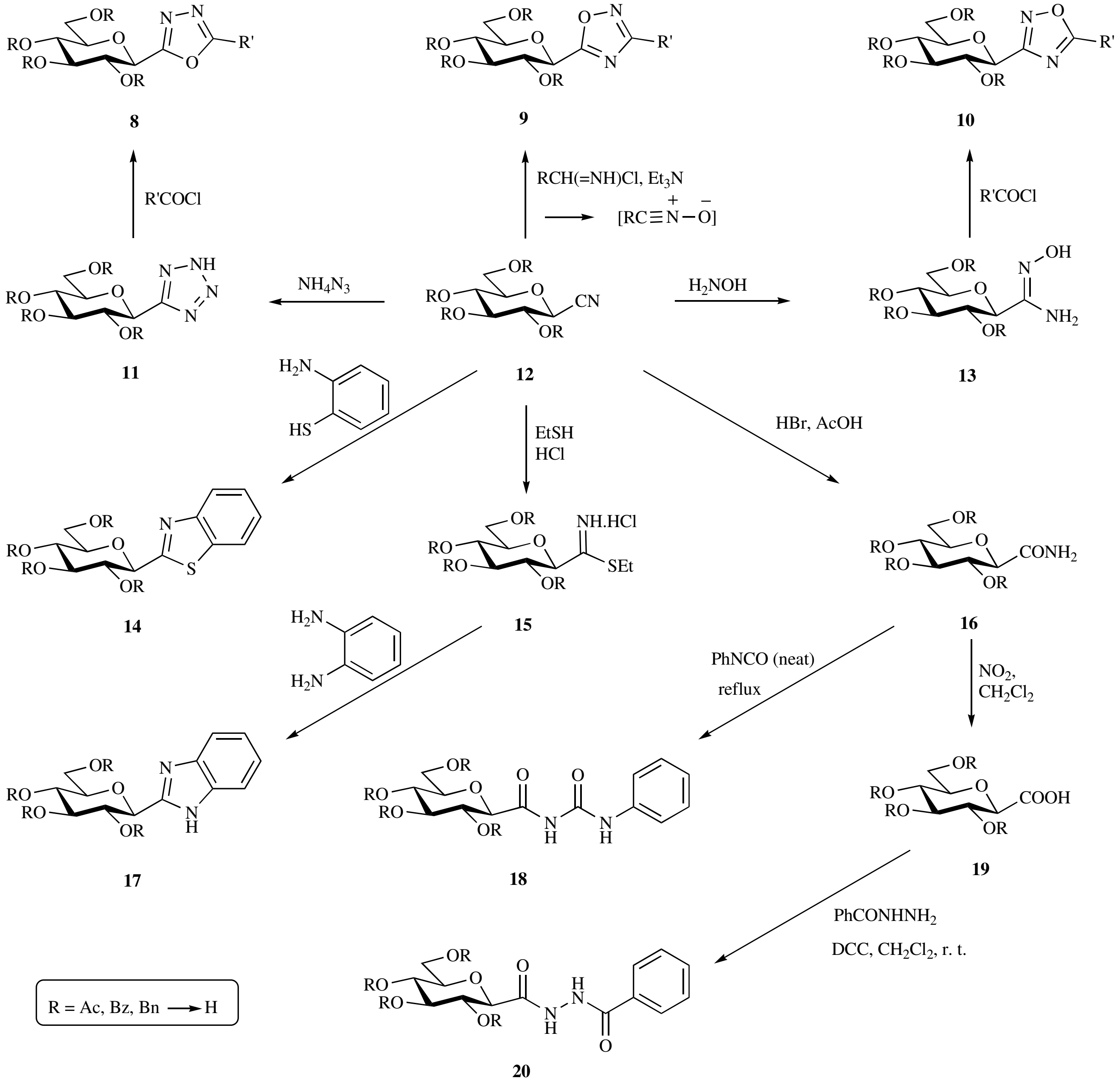

Scheme 2.

Table 10. Comparison of *C*-β-D-Glucopyranosyl Derivatives (K_i [µM] RMGPb)

	Entry	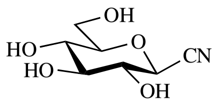 OH O HO HO CN OH	Entry	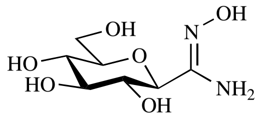 OH O N OH HO HO NH₂ OH	Entry	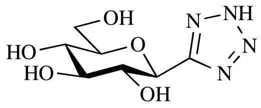 OH O N–NH N N HO HO OH
	1.	130 [95]	9.	no inh. at 625 µM	18.	no inh. [95]
R'		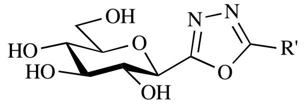 OH N–N HO O R' HO O OH		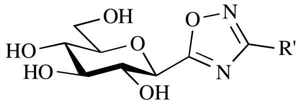 OH O–N HO O R' HO N OH [97]		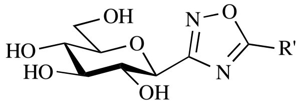 OH N–O HO O R' HO N OH [98]
$-CH_3$	2.	212 [95] 145 [96]			19.	5 % at 2 mM
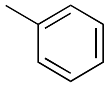	3.	no inh.	10.	26.5	20.	842
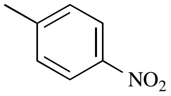			11.	243	21.	10 % at 1 mM
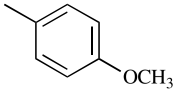			12.	12.7	22.	193
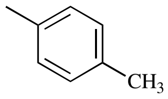			13.	7.5	23.	107
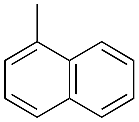	4.	1400			24.	270
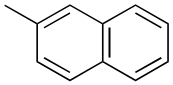	5.	43 % at 4 mM	14.	2.4	25.	38

(Table 10). Contd…..

	6.	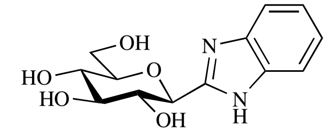	15.	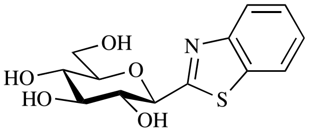			
		11 [95] 9 [96]		229 [95] 76 [96]			
	7.	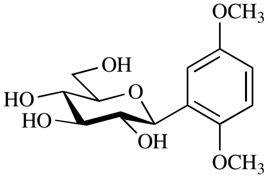	16.	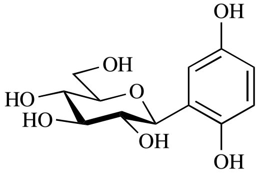	26.	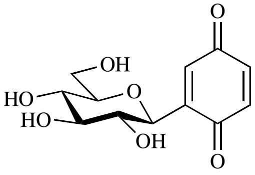	
		no inh. [99]		900 [99]		1300 [99]	
	8.	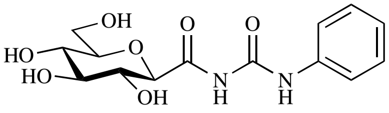	17.	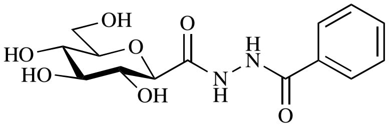		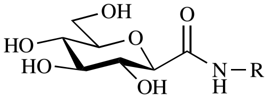	
		no inh. at 625 µM*		no inh. at 625 µM*	27. 28. 29. 30. 31.	R = H 440 CH_3 160 Ph 5400 NH_2 400 $NHCH_3$ 1800	[76]

*Czifrák, K.; Felföldi, N.; Docsa, T.; Gergely, P.; Chrysina, E.D.; Kiritsi, C.; Siafaka-Kapadai, A.; Leonidas, D.D.; Zographos, S.E.; Oikonomakos, N.G.; Somsák, L. *in preparation*.

pounds 1,3,4-oxadiazole **8**, tetrazole **11**, benzothiazole **14**, and benzimidazole **17**. As a common starting material for the synthesis of these derivatives, *O*-acetyl or *O*-benzoyl protected anhydro-aldononitrile **12** (β-D-glucopyranosyl cyanide) was used. 1,3-Dipolar cycloaddition of **12** with azide ion gave 5-β-D-glucopyranosyl tetrazole **11**, which was acylated by acid chlorides to give 5-β-D-glucopyranosyl-2-substituted-1,3,4-oxadiazoles **8** *via* *N*-acyl nitrilimine intermediates. Ring closure of **12** by 2-amino-thiophenol yielded 2-β-D-glucopyranosyl benzothiazole **14**. Similar reaction with 1,2,-diamino-benzene was unsuccesful with **12**, but the more reactive thioimidate salt **15** gave 2-β-D-glucopyranosyl benzimidazole **17**. Deprotections were effected by the Zemplén method to give the test compounds listed in Table **10**.

Glucosyl cyanide **12** proved also useful for the syntheses of other series of oxadiazoles. Thus, 1,3-dipolar cycloaddition with *in situ* obtained nitrile-oxides furnished 3-substituted-5-β-D-glucopyranosyl-1,2,4-oxadiazoles **9** [97]. The reversed substitution pattern could be achieved by transforming **12** using hydroxylamine into the corresponding amidoxime **13** which was ring-closed by acid-chlorides to give 5-substituted-3-β-D-glucopyranosyl-1,2,4-oxadiazoles **10** [98]. The deprotected test compounds are listed in Table **10**.

Kinetic investigations with these compounds showed β-D-glucopyranosyl cyanide (Entry 1) to have weak activity, while *C*-(β-D-glucopyranosyl)formamidoxime and 5-β-D-glucopyranosyl tetrazole (Entries 9 and 18, resp.), in spite of their hydrogen bond donor capacities, proved inactive.

The general trend for the three series of oxadiazoles shows the 3-substituted-5-β-D-glucopyranosyl-1,2,4-oxadiazoles to be the most active (compare Entries 2-5, 10-14, and 19-25). For strong inhibition within one series the substituent of the heterocycle must be a large and properly oriented aromatic ring: 2-naphthyl derivatives are superior as compared to 1-naphthyl compounds (Entries 4, 5, and 24, 25). This latter tendency goes in parallel with the observations for the *N*-acyl-β-D-glucopyranosylamine and *N*-substituted-*N*'-β-D-glucopyranosyl urea series (cf. Table **5**).

Inhibition by compounds having a condensed aromatic system attached directly to the anomeric carbon of the sugar like benzimidazole and benzothiazole derivatives in Entries 6 and 15, respectively, again underlines the significance of a large aromatic ring system. The higher affinity of the benzimidazole derivative is due to the hydrogen bond between imidazole NH and His377 main chain carbonyl which is necessarily absent in the benzothiazole.

Glucosyl cyanide **12** was used for the preparation of constitutional isomers of *N*-acyl-*N*'-β-D-glucopyranosyl ureas[*]. Thus, **12** was hydrated to anhydro-aldonamide **16** which, by heating in neat phenyl isocyanate, gave **18**. Nitrosation of **16** furnished anhydro-aldonic acid **19** to be used to acylate benzoyl hydrazine by way of a dicyclohexyl-carbodiimide mediated coupling to give diacyl hydrazine derivative **20**. The deprotected test compounds (Table **10**, Entries 8 and 17) exhibited no inhibitory effect (cf. Table **6**, Entries 5 and 10). For comparison, also shown are inhibitor constants for anhydro-heptonamide, its *N*-methyl and *N*-phenyl derivatives (Entries 27-29, resp.), as well as anhydro-heptonohydrazide and its *N*-methyl derivative (Entries 30 and 31, resp.). All these compounds had moderate affinity towards RMGPb.

Other derivatives of aromatic systems [99] (Scheme **3**) were obtained from 2-(β-D-glucopyranosyl)-1,4-dimethoxybenzene **22** prepared by electrophilic aromatic substitution with a glucosylium ion generated from **21**. Compound **22** was oxidized to protected 1,4-benzochinon derivative **24**, however, deprotection gave only impure material **25**. Reduction of **24** to *C*-glucosyl hydrochinon derivative **26**, deprotection to **27**, and subsequent oxidation furnished **25** without impurities. The deprotected compounds **23**, **25**, and **27** were also tested as inhibitors of GP, but showed either no (Table **10**, Entry 7) or moderate inhibition (Entries 16 and 26).

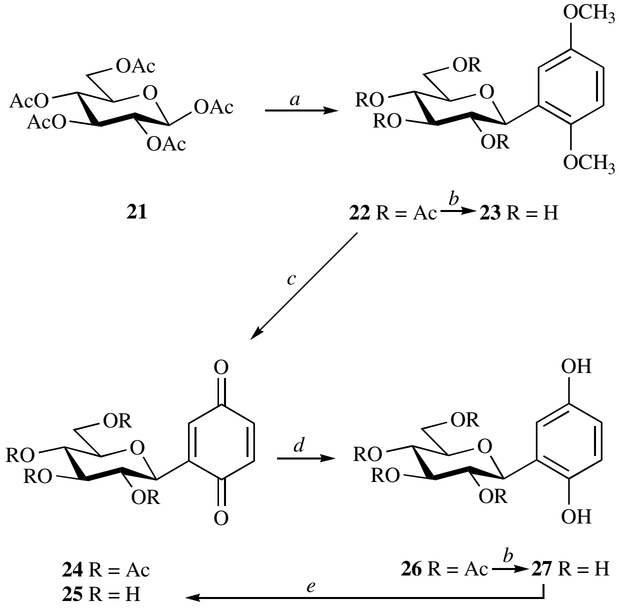

Scheme 3. *a*) 1,4-dimethoxybenzene, $SnCl_4$, CF_3CO_2Ag, CH_2Cl_2, 25-30 °C; *b*) NaOMe, MeOH, r. t.; *c*) CAN, CH_3NO_2, H_2O; *d*) $NaBH_4$, EtOAc, r. t.; *e*) Ag_2O, 2-propanol, r. t. or $PhI(OAc)_2$, MeOH, r. t.

Iminosugars

Several representatives of iminosugar derivatives were covered in our last reviews [38, 45].

New developments have been reported [54] in the synthesis of 1,4-dideoxy-1,4-imino-D-arabinitol (DAB, Scheme **4**): reductive amination of D-arabinose (**28**) gave benzylamine **29** which was debenzylated to **30**. *N*-Formylation produced **31** which furnished **32** in a fermantative oxidation. One-pot hydrolytic removal of the *N*-formyl group followed by intramolecular reductive amination gave DAB isolated as the hydrochloride salt in 26 % overall yield. Besides this expedient procedure other recent syntheses for DAB were elaborated based on chiral epoxyaldehydes [100], D-fructose [101], D-serine [102], D-lyxose [103], and procedures were published also for the preparation of the L-arabinitol derivative [104-106]. DAB (Table **11**, Entry 1), isofagomine and its *N*-(3-phenylpropyl) derivative (Entries 2 and 3, resp.) were tested as inhibitors of several GP enzymes. These compounds binding at the catalytic site can be regarded as oxocarbenium ion mimics. A "*C*-glycosyl" derivative of fagomine (Entry 4) showed no inhibition towards RMGPb [107], while a seven membered iminosugar analog (Entry 5) also had no effect on RMGPb [108].

---

[*] Czifrák, K.; Felföldi, N.; Docsa, T.; Gergely, P.; Chrysina, E.D.; Kiritsi, C.; Siafaka-Kapadai, A.; Leonidas, D.D.; Zographos, S.E.; Oikonomakos, N.G.; Somsák, L. *in preparation.*

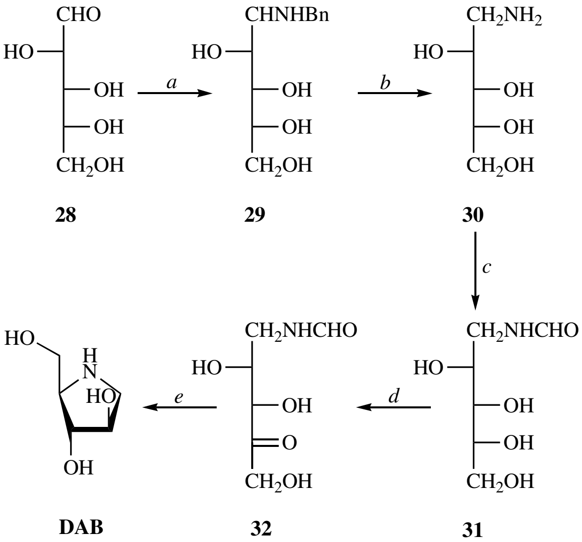

Scheme 4. *a*) $BnNH_2$, H_2 (5 bar), Ra-Ni, 95 % EtOH, 40 °C; *b*) H_2 (5 bar), Pd/C, 95 % EtOH, 70 °C; *c*) CH_3OCHO, CH_3OH, r. t.; *d*) *Gluconobacter oxidans*, pH 6.3, 28 °C; *e*) NaOH, H_2O, H_2 (5 bar), Pd/C, r. t.

In summary, most efficient inhibitors of the catalytic site can be found among *N*-acyl-*N*'-β-D-glucopyranosyl ureas, *N*- and *C*-β-D-glucopyranosyl heterocycles, and some iminosugars (especially DAB). While the latter's efficiency can be attributed to its resemblance to a glucosylium ion, the other classes of compounds exploit extensive interactions with the β-channel part of the catalytic site. These features may form the basis of further inhibitor design supported by X-ray structural elucidation of enzyme inhibitor complexes, as well as computational studies. However, due to extremely high flexibility of the 280s loop, the structures of the ideal substituents are difficult to optimize and further extensive synthetic work cannot be avoided.

Storage Site

The glycogen storage site, which might serve as a region through which the mammalian enzyme is attached to glycogen particles *in vivo*, is on the surface of the molecule, some 30 Å from the catalytic site. This site was identified from crystallographic binding studies with maltopentaose (G5) and maltoheptaose (G7) [109, 110 and references therein]. In GPb, G5 can bind to the glycogen storage site by filling 5 major and 2 minor subsites. The major site, made up of helices α12 and α13 (residues 396-418 and 420-429, respectively) and the loop connecting the two antiparallel strands, β15 (residues 430-432) and β16 (residues 437-411), binds five glucose units in subsites S3-S4-S5-S6-S7 with the reducing end of the oligosacharide bound in subsite S3. The minor site, located above the nonreducing end of the major site and made up of helix α12, the loop connecting the antiparallel β sheets β8 (residues 198-209) and β9 (residues 212-223) and Val354 from helix α9 (residues 344-355), binds glucosyl residues at subsites S8 and S9.

In contrast to the other binding sites of GP, the storage site has received less attention as a possible target in modifying activity of GP. In an attempt to fill this gap α-, β-, and γ-

Table 11. Iminosugar Derivatives as Inhibitors of GP (IC_{50} [μM])

Entry	Structure	RMGPb	RMGPa	RLGPa	PLGPa	Ref.
1.	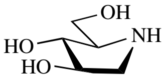	0.39	0.33	0.37	0.49	[54]
2.	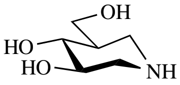	1.21	0.76	0.68	0.67	[54]
3.	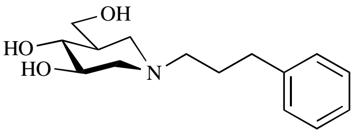	0.84	-	1.22	0.85	[54]
4.	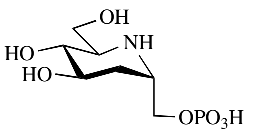	no inh.	-	-	-	[107]
5.	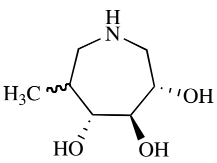	no inh.*	-	-	-	[108]

*By either isomer up to 1 mM.

cyclodextrins (CD, cyclooligosaccharides of glycosidically α-1,4-linked 6, 7, or 8 D-glucopyranosyl units, respectively) were studied kinetically and by protein crystallography. Inhibition of RMGPb was observed in the millimolar range (α-CD K_i = 47.1 mM, β-CD K_i = 14.1 mM, γ-CD K_i = 7.4 mM) [110].

Inhibitor Site

The inhibitor or caffeine binding site is situated on the surface of the enzyme, at the entrance to the catalytic site (some 12 Å from it); it is a hydrophobic binding pocket and comprises residues from both domains 1 and 2. In the T state, Phe285 from the 280s loop is stacked close to Tyr613, from α19 helix (residues 613-631), and these two aromatic residues form the inhibitor site. Occupation of this site stabilizes the T-state conformation of the enzyme and blocks access to the catalytic site, thereby inhibiting the enzyme. Inhibition at this site is generally synergistic with glucose, suggesting that inhibition could be regulated by blood glucose levels and would decrease as normoglycaemia is achieved without producing hypoglycaemia. This site has been probed with purines, nucleosides, nucleotides [38] and, more recently, flavopiridol [111]. The affinity of these ligands for the inhibitor site is mainly due to the π-π stacking interactions of their aromatic rings between the side chains of Phe285 and Tyr613; they are more potent in the presence of high glucose concentrations.

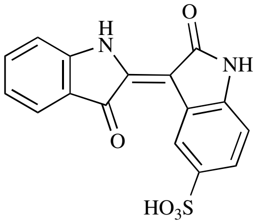

Indirubin-5-sulfonate
K_i = 13.8 μM (RMGPb)

Indirubin-5-sulfonate [112] has a low micromolar inhibitor constant and binds at the inhibitor site of the enzyme.

Indirubin-3'-aminooxy-acetate [113] (E243) inhibits GP in the low micromolar range and occupies the inhibitor site, but binds also to the allosteric site (Fig. **11**).

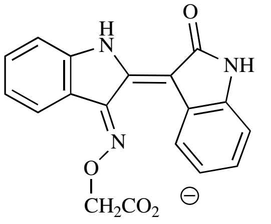

E243 - Indirubin-3'-aminooxy-acetate
K_i = 21 μM (RMGPb)

Flavopiridol (Table **12**, Entry 1) was shown to exert significant inhibition against RMGPb [111, 114]. Analogues of this inhibitor with a flattened tetrahydro-pyridine ring were synthesized (Scheme **5**) starting either with **33** or **34** to give **35** in a selective demethylation and/or acetylation followed by a Lewis-acid catalyzed Fries-rearrangement. Benzoylation by the corresponding acid chloride gave compounds **36** which, on basic treatment and subsequent dehydration, yielded **37** which were demethylated to give test compounds **38** (Table **12**, Entries 2-10) [115]. Compounds in Entries 2-8 were found to inhibit RMGPb with similar potencies, while replacement of the phenyl group by aliphatic moieties gave

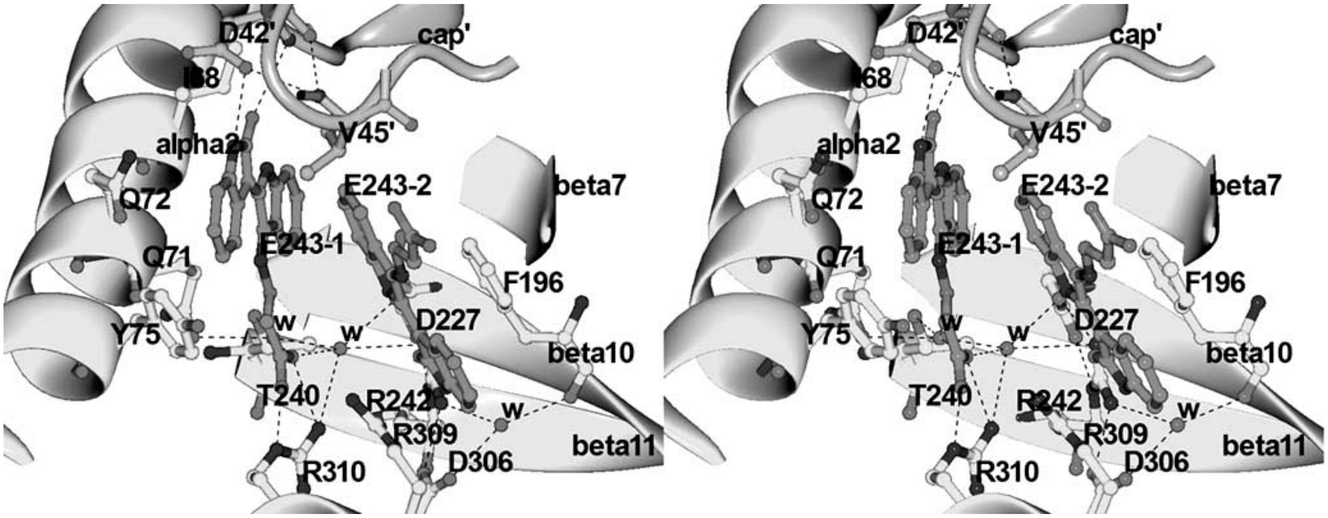

Fig. (11). Binding of two E243 molecules, E243-1 and E243-2, at the allosteric activator AMP binding site and a new sub-site in the vicinity of the allosteric site, respectively, with their indole-aminooxy-acetate rings inclined approximately 40°. E243-1 binds between residues of the α2 helix, Arg310 and residues of the cap' region, and it is partially occupying the AMP binding site. E243-2 binds at a new subsite, formed by residues Phe196, Arg309, Arg242, and Val45' by stacking against the side chains of Phe196 on one side and Arg309 on the other.

Table 12. Flavopiridol and Analogues as Inhibitors of RMGPb* [115]

Entry	Structure		K_i [μM]
1.	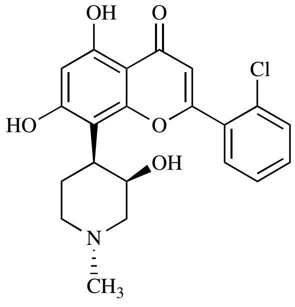 Flavopiridol		1.16
	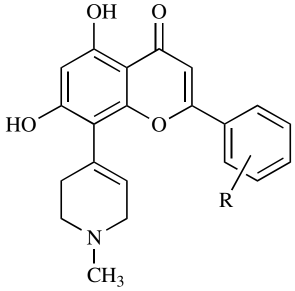	R	
2.		H	1.28
3.		2-Cl	0.99
4.		3-Cl	0.83
5.		4-Cl	1.89
6.		2-F	2.75
7.		2-Br	1.50
8.		3,5-diCl	2.50
9.	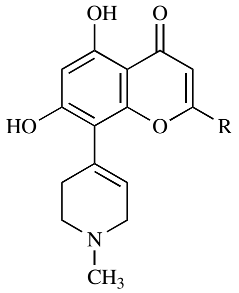	CH_3	241
10.		$C(CH_3)_3$	no inh.

*Ganotidis, M.; Tiraidis, C.; Kosmopoulou, M.N.; Elemes, Y.; Sakarellos, C.; Agius, L.; Leonidas, D.D.; Zographos, S.E.; Oikonomakos, N.G. *unpublished results.*

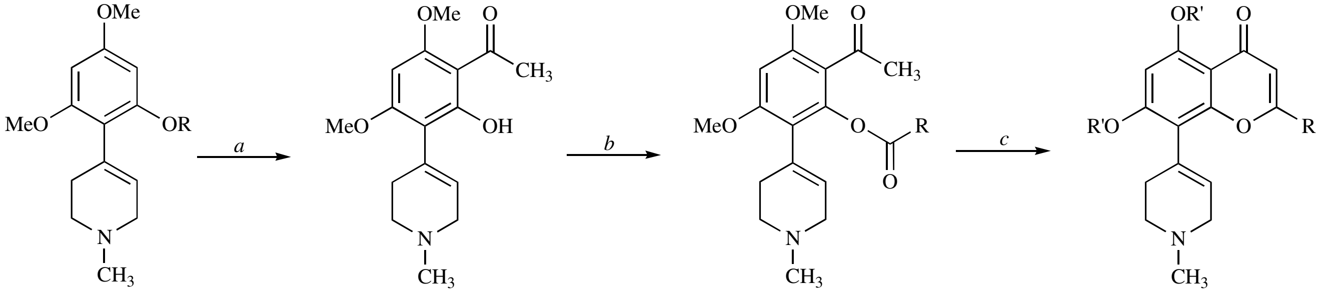

33 R = Me
34 R = H
35
36
d
37 R' = Me
38 R' = H

Scheme 5. *a*) $BF_3 \cdot OEt_2$, Ac_2O, dry CH_2Cl_2; *b*) RCOCl, 10% DMAP, dry pyridine; *c*) (i) NaH, dry THF, (ii) H_2SO_4, AcOH; *d*) pyridine hydrochloride.

compounds of much less efficiency (Entries 9 and 10). To elucidate the mechanism of inhibition of these inhibitors, we have recently analysed the crystal structures of this series in complex with RMGPb*. The structures were determined and refined to 2.30-1.90 Å resolution; the binding studies demonstrated that, with the exception of the *tert*-butyl derivative (Entry 10), all inhibitors bound at the inhibitor site, where they occupy a position similar to that of flavopiridol (Fig. **12**).

Compounds binding to the inhibitor or caffeine site were screened by surface plasmon resonance (SPR) [116]. The affinities of a series of compounds (K_D values of 17-550 μM)

---

[*] Ganotidis, M.; Tiraidis, C.; Kosmopoulou, M.N.; Elemes, Y.; Sakarellos, C.; Agius, L.; Leonidas, D.D.; Zographos, S.E.; Oikonomakos, N.G. *unpublished results.*

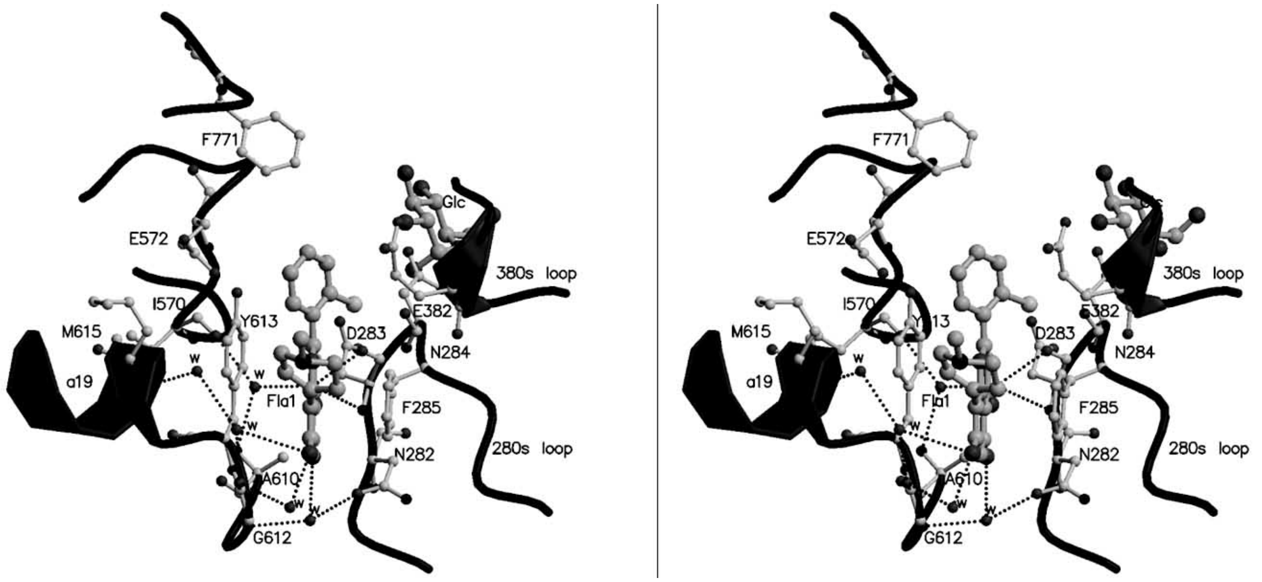

Fig. (12). Binding of flavopiridol analogue (Table **12**, Entry 3), at the inhibitor site. The hydrogen bonding pattern between ligand, protein residues, and water molecules (w) is represented by dotted lines. The location of the catalytic site where the glucose molecule (Glc) binds at the catalytic site of the enzyme is also shown.

were determined and the crystal structures of uric acid, caffeine and riboflavin in complex with HLGPa were solved. Hypoxanthine, uric acid, allopurinol, 3-methylxanthine, folic acid, xanthine, 7-methylxanthine, 1-methylxanthine, xanthine and theophylline bind at the purine nucleoside site, but with weaker affinity than caffeine (K_D=108 μM), whereas xanthopterine (K_D=85 μM), FAD (K_D=80 μM), FMN (K_D=70 μM), lumiflavine (K_D=20 μM), and riboflavin (K_D=17 μM) bind with higher affinity. The main features of binding of uric acid, caffeine, and riboflavin to HLGPa are the stacking interactions between the the planar ligands and the aromatic rings of Phe285 and Tyr613. In addition, each compound forms a specific set of water-mediated hydrogen bonding interactions to residues in the vicinity of the inhibitor site.

The structure of the inhibitior site requires planar molecules to bind. While no real breakthrough could be achieved by the recently investigated compounds several of those with unknown binding site (see corresponding section) may occupy this site and form the basis of further inhibitor design.

Allosteric (or AMP-Binding) Site

The allosteric site is situated where the C termini of the helices α2 (residues 47-78) and α8 (residues 289-314) come together forming a V; it is lined by the β-sheet strands β4 (residues 153-160), β10 (residues 222-232) and β11 (residues 237-247) , the short β7 strand (residues 191-193), and the following loop (residues 195-197), and is closed by the cap' region (residues 36' to 47') (superscript prime refers to residues from the symmetry-related subunit). The allosteric site, which binds the classical allosteric activator AMP, and allosteric inhibitor Glc-6-P, has been shown to bind the Bayer compound W1807, and several dihydropyridine diacid analogues [117-119]. Ligands occupying this site are able to inhibit GP by either direct inhibition of AMP binding and/or indirect inhibition of substrate binding through stabilization of the T- or T'-state conformation.

The acyl urea derivative Entry 1 (Table **13**) was identified by focused screening of 60 compounds exhibiting pharmacophoric similarities to known GP inhibitors. An array of 44 acyl ureas were prepared by reaction of acyl isocyanates **39** with R^4-amines (Scheme **6**), a route amenable to parallel synthesis, or reacting carboxamides **40** with R^4-isocyanates to give acyl ureas **41** [120]. Modifications were guided by an X-ray crystallographic structure determination of the lead complexed with RMGPb. Most important features of SAR were: R^1 = Cl more active than F; for R^2 F > Cl > H; in position 2 of the R^4 ring a substituent (Cl, OMe, OCF_3) larger than H was advantageous; in position 4 an acidic moiety (COOH, tetrazole) was better than SO_2NH_2 or COOMe. Phenolic OH in position 5 of R^4 was more efficient than the similar 4-carboxylic acid (Entries 2 and 3). The structure of compound in Entry 3 in complex with HLGPa was determined at 1.9 Å resolution. There are hydrogen-bonding interactions of the central acyl urea moiety with the carbonyl group of Val40', the backbone amide group of Asp42', and an ordered water molecule in the upper part of the AMP pocket. The 2-chloro-4-fluoro-substituted benzoyl ring tightly packs against Trp67, Arg193, Val40', and Lys41'. In addition to these interactions the phenolic ring makes hydrophobic van der Waals interactions with Gln72, additional van der Waals interactions are mediated by the methoxy substituent positioned near Tyr75, and the phenolic ring also induces additional hydrogen bonds between the side chains of Asp42' and Asn44' and the phenolic hydroxyl group (Fig. **13**). These interactions may provide an explanation for its high potency. Elongating the acyl urea with an sp^3 carbon (Entry 5) or replacing a carbonyl by a sulfonyl moiety (Entry 6) resulted in loss of enzymatic activity. The best phenolic compound was less active in the cell assay, therefore, based on a 3D pharmacophore model, further optimization was carried out revealing the methyl urea derivative in Entry 4 to have the best cellular activity. This compound was tested in Wistar rats, and significantly reduced glucagon-induced hyperlycemic peak.

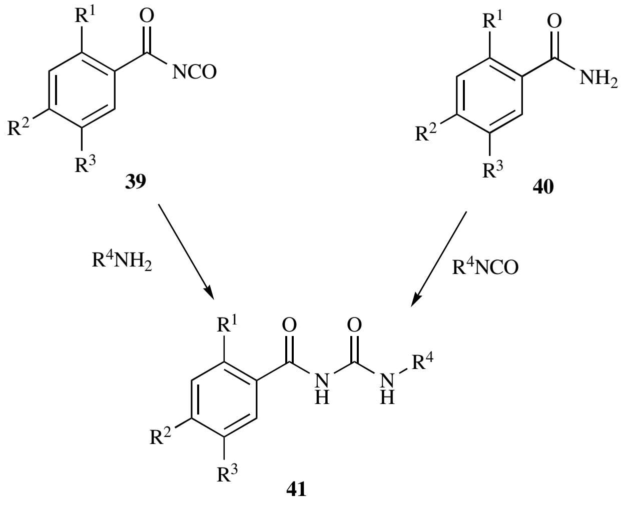

Scheme 6.

Table 13. Acyl Ureas as Inhibitors of GP and their Effect in Cell Based Assay [120, 121] (IC_{50} [µM])

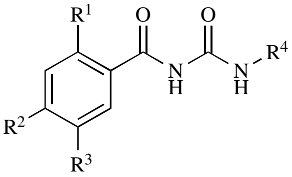

Entry	R^1	R^2	R^3	R^4	HLGPa	Hepatocyte
1.	Cl	H	H	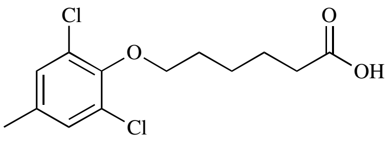	2	80
2.	Cl	F	H	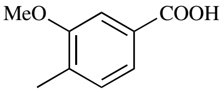	0.21	2
3.	Cl	F	H	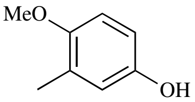	0.023	6.2
4.	Cl	F	F	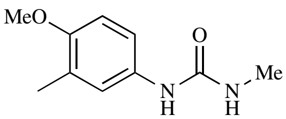	0.053	0.38
5.	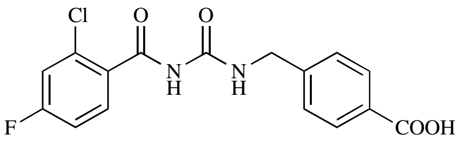				10	nd
6.	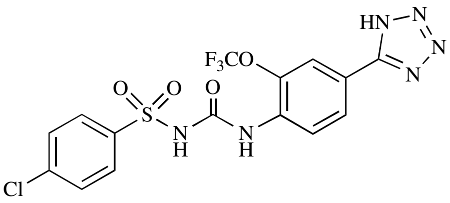				10	nd

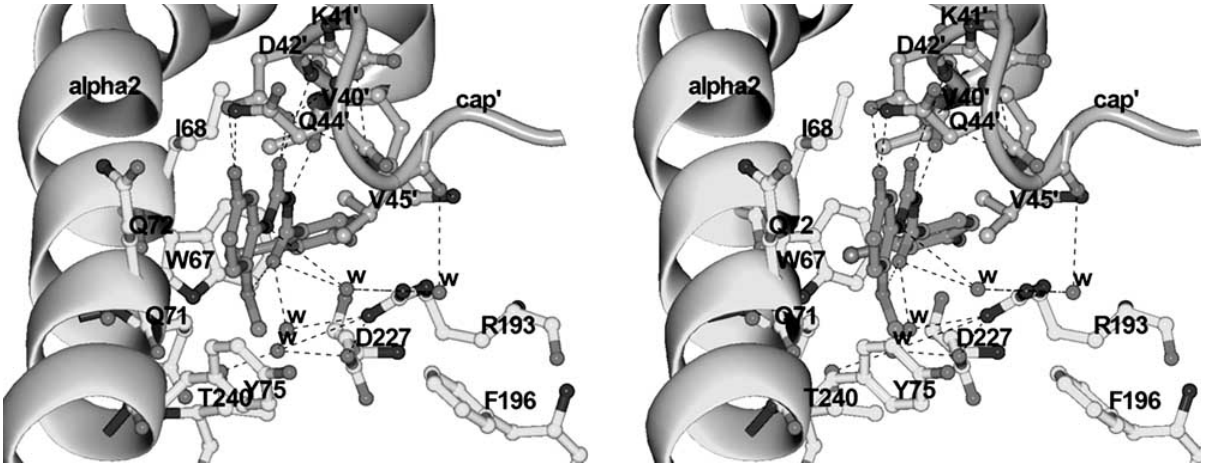

Fig. (13). Binding of acyl urea derivative (Entry 3 in Table **13**), derived from chemical optimisation exploiting X-ray structural data of a screening hit [120] that binds at the allosteric site of HLGPa. The compound binds with benzoyl ring buried deep in the allosteric site, while the phenolic ring points toward the entrance of the site. Based on PDB code 2ATI.

To describe the inhibitory activity of the above series of acyl ureas, linear and non-linear QSAR models were derived by using multiple linear regression (MLR) and least squares support vector machines (LS-SVM) statistical methods, respectively [122]. The six independent descriptors selected to correlate with the inhibitor binding affinities mainly described hydrogen bond, electrostatic, steric and hydrophobic interactions. Although both methods, MLR and LS-SVM, gave activity results in good agreement with experiment (correlation coefficients $r \sim 0.9$) and therefore both provide useful input for the design of further acyl urea inhibitors, the LS-SVM method yielded better overall performance statistics than MLR.

Two series of phthalic acids (incorporating a substituted benzene or naphthalene ring) were prepared (Scheme **7**) either by etherifying the 4-position by coupling **42** with a hydroxyphthalate derivative to give **43** which was reduced to **45**, or starting with aminophenol **44** to furnish **45** directly. *N*-Acylation of **45** gave test compounds **46** listed in Table **14**. A solid phase method was also applied to get compounds **46** starting with resin bound hydroxyphthalic acid **47** obtained by carbodiimide mediated coupling of 4-hydroxyphthalic acid to the hydroxymethyl functionalized commercial Wang resin. Further transformations were carried out by similar chemistry used in the conventional synthesis.

Effects of substituents in ring ***A*** showed a strong preference for the 3-NO_2 group (Table **14**, Entry 1) since other derivatives (3-Cl, -OMe, -Ac, -COOH, 4-Cl, -Me, 3,4-di-Cl, or unsubstituted ***A*** ring) were at least 30-fold weaker inhibitors than the 3-nitro compound. Methyl substitution in ring ***B*** gave more efficient derivatives (Entries 2 and 3), the 5'-Me compound being ~15-fold better than the unsubstituted one. Carboxamido substitution in position 4' (Entries 4-7) resulted in similar efficiency but the presence of both the amide and methyl groups proved not advantageous (Entry 8).

Molecular modeling computations [124] were used in the development of a similar series of inhibitors using Entry 8 of Table **15** as a lead. Competitive binding studies were not available to help identify the binding site of inhibitors of this type, therefore 3D-similarity/superimposition using SQ [125] of conformers of the lead were compared to the crystal structures of Bayer diacid W1807 bound at the AMP allosteric site (PDB entry 3AMV [118]), caffeine at the inhibitor site (PDB entry 1GFZ [111] and Pfizer compound CP320626 at the dimer interface site (PDB entry lC50 [126]). The AMP allosteric site was identified as the most likely binding site. This prediction was confirmed by the solved X-ray structure of RMGPb complexed with the lead compound [127]. ICM docking [128] of the lead to the AMP allosteric site of the

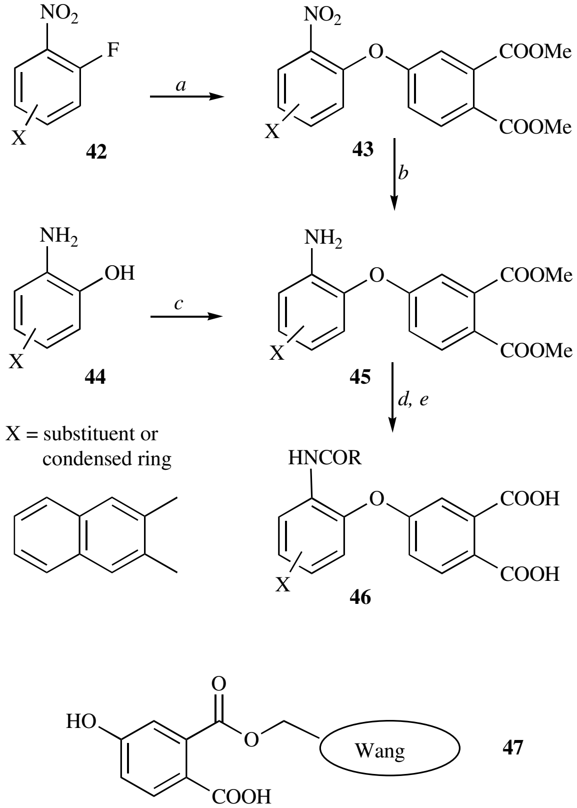

Scheme 7. *a*) dimethyl-4-hydroxyphthalate, K_2CO_3, DMF, 100 ºC; *b*) H_2, Pd/C, CH_2Cl_2; *c*) dimethyl-4-nitrophthalate, K_2CO_3, DMF, 100 ºC; *d*) RCOCl, DIEA, CH_2Cl_2 or RCOOH, EDC, DIEA, CH_2Cl_2 or RCOCl, TEA, acetone; *e*) PhTMS, I_2, 110 ºC or NaOH, MeOH/H_2O or 2N NaOH, dioxane, r. t.

Table 14. Inhibition of GP by Phthalic Acid Derivatives I [123] (IC_{50} [μM])

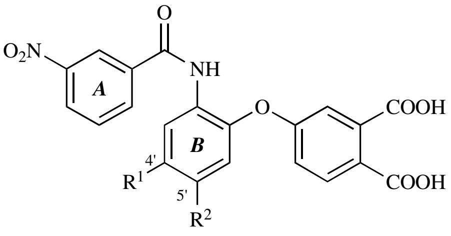

Entry	R^1	R^2	PLGPa
1.	H	H	1.3
2.	CH_3	H	0.45
3.	H	CH_3	0.09
4.	CH_3-CONH	H	0.14
5.	C_6H_5-CONH	H	0.12
6.	4-I-C_6H_4-CONH	H	0.09
7.	3-NO_2-C_6H_4-CONH	H	0.074
8.	3-NO_2-C_6H_4-CONH	CH_3	0.7

receptor derived from the crystal structure of T-state GPa with W1807 correctly predicted the crystallographic ligand binding conformation. Grid based hydrophobic/hydrophilic surfaces calculated using the docking model revealed an unfilled hydrophobic region near the central phenyl ring *B*. This information was exploited to design and synthesize a series of napthyl analogues with stronger affinity to the enzyme (Table **15**, Entries 1-4).

In these investigations the isoform selectivity was also addressed [127]. Among the naphthalene derivatives (Table **15**, Entries 1-4) the 4-nitro-2-pyridyl derivative (Entry 4) was the most efficient. Although the liver/muscle enzyme selectivity was not as good as for the 4-Cl compound (3 *vs*. 5), the 4-NO_2 performed better in the cellular assay. Compounds with other substituents in the pyridine ring (e. g. 4-Cl in Entry 3, or 4-Me, -Et, -OMe, -CF_3) were weaker *in vitro* and ~10-fold less efficient in the cellular test. Both the 4-chloro- and the 4-nitro-2-pyridyl derivatives exhibited higher liver enzyme selectivity (10 and 8, Entries 5 and 8, resp.) in the benzene compound series. Introduction of a 3'-F was necessary to get effective compounds in the cell (Entries 6 and 9) while the 4'-F derivatives (Entries 7 and 10) were much less active in every respects. *In vivo* efficacy of the compound in Entry 6 was tested in the glucagon challenge PD model to show significant lowering of blood glucose levels before (~50 %) and after (lower than vehicle) glucagon treatment.

In order to establish SAR for the dihydropyridine-diacid U6751 (Table **16**, Entry 1) a series of compounds with various substituents on the pyridine ring as well as the 2-

Table 15. Inhibition of GP by Phthalic Acid Derivatives II [127] (IC_{50} [μM])

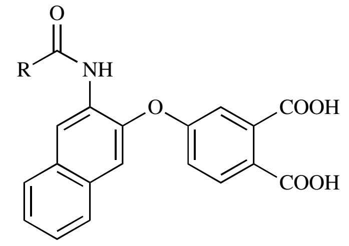					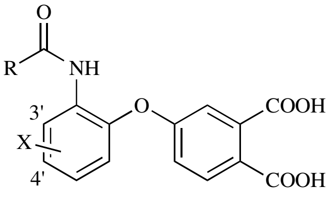				
Entry	**HLGP**	**HMGP**	**Graph**	**R**	**Entry**	**X**	**HLGP**	**HMGP**	**Graph**
1.	2.88	12.3	>20	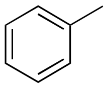					
2.	0.023	0.14	7.5	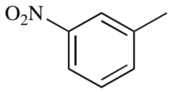					
3.	0.002	0.012	1.5	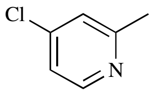	5.	H	0.017	0.181	8
					6.	3'-F	0.01	0.06	0.3
					7.	4'-F	0.078	0.647	11
4.	0.001	0.003	0.3	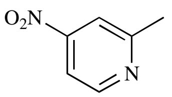	8.	H	0.003	0.025	1
					9.	3’-F	0.001	0.009	0.3
					10.	4'-F	0.013	0.109	1.8

chlorophenyl moiety (R^3 = Cl) was synthesized (Scheme **8**) [129]. β-Amino-acrylic ester **50** and benzylidene acetoacetic ester **51** obtained from propiolic ester **48** and benzaldehyde **49**, respectively, were condensed to give dihydropyridines **52**. The C-5 ester in **52** was transformed into amides and both types of compounds were hydrolyzed to acids **53**.

Removal of Cl from position 2' of U6751 (Table **16**, Entry 1) resulted in a compound showing ~10-fold weaker inhibition. This revealed that a nearly perpendicular arrangement of the phenyl and pyridine rings was essential for the binding. Another compound lacking the carboxyl group in position 2 was ~200-fold weaker, thus the diacid functionality cannot be omitted. Replacement of the highlighted isopropoxyl group to give various amides furnished very poor inhibitors. An *N*-desalkyl derivative (R^2 = H) was again less effective by a factor of ~20 as compared to the lead, however, *N*-benzylation (Entry 2) increased the efficiency. From the different substitutions in the benzyl group selected examples show the most active compounds in Entries 3-6. In hepatocytes the dimethoxy derivative (Entry 6) proved most efficient, and the compound was shown to very efficiently lower blood glucose levels in *db/db* mice.

Corosolic acid (**CA**) and maslinic acid (**MA**) were identified as micromolar inhibitors of RMGPa [130]. The former is the primary active component of a plant extract marketed in Japan and USA for reducing blood sugar levels, while the latter is abundant in olive fruit. Because of limited availability of these compounds by plant extraction, their synthesis was elaborated starting with ursolic acid (**UA**) and oleanolic acid (**OA**), respectively, as shown in Scheme **9**. Thus **UA** or **OA** were transformed to the corresponding C-28 benzylesters **54** followed by oxidation to give ketones **56**. These were either reacted to enol-acetate **63** or stereoselectively hydroxylated (only from **OA**) to **62**. Hydroboration–oxidation of **63** and subsequent debenzylation afforded **68** (**CA** or **MA**). Stereoselective reduction of **62** followed by debenzylation gave **MA** and 3-epi-**CA**. Basic treatment of **62** gave the unsaturated ketone **65** of the **MA** series. Hydroxy enone **65** in the **CA** series was reduced to give 2-epi-**CA**. Both **CA** [131] and **MA** [132] was further functionalized at the C-28 carboxylic acid moiety by forming several esters **69** also containing other appendages (see Scheme **9**, R^7). The 2- and 3-OH groups in **CA** were acylated mostly by the corresponding anhydrides into mono- and diesters of C-2−C-4 and C-7 alkanoic acids, benzoic acid, succinic acid, and were also tosylated and mesylated, and closed to an epoxide [131]. **OA** (being in active clinical use as an anti-hepatitis drug in China) itself had *in vivo* hypoglycemic effect and proved to be a good inhibitor, therefore, several modifications were carried out to study SAR [133]. The 3-OH was esterified to give **55** (for R^5 see Scheme **9**), oxidized, and oximated to **57**. Ketone **56** was nitrosated to oxime **61** (R^6 = H) which was also etherified (for R^6 see Scheme **9**). Reduction of **61** gave alcohol **64** while further oximation furnished **67** which was cyclized to oxadiazole **66**. Isoxazole **59** was obtained from **56** by formylation to give **58** which was cyclized by hydroxylamine. Similar transfromations of **UA** were also car-

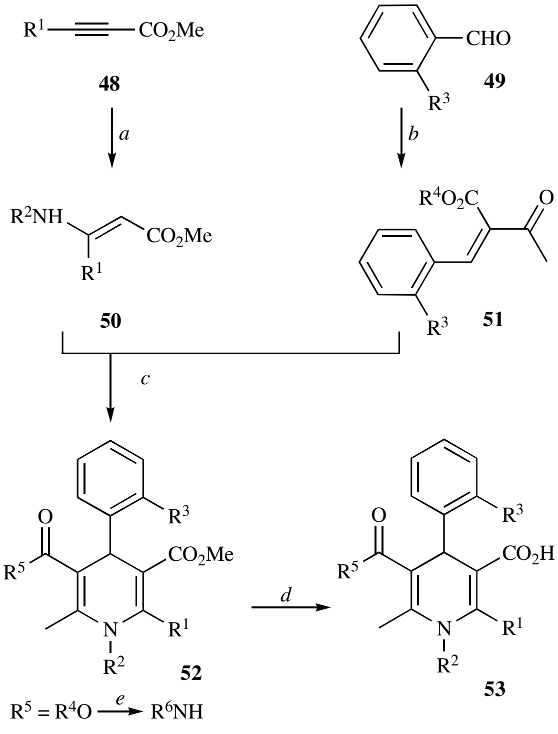

R^1 = H, COOMe, COOH
R^2 = H, Et, CF$_3$CH$_2$, Bn, 2- or 3- or 4-Cl-C$_6$H$_4$-CH$_2$, 2,3- or 2,4- or 2,5- or 3,4- or 3,5-diCl-C$_6$H$_3$-CH$_2$, 3-NO$_2$-C$_6$H$_4$-CH$_2$, 3,4-diOMe-C$_6$H$_4$-CH$_2$
R^3 = H, Cl
R^4 = *i*Pr, allyl;
R^6 = Et, *i*Pr, *i*Bu, Bn

Scheme 8. *a*) R$_2$NH$_2$, MeOH, r.t.; *b*) cat pTSA, CH$_3$C(O)CH$_2$COOR^4, benzene, reflux; *c*) 140 °C, neat; *d*) NaOH, dioxane/H$_2$O (1:1), 50 °C; *e*) R^4 = Allyl (1) Pd(PPh$_3$)$_4$, dimedone, (2) R^{6}NH$_2$, EDC, HOBt.

Table 16. Dihydropyridine-diacid Derivatives [129] (IC$_{50}$ or *EC$_{50}$ in Hepatocytes [μM])

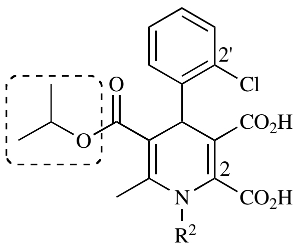

rac-U6751
(Entry 1)

Entry	R^2		HLGPa	HMGPa	Cell*
1.	-CH$_2$CH$_3$		0.039	0.138	2.23
	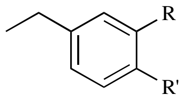				
	R	R'			
2.	H	H	0.011	0.026	1.13
3.	H	Cl	0.002	0.006	0.48
4.	Cl	Cl	0.013	0.041	1.06
5.	NO$_2$	H	0.005	0.01	0.44
6.	OMe	OMe	0.004	0.011	0.27

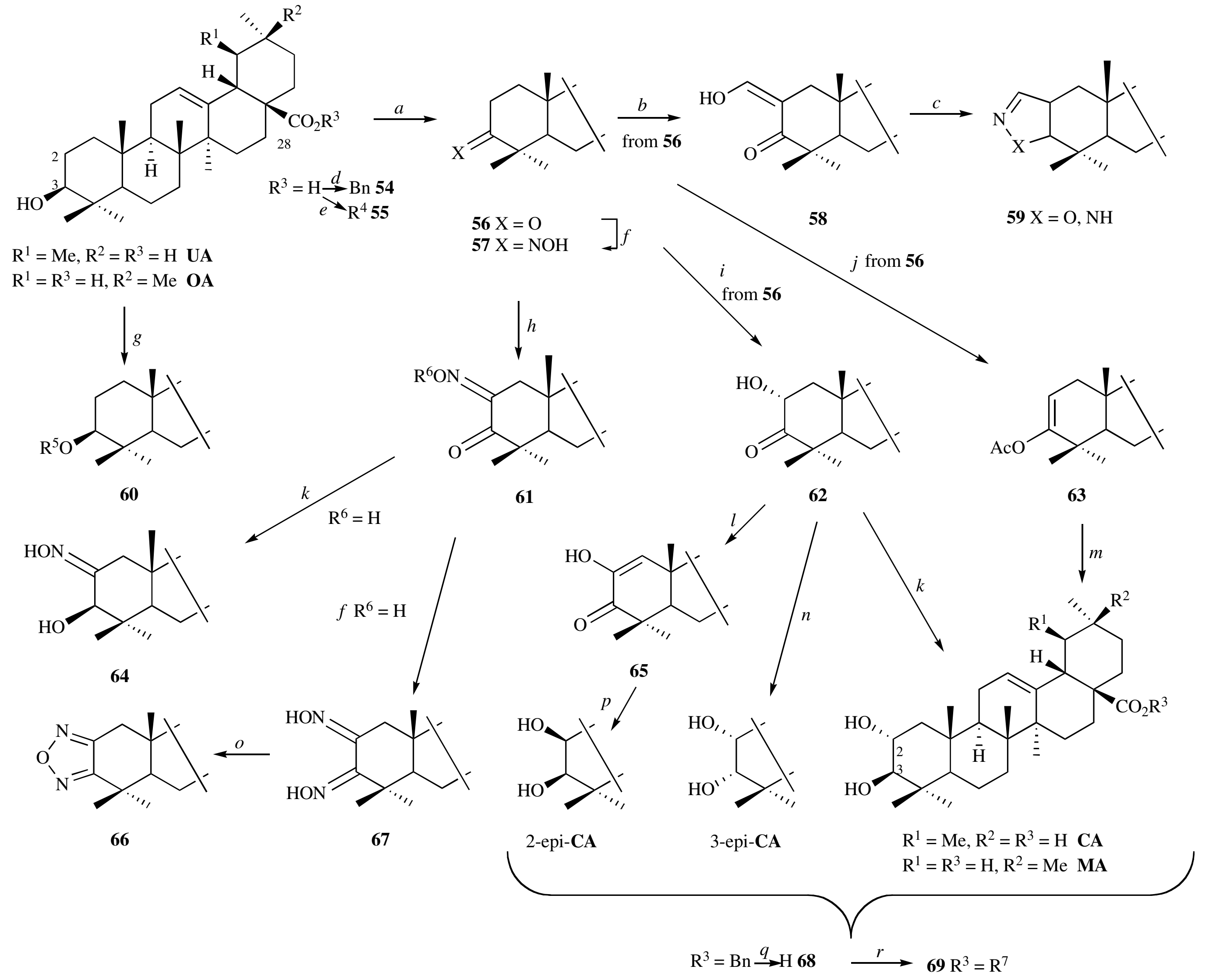

R^4 = Et, allyl, $(CH_2)_{1\text{ or }3}COOEt$, $(CH_2)_{1\text{ or }3}COOH$, CH_2CH_2Br, CH_2CH_2OH, CH_2CH_2NHMe, $CH_2CH_2NEt_2$

R^5 = Ac, $HOOCCH_2CH_2C(=O)$–, *n*PrC(=O)–, 4-Cl–C_6H_4–CH=CH–C(=O)–, 4-MeO–C_6H_4–CH=CH–C(=O)–

R^6 = H, Bn, 2,4-diCl–C_6H_3–CH_2–

R^7 = **CA**: $C_{1\text{-}4}$ alkyl, allyl, pyrazol-1-ylmethyl, CH_2COOEt, CH_2COOH, 2,3,4,6-tetra-*O*-acetyl-β-D-glucopyranosyl, β-D-glucopyranosyl

MA: Me, pyrazol-1-ylmethyl, CH_2COOEt, CH_2COOH, $(CH_2)_{2\text{ or }4}Br$, $(CH_2)_{2\text{ or }4}OH$, $(CH_2)_{2\text{ or }4}NEt_2$, pyperidin-1-yl-($C_{2\text{ or }4}$)alkyl, morpholin-1-yl-($C_{2\text{ or }4}$)alkyl

UA = ursolic acid, **OA** = oleanolic acid, **CA** = corosolic acid, **MA** = maslinic acid

Scheme 9. *a*) PCC, CH_2Cl_2, r. t.; *b*) HCOOEt, CH_3ONa, CH_2Cl_2, r. t.; *c*) $HONH_3Cl$, EtOH-H_2O, reflux or $H_2NNH_2 \cdot H_2O$, EtOH, reflux; *d*) BnCl, K_2CO_3, DMF, 50 °C; *e*) R^4-Hlg, K_2CO_3, DMF, r. t. to 50 °C; *f*) $HONH_3Cl$, Py, 80 °C; *g*) standard acylation conditions; *h*) $NaNO_2$, H_2SO_4, CH_3OH, THF, H_2O, r. t.; *i*) mCPBA, cc. H_2SO_4 (cat.), MeOH, CH_2Cl_2, 0 °C; *j*) $AcOCH=CH_2$, cc. H_2SO_4 (cat.) 100 °C; *k*) $NaBH_4$, THF, 0 °C; *l*) KOH, MeOH, DMF; *m*) 1. BH_3, THF, 2. H_2O_2, NaOH; *n*) Al(O*i*Pr)$_3$, *i*PrOH, reflux; *o*) NaOH, 1,2-ethanediol, 200 °C; *p*) $NaBH_4$, MeOH/THF, r. t.; *q*) H_2, Pd/C, THF, r. t.; *r*) R^7-Hlg, K_2CO_3, DMF, r. t. or 50-60 °C.

ried out [134]. In each of these derivatives the temporary benzyl protection was removed by hydrogenolysis.

In Table **17** inhibition data for modified derivatives of **UA** and **OA** and their frequently prepared intermediate benzylesters are collected. It can be established as a general trend that the benzylesters are weaker inhibitors than the acids. Esterification of the 3-β-OH (Entries 2,3 and 11-13) had different effects, a large hydrophobic group (Entry 13) providing improved inhibition. Oxidation of this hydroxyl weakens the binding (Entries 4 and 14) and several functional groups attached by a double bond to positions 2 and 3 (Entries 5, 6, and 15-19) had no significant effect or even caused loss of the inhibitory effect. Interestingly, in the benzylester series a large hydrophobic substituent and a hydroxymethylene group gave the best results (Entries 17

Table 17. C-28 Carboxylic Acids (and their Benzyl Esters) of Ursolic Acid (UA) [134] and Oleanolic acid (OA) [133] as Inhibitors of RMGPa (IC$_{50}$ [μM])

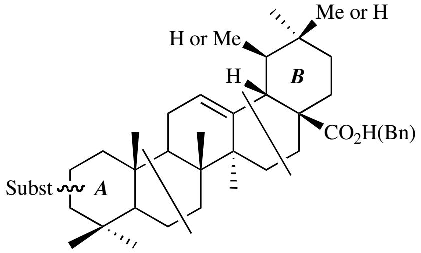

	R		Entry	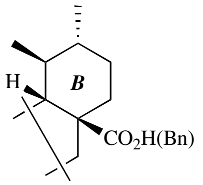	Entry	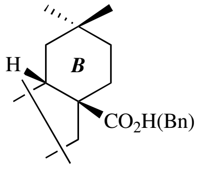
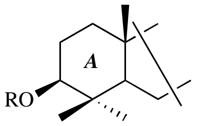	H		1.	**UA** 9	10.	**OA** 14 (461)
	CH_3CO		2.	131	11.	no inh.
	$HOOCCH_2CH_2CO$		3.	27.6	12.	8
	4-Cl-C_6H_4-CH=CH-CO				13.	3.3
	Y	Z				
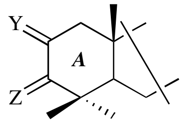	H, H	O	4.	56.5 (no inh.)	14.	17.9
	H, H	NOH			15.	225
	NOH	O	5.	(82.9)	16.	26.1 (46.8)
	2,4-diCl-C_6H_3-CH_2O-N	O			17.	nd (8)
	NOH	NOH	6.	(314)	18.	nd (22.3)
	CHOH	O	7.	(no inh.)	19.	nd (6.3)
	αOH, H	O			20.	(29)
	NOH	βOH, H			21.	28.2 (179)
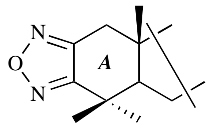			8.	66.3 (no inh.)	22.	11.2 (1002)
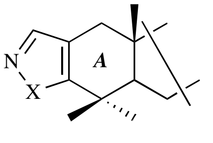			9.	40.4 (72.9) (X = NH)	23.	12.7 (19.6) (X = O)

and 19, resp.). Annelation of a heterocycle at the 2,3-positions of **UA** gave weaker inhibitors, while with **OA** this effect was not present (Entries 8, 9, and 22, 23, resp.).

Esterification of the C-28 carboxyl (Table **18**) resulted in varied influences on binding. In the **UA** series introduction of an ethoxycarbonylmethyl moiety gave a stronger inhibitor (Entry 4), while the same type of substitution produced an inactive compound in the **OA** series (Entry 15). Analogous esterification of **MA** strengthened the inhibition (Entry 20) contrary to **CA** (Entry 8), and a four-fold increase could be achieved by introducing an ω-bromobutyl group in the **MA** series (Entries 18 and 23, resp.).

Modifications in ring *A* of corosolic acid (**CA**) (Table **19**) concerning the stereochemistry of the 2,3-dihydroxyl moiety weakened the binding in both the free acid and the benzylester series (compare Entries 1-3 and 5-7, respectively). Oxidation of both hydroxyls to a diketone made the best inhibitor among the benzylated derivatives (Entry 8). Esterification in

Table 18. C-28 Carboxylic Esters of Pentacyclic Triterpenoids as Inhibitors of RMGPa [130-134] (IC_{50} [μM])

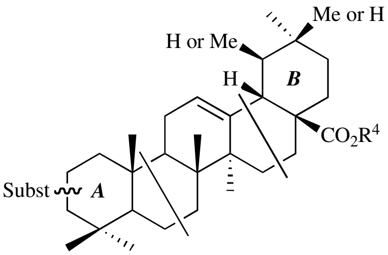

	R^4	Entry	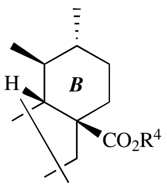	Entry	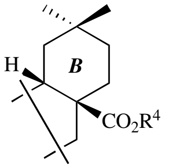
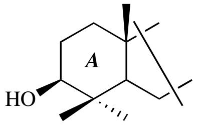	H	1.	9 (**UA**)	12.	14 (**OA**)
	Et	2.	911	13.	no inh.
	Allyl	3.	no inh.	14.	no inh.
	CH_2CO_2Et	4.	4.1	15.	no inh.
	CH_2CO_2H	5.	188	16.	62.6
	$CH_2CH_2NHCH_3$			17.	53.2
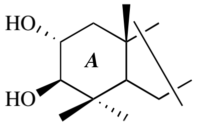	H	6.	20 (**CA**)	18.	28 (**MA**)
	CH_3	7.	34	19.	393
	CH_2CO_2Et	8.	102	20.	19
	CH_2CO_2H	9.	no inh.	21.	1651
	$(CH_2)_2Br$			22.	50
	$(CH_2)_4Br$			23.	7
	Ac_4-β-D-Glc_p	10.	373		
	β-D-Glc_p	11.	106		

general was also not beneficial for the inhibition (Entries 9-15), however, a mono-heptanoyl or -benzoyl derivative in the 2-position exhibited low micromolar binding (Entries 16 and 17, respectively).

Based on docking studies it was suggested [132] that these triterpene derivatives might occupy the inhibitor site, however, protein crystallography of the RMGPb–complex revealed binding at the AMP-site [135]. The crystal structures of the RMGPb-maslinic acid and RMGPb-asiatic acid complexes demonstrated that both maslinic acid (**MA** in Scheme **9**) and asiatic acid (Fig. **14**) bind at the allosteric activator site, where they partially overlap with the position of AMP. The contacts from maslinic acid to RMGPb include ionic interactions from the carboxylate group to the Arg310 of the allosteric phosphate-recognition subsite, and also nonpolar van der Waals interactions to Tyr75, Phe196, and Val45' (from the symmetry related subunit).

Isolated from the cultured broth of a fungal strain No. 13835, FR258900 was shown to inhibit HLGPa [136]. The compound proved effective in lowering plasma glucose levels in animal models of diabetes [137]. The structure of the co-crystallised GPb-FR258900 complex [138], determined to 2.2 Å resolution, revealed that FR258900 binds at the allosteric site where the natural allosteric activator AMP, and the natural allosteric inhibitor Glc-6-P bind. The inhibitor has no structural similarity to these natural regulators of GP. The contacts from FR258900 to the enzyme are dominated by nonpolar van der Waals interactions to Gln71, Gln72, Phe196, and Val45′ (from the symmetry related subunit), and also by ionic interactions from the carboxylate groups to the three arginine residues (Arg242, Arg309, and Arg310) that form the allosteric phosphate-recognition subsite.

The allosteric site can accommodate diverse structures such as acyl ureas, phthalic acid derivatives, dihydropyridine

Table 19. Effects of Modifications in Ring *A* of Corosolic Acid (CA) on the Inhibition of RMGPa [131]

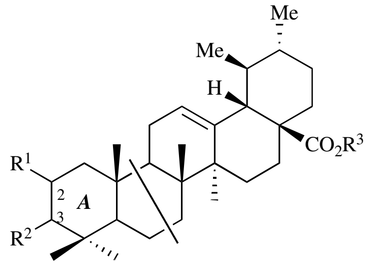
Me
Me
H
CO_2R^3
R^1
2
3
A
R^2

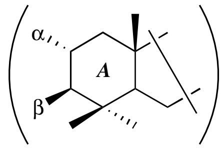

Entry	R^1	R^2	R^3	IC$_{50}$ [μM]
1.	α-OH	β-OH	H	20
2.	α-OH	α-OH	H	212
3.	β-OH	β-OH	H	115
4.	α-OH	=O	Bn	32
5.	α-OH	β-OH	Bn	41
6.	α-OH	α-OH	Bn	323
7.	β-OH	β-OH	Bn	108
8.	=O	=O	Bn	7.3
9.	α-$OCOCH_3$	β-$OCOCH_3$	H	35
10.	α-$OCOCH_2CH_3$	β-$OCOCH_2CH_3$	H	74
11.	α-$OCO(CH_2)_2CH_3$	β-$OCO(CH_2)_2CH_3$	H	79
12.	α-$OCO(CH_2)_2COOH$	β-$OCO(CH_2)_2COOH$	H	no inh.
13.	α-$OCOCH_3$	β-OH	H	38
14.	α-$OCOCH_2CH_3$	β-OH	H	97
15.	α-$OCO(CH_2)_2CH_3$	β-OH	H	78
16.	α-$OCO(CH_2)_4CH_3$	β-OH	H	3.3
17.	α-$OCOC_6H_5$	β-OH	H	5.1

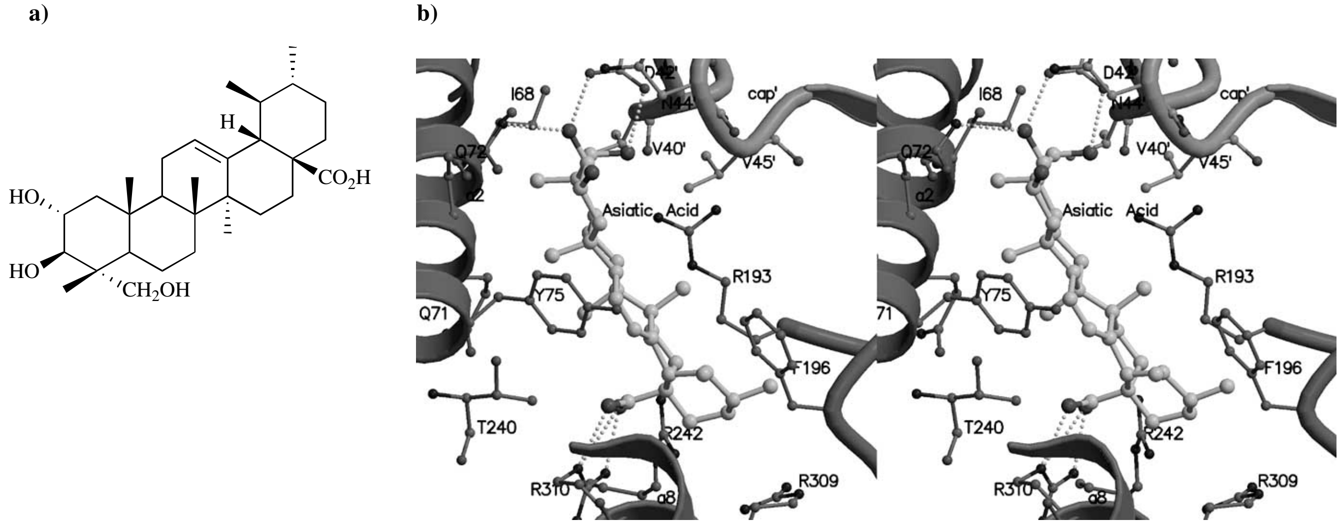
a)
H
CO_2H
HO
HO
CH_2OH
b)
I68
D42'
N44'
cap'
Q72
α2
V40'
V45'
Asiatic Acid
R193
Y75
Q71
F196
T240
R242
R310
α8
R309

Fig. (14). Structure of asiatic acid (**AA**) (**a**), and interactions between asiatic acid and GPb at the allosteric site (**b**), based on PDB code 2QN1.

diacids, triterpenoids, and FR258900 surveyed in this review. It is difficult to make similarity based comparisons of these types of compounds, therefore, each class may serve as a lead for further inhibitor design.

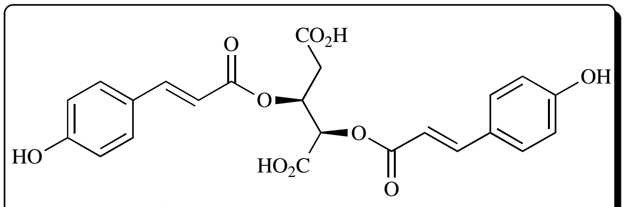
FR258900
IC_{50} = 2.5 μM with HLGPa [136]
K_i = 0.46 μM with RMGPb [138]

New Allosteric Site

The new allosteric (or indole) binding site, located inside the central cavity of the dimeric enzyme, is formed on association of the two subunits; the central cavity is partially closed at one end by residues from the cap' region and α2 helices (Arg33, His34, Arg60 and Asp61 and their symmetry related equivalents) and at the other end by the α7 tower helices (residues Asn270, Glu273, Ser276 and their symmetry-related equivalents). The new allosteric site was discovered from crystallographic studies of the binding of indolecarboxamide **70** and related synthetic counterparts like **71**, **72** [126] and **73**, **73a** [139]. The CP320626 (**72**) binding site in the central cavity is some 15 Å from the allosteric effector site, 33 Å from the catalytic site and 37 Å from the inhibitor site. The 18 amino acid residues (9 from each subunit) implicated in CP320626 binding to RMGPb are highly conserved in human muscle, human liver, human brain, rat muscle, rat liver and rat brain GPs [140]; with the exception of Ala192 (which is serine in the human liver isoenzyme), a total of 17 residues that come in close contact with CP320626 are identical in rabbit muscle and human liver phosphorylases (Fig. **15**).

Inhibitors **74** and **75** also recognized by HTS show strong relationship to the indole-carboxamides. The similarities allow consideration of these derivatives as general *N*-aroylglycylamides (*N*-aroyl phenylalanylamide if aAr^2 = CH_2Ph) shown in **75a**. Further derivatives were designed by changing Ar^1, omitting aAr^2, or translocating bond c to b.

The syntheses for such derivatives are summarized in Scheme **10**. Carboxylic acids of halogenated thieno[3,2-b]pyrroles **83** and thieno[2,3-b]pyrroles **84** were obtained from the corresponding thiophene carboxylic acids **77** or, alternatively for **83**, from vinylazide **80**. A series of substituted indole-2-carboxylic acids **89** was obtained from anilines **85**. Under standard amide coupling conditions acids **83**, **84**, **89**, and glycyl(or phenylalanyl)amides **86** gave compounds **87**. Amino quinolones **92** were prepared in multistep transformations from *N*-protected phenylalanine **94** or *N*-protected phosphonoglycinate **90**. Seven-membered amino lactames **93** were obtained from a commercial starting compound (**93** R^7 = H) by manipulations similar to those for **91**

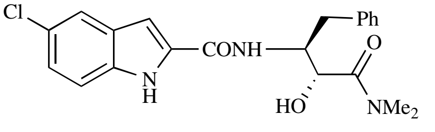 **70** CP-91149 [141] IC_{50} 0.13 μM HLGPa	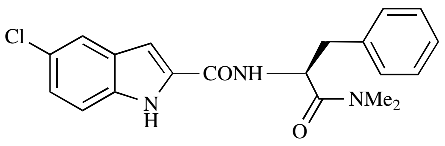 **71** IC_{50} 0.082 μM HLGPa [142]
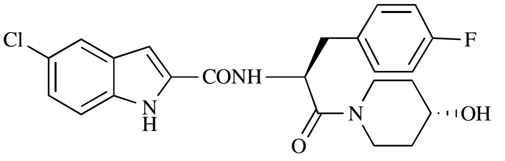 **72** CP320626 [142] IC_{50} 0.2 μM HLGPa, 0.083 μM HMGPa	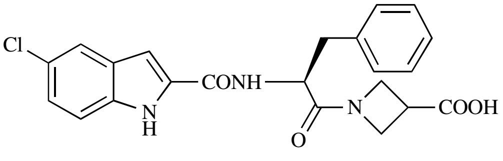 **73** CP403700 [139] IC_{50} 0.045 μM HLGPa
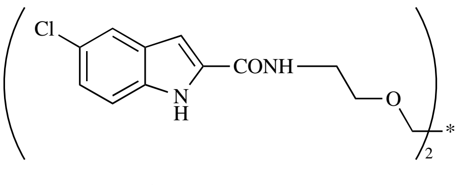 **73a** CP-526423 [139] IC_{50} 0.006 μM HLGPa	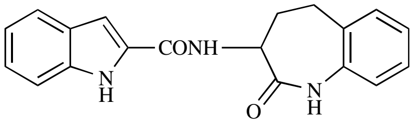 **74** IC_{50} 1.06 μM HLGPa, 2.44 μM HMGPa [143]
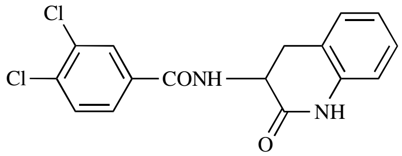 **75** IC_{50} 1.37 μM HLGPa, 2.31 μM HMGPa [143]	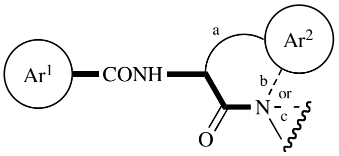 **75a**

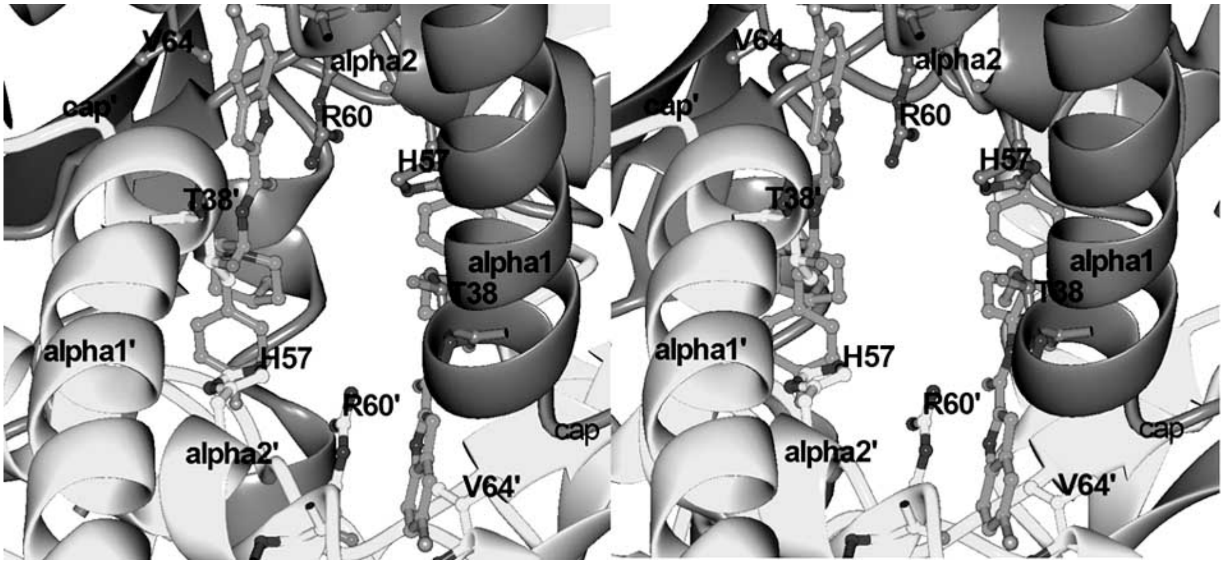

Fig. (15). Binding of CP320626 (**72**) to the new allosteric binding site. The CP320626 binding pocket is formed by residues of the α2 helix (47-78), the cap region (36-47), the 11-residues loop 180-190, and the β7 strand (191-193) from each subunit [144]. Based on PDB code 1H5U.

and **92**. Standard amide couplings of **92** and **93** with acids **83**, **83**, and **89** gave compounds **88**.

SAR for the Ar^1 = indole compounds was investigated with dihydroquinolones (selected examples shown in Table **20**, Entries 10-15) and showed the superiority of 5-substituted-indole derivatives among them 5-chlorides and 5-bromides being the best. All other substituents (Scheme **10**, R^3 in **89**) tested gave worse *in vitro* results.

Further changes in the Ar^1 group are compiled in Table **21**. Thienopyrroles of both annelation type (Entries 2 and 6) are poor inhibitors, however, mono- or dichlorination (Entries 3 and 9, resp.) makes better inhibitors than the 5-chloroindol derivative (Entry 1). Bromination had varying effects (Entries 5 and 10).

Translocation of a bond of the amide nitrogen to the Ar^2 moiety (turning from bond c to b in **75a**) may result in a rigidification of that part of the molecule. This was investigated by applying each efficient Ar^1 residues (Table **20**). Among the 5-chloroindole derivatives the six-membered lactames were more efficient than the seven-membered ones (compare Entries 7 and 9), and *R* configuration was better than *S* (compare Entries 7 and 8). Methyl substitution of the quinolone nitrogen had no significant effect either with 5-chlorine or 5-bromine (Entries 12, 13), however, hydroxyalkyl groups were beneficial for the cell efficiency (Entries 16, 17). This was further enhanced in the thienopyrrole series (compare Entries 1, 2 and 5, 6). Thienopyrrole compound shown in Entry 18 had the best pharmacokinetic profile and in a glucagon challenge model test in Zucker rats lowered blood glucose increase by 46 %.

Indane derivatives (Entries 3, 4) were similarly active with the dichloro thieno[3,2-b]pyrrole system but were much less efficient in combination with the chloro thieno[2,3-b]pyrrole ring system.

Turning to glycinamides from the phenylalanine derivatives offered the advantage of achirality as well as diminished hydrophobicity. By maintaining the 5-chloroindole group variations in *N*-substituents of the terminal amide were investigated (Table **22**). Keeping an *N*-methyl group constant (Entries 1-4) the cyclopentyl derivative proved the best. In the next series with the cyclopentyl as a constant substituent (Entries 5-8), 2-hydroxypropyl derivative (Entry 5) gave the best *in vitro* result but the 2-hydroxyethyl compound (Entry 8) performed better in the cellular assay. Therefore, this was chosen to be kept constant for further analog design and it was shown that a broad variety of saturated and aromatic carbo- and heterocycles and alkyl groups showed good enzymatic activity (Entries 9-12). In the cell-based assay the phenyl derivative in Entry 12 proved the most efficient.

GPa docking calculations were performed [148] for a set of 25 indole-2-carboxamide inhibitors [142] employing the Lamarckian Genetic Algorithm (LGA) of the AutoDock 3.0 program [149, 150]. The receptor from the crystal structure of HLGPa–CP403700 (PDB entry 1EXV [139]) was used. Predictive 3D-QSAR models using both CoMFA and CoMSIA methods were derived directly from the alignment conformations of the docked ligands in the receptor cavity. Good correlation (r^2 = 0.710) between the ligand docking scores and their experimental activities ($-\log IC_{50}$) was obtained, giving added credibility to the docked ligand binding conformations. From the docking results, it was estimated that the average electrostatic contribution to ligand binding was just ~ 6.1%, non-electrostatic interaction therefore dominating in agreement with hydrophobic nature of the new allosteric site binding pocket [139]. The major objective of the CoMFA and CoMSIA analyses was to obtain better predictive models. For a training set of 21 ligands, a CoMFA model with $r^2 = 0.996$ and cross validated r^2 (q^2) = 0.697, and COMSIA model with $r^2 = 0.965$ and $q^2 = 0.622$ were derived, with the predictive ability of both models validated by application to an external test set of 4 ligands not included in the original models. The quality of the results indicate that these models can be exploited for new indole-2-carboxamide inhibitors design. Similar binding conformations of the

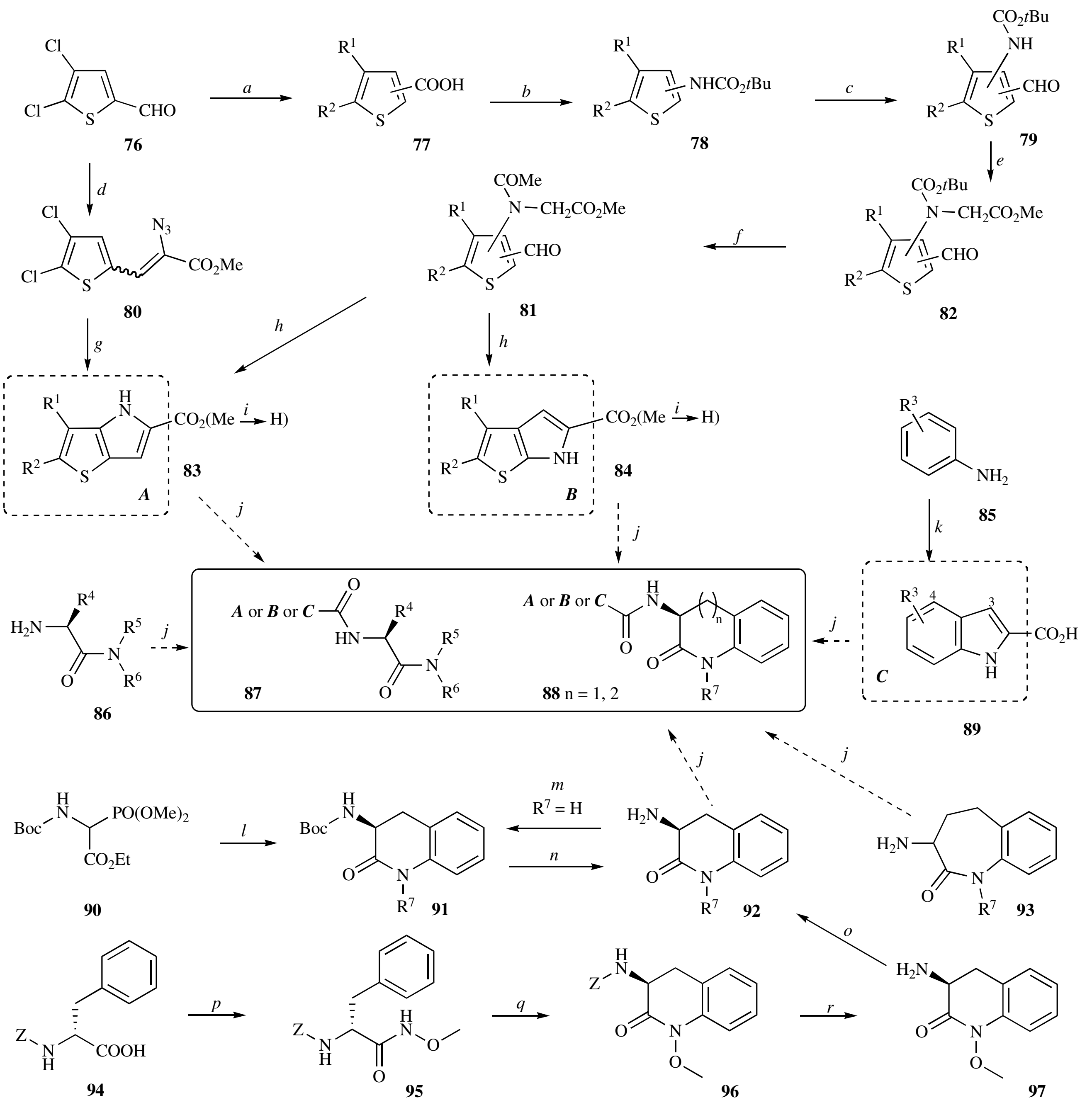

R^1 = H, Cl, Br

R^2 = H, Cl, Br

R^3 = (indole numbering in **89**) = H, 4-Cl, 5-Cl, -Br, -F, -Me, -Et, -OMe, -CN, $-CF_3$, -Ph, -COOMe, 6-Cl, -Ph, 7-Cl, $-NO_2$, $-NH_2$, 4-COOMe–5-Cl, 5-Cl–6-COOMe, 5-Cl–7-F

R^4 = H, CH_2Ph

R^5 = Me, CH_2CH_2OH, cyclopentyl

R^6 = C_{1-4} alkyl and isoalkyl, C_{3-10} cycloalkyl, Ph, aralkyl, heteroaryl and hetarylalkyl, $(CH_2)_{2-3}NH_2$ and *N*-substituted derivatives, $(CH_2)_{2-3}OH$ and Me, *i*Pr, Ph ether derivatives, CH_2CH_2CN, CH_2CONH_2, CH_2COOEt, $CH[(CH_2)_2]_2SO_2$, $CH[(CH_2)_2]_2O$

R^7= H, Me, CH_2CH_2OH, CH_2CH_2OMe, CH_2COOH, CH_2CONH_2 and *N*-substituted derivatives, CH_2CN, CH_2CH_2SMe and oxidized derivatives, $CH_2CH(OH)CH_2OH$

Scheme 10. *a*) $KMnO_4$, NaOH, 50 ºC; *b*) DPPA, Et_3N, *t*BuOH, reflux; *c*) *n*BuLi, THF, DMF, –78 ºC to r. t.; *d*) $MeO_2CCH_2N_3$, NaOMe, MeOH; *e*) $BrCH_2CO_2Me$, $KHCO_3$, DMF, 60 ºC; *f*) AcOH, Ac_2O, 120 ºC; *g*) $PhCH_3$, reflux; *h*) K_2CO_3, DMF, 60 ºC; *i*) LiOH, MeOH, H_2O; *j*) standard amide coupling conditions; *k*) 1. Ag_2SO_4, I_2, EtOH, r. t., 2. pyruvic acid, DABCO, $Pd(OAc)_2$, DMF, 105 ºC; *l*) 1. 2-nitrobenzaldehyde, NaH, THF, 0 ºC to r. t., 2. Pd/C, MeOH, H_2 (40 psi) than EtOAc, reflux; *m*) 1. $(Boc)_2O$, DCM, 2. NaO*t*Bu, R^7-X, DMF, r. t.; *n*) AcCl, MeOH, 50 ºC; *o*) EtOH/ water (1:1), 2 M HCl to pH 3, H_2, 10 % Pd/C, 3 bar, 25 ºC; *p*) $CH_3ONH_2{\cdot}HCl$, Et_3N (2 eq), EDAC, HOBt, DMF, r. t.; *q*) 1. DCM, argon 0 ºC, TFA (2.7 eq), 2. $(CF_3CO_2)IPh$ (1.05 eq), excess aq Na_2CO_3; *r*) H_2, 10 % Pd/C, 1 bar, EtOAc.

Table 20. Indole-2- and Thienopyrrol-carboxamide Derivatives as Inhibitors of GP (IC_{50} [µM])

Entry	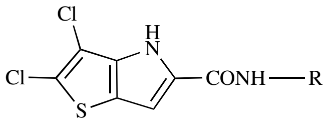 R		HLGPa	Cell	Ref.
1.	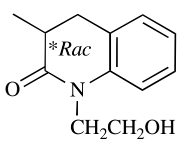		0.007	0.6	[145]
2.	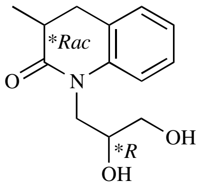		0.002	0.26	
3.	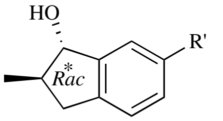	R' = H	0.009	1.5	[146]
4.		R' = F	0.049	1.3	

Entry	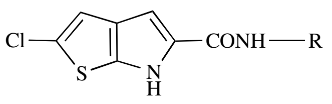 R	HLGPa	Cell	Ref.
5.	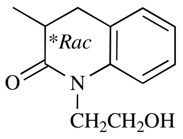	0.026	0.79	[145]
6.	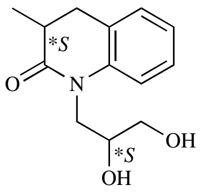	0.012	-	

Entry	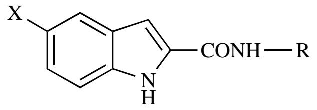 X	R	HLGPa	HMGPa	Ref.
7.	Cl	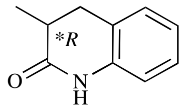	0.025	0.014	[143]
8.	Cl	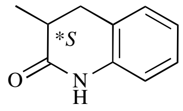	0.047	0.039	
9.	Cl	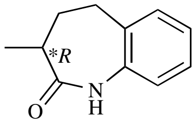	0.099	0.083	
10.	H	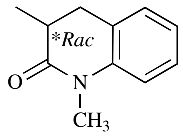	0.16	0.056	[143]
11.	F		0.12	0.089	
12.	Cl		0.025	0.032	
13.	Br		0.030	0.073	
14.	Me		0.12	0.098	
15.	CN		0.18	0.11	
				Cell	
16.	Cl	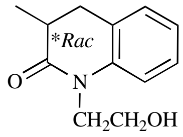	0.017	4.0	[145]
17.	Cl	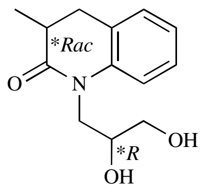	0.044	1.3	

Entry			
18.	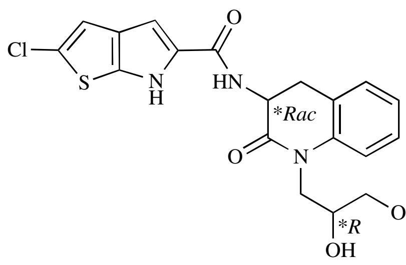	HLGPa 0.029 Cell 1.1	[145]

Table 21. Comparison of Effects of the Ar^1 Aromatic Moiety in *N*-acyl-phenylalanylamides(IC$_{50}$ [μM], HLGPa)

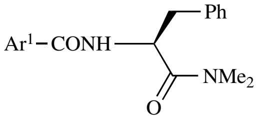

Entry	Ar^1				Ref.
1.	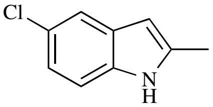			0.082	[142]
				0.051	[146]
		R^1	R^2		
2.	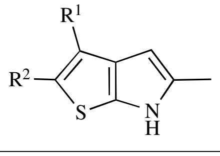	H	H	2.31	[146]
3.		H	Cl	0.017	
4.		H	Br	0.031	
5.		Br	Br	20 % at 10 μM	
6.	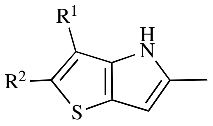	H	H	35 % at 100 μM	[146]
7.		H	Cl	0.577	
8.		Cl	H	0.390	
9.		Cl	Cl	0.005	
10.		Br	Br	0.023	

ligands reveal that they interact with HLGPa in a very similar way, but suggestions for improvement of affinities can be extracted from the 3D-QSAR models.

Docking and 3D-QSAR analysis have also been performed [151] on the same series of indole-2-carboxamide derivatives [142] to quantitatively correlate variations in structure and physiochemical properties of the ligands with their *in vitro* HLGPa activities. The data set of 25 ligands was divided into a training set of 20, each member selected by clustering of molecules based on the Euclidean distances between descriptors for the molecules, and a test set of 5. Training set selection was performed in this methodical manner so as to compensate for deficiencies in the limited size of the data set. However, a different approach to that used in ref [148] was applied: 3D-QSAR CoMFA/CoMSIA models for the GPa inhibitors were derived using pharmacophoric alignment and the HIPHOP module of Catalyst 4.5 [152]. The final CoMFA model was assessed for complementarity with the active site of GPa by rigid docking to the HPGPa enzyme receptor in complex with CP320626 (PDB entry 1LWO [153]) using InsightII [154] and LUDI [155, 156] scoring functions. More specifically, the common feature pharmacaphore aligned conformers were manually docked into the active site by superimposing them onto CP320626. The pharmacophoric model (hypothesis) consisted of four features: hydrophobic, hydrogen bond donor, hydrogen bond acceptor and ring aromatic, and its mapping to CP320626 corresponded well to the major interactions between the ligand and GPa enzyme. The CoMFA model yielded quality statistics for both the training (r^2 = 0.98, q^2 = 0.68) and test sets (r^2 = 0.85) but for the docking calculations, in contrast to the other approach outlined above [148], the correlation between docking scores and ligand binding affinities was not so reasonable (r^2 = 0.57, compare r^2 = 0.71 in reference [148]). Errors introduced by rigid-body docking, the scoring function and docking to a monomer GPa receptor (it is not clear whether the dimer was generated for docking by symmetric operations) from the GPa-CP320626 (PDB entry 1LWO [153]) complex all have to be considered in this regard.

In summary, extensive efforts were made to improve inhibition by compounds occupying the new allosteric site. The original indolcarboxamides were replaced by thienopyrrol derivatives, and rigidification of the original stuctures was also acheived by quinolones. Glycinamide surrogates were made to replace phenylalanylamides. In these series of compounds the inhibitory efficiency remained in the low nanomolar range.

Inhibitors with Unknown Binding Mode

3-Anilino-quinoxalinone (Table **23**, Entry 1) was identified as a new lead by high throughput screening and pharmacophore based electronic database searching. In order to test changes in the imidazole portion, the substituents of the homoaromatic ring and at *N*-1 of the quinoxaline, as well as in the 4-position of the aniline moiety, a series of compounds were prepared as outlined in Scheme **11**. Diamino benzene (or pyridine) derivatives **100**, either commercially available or obtained from **98** *via* **99**, were ring-closed to **101** which was chlorinated to give **102**. This was substituted by various aniline derivatives to yield **103**, **105**, and **107** suitable to build up further appendages. Thus **103** was directly linked to heterocycles by a palladium-catalyzed cross coupling to give **104**; **105** was acylated to amide linked heterocyclic deriva-

Table 22. Glycinamides as Inhibitors of GP [147] (IC$_{50}$ [μM])

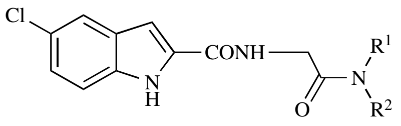

Entry	R^1	R^2	HLGPa	SK-Hep
1.	CH_3	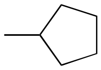	0.055	1.7
2.		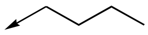	0.150	1.4
3.		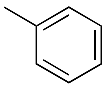	0.210	7.1
4.		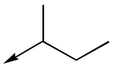	0.230	0.62
5.	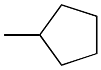	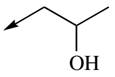	0.016	1.3
6.		$-CH_2CN$	0.030	0.68
7.		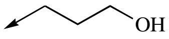	0.042	0.76
8.		$-(CH_2)_2OH$	0.057	0.14
9.	$-(CH_2)_2OH$	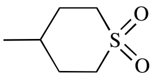	0.012	>30
10.		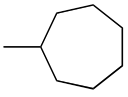	0.030	2.3
11.		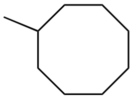	0.32	12
12.		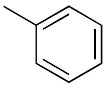	0.12	0.27

tives **106**, and the reversed amide linkage of **108** was obtained by amidation of **107**.

Change of imidazole directly linked to aniline by directly bound 2-pyrrolyl or 3-furyl or through NHCO-linked 2-pyrrolyl (not shown) and 2-furyl groups (Table **23**, Entry 2) gave no better inhibitors. However, amide linked isoxazoles (Entries 3, 4) proved much better, and a reversal of the amide group brought about a further improvement (compare Entries 3 and 5, 6). Inserting a methylene bridge between the amide nitrogen and the heterocycle gave inhibitors of similar efficiency (Entries 7, 8) but a dimethylene linker resulted in loss of activity (Enty 9). Changes in the quinoxaline part were investigated with the 2-thienylmethyl derivatives (Entries 10-18). Removal of the *N*-methyl group or substitutions in the phenyl part in the quinoxaline resulted in no significant change of activity (compare Entry 8 to 10-12). Replacement of the *N*-methyl group by ethyl had no influence on the inhibition (Entries 8 and 13) while larger or more polar substituents (Entries 14-17) weakened the effect. Introduction of a further nitrogen into the quinoxalin part also gave a good inhibitor (Entry 18). The compounds failed in cellular assays most probably due to poor bioavalibility.

Identified by high-throughput screening an amide derivative of 3,4-dichloro-cynnamic acid (Table **24**, Entry 1) was

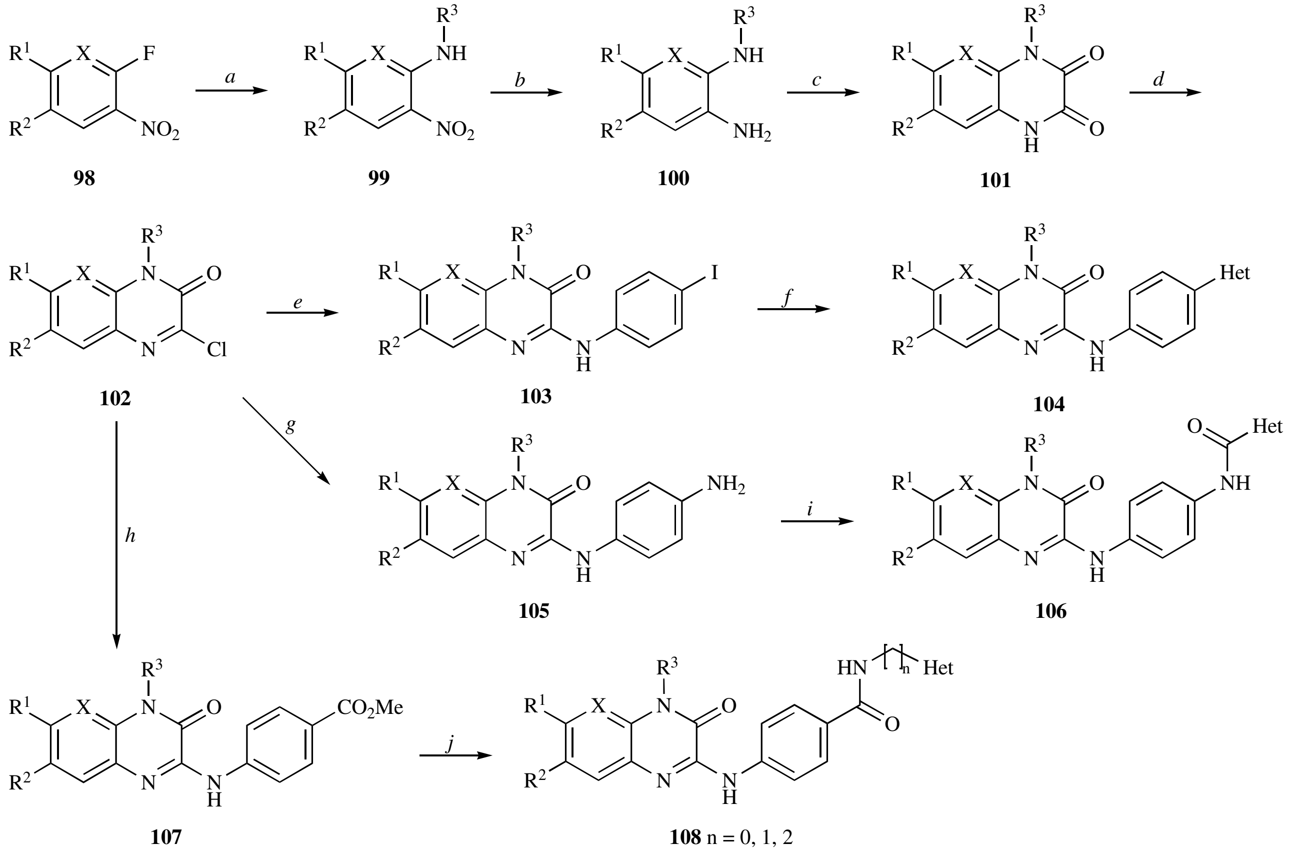

R^1 = H, CH_3; R^2 = H, F; R^3 = H, Me, Et, *i*Pr, CH_2CH_2OH, CH_2CO_2H, $CH_2CH_2NMe_2$, CH_2CH_2-2-pyridine, CH_2CH_2-*N*-piperidine, CH_2CH_2-*N*-morpholine; X = CH, N.

Het = furan, thiophene, pyrrole, pyrazole, thiazole, isoxazole, pyrazine

Scheme 11. *a*) R^3NH_2, NaOAc, 80 ºC, *b*) H_2 (50 psi), 10 % Pd/C, EtOH; *c*) $Cl(CO)CO_2Et$, Et_3N, CH_2Cl_2 or $(CO_2Et)_2$, r. t.; *d*) $POCl_3$, Hünig base, $PhCH_3$, 110 ºC or $POCl_3$, DMF, 95 ºC; *e*) H_2N-C_6H_4-I, CH_3CN, 80 ºC; *f*) Het-$B(OH)_2$, $Pd(PPh_3)_4$, 2N Na_2CO_3, DME, 90 ºC; *g*) H_2N-C_6H_4-NH_2, CH_3CN, 80 ºC; *h*) H_2N-C_6H_4-CO_2Me, CH_3CN, 80 ºC; *i*) Het-COCl, Et_3N, CH_2Cl_2, r. t.; *j*) Het-$(CH_2)_n$-NH_2, $AlMe_3$, $PhCH_3$, 120 ºC.

shown to have significant activity against HLGPa in the presence of glucose but was practically inactive without glucose [158]. This compound served as a lead to synthesize a variety of related propenamide derivatives. A solid phase synthetic methodology (Scheme **12**) was developed starting by attachment of ω-amino-alcohols to a resin-bound aldehyde **109** using reductive amination to give secondary amines **110**. Acylation by a carbodiimide-mediated protocol gave the expected **112** with phenylpropenoic acids, while with benzoic acids 15-20 % of diacylated **113** was also obtained. Alkanoic acids furnished only type **114** compounds, which could be selectively *O*-deacylated to **112** by basic treatment. Alcohol **112** was tosylated to **114** and then reacted with a cyclic amine to give **111**. Compounds **111** were transformed into ureas by isocyanates followed by cleavage from the resin to yield compounds **115**. Reactions of **111** with acyl and sulfonyl chlorides and isothiocyanates were also carried out (not shown).

Extensive SAR investigations revealed that replacement of the phenyl-urea part by phenylamide, sulfonamide, and thiourea, changing the aryl group on the urea by hydrogen, heteroaryl, and diverse alkyl groups, as well as substitutions on the phenyl ring by electron releasing groups gave ineffective (IC_{50} >20 μM) derivatives. 3,4-Dihalogeno substitution proved very efficient both in piperazines and homopiperazines (Table **24**, Entries 1, 2, and 5, 6, resp.), and was superior to monochloro substitution either in position 3 or 4 in both series (Entries 3, 4, and 7, 8). The effect of the heterocyclic ring size seemed not very important with a 5-carbon spacer (Entries 1, 2, and 5, 6), but was more pronounced in case of 4- and 6-membered chains (Entries 11, 15, and 13, 17). Saturation of the double bond in the cinnamoyl moiety to $–CH_2CH_2–$, its replacement by a cyclopropyl ring, or total removal to form a benzamide derivative, as well as various substitutions in the phenyl ring instead of the 3,4-dichloro pattern gave inactive compounds.

A large series of bicyclic sugar derivatives [159] **118** (Scheme **13**) was obtained by reductive amination of sugar aldehydes **116** by β-amino esters **117**. Reduction of the ester group gave amino alcohols **119**. Although the number of the investigated compounds does not allow a meaningful SAR to be discussed, significant inhibition of RLGP was observed by alcohols rather than with esters (Table **25**, Entries 2 and 4, 3 and 5, as well as 8).

Several natural flavonoid derivatives (flavones, flavonols, flavanones, isoflavones, catechins, and anthocyanidines) were investigated as inhibitors of RMGP (the most efficient compounds are shown in Table **26**) [160]. Satura-

Table 23. 3-Anilino-Quinoxalinones as Inhibitors of RMGPb [157]

<table>
<tr><th>Entry</th><th colspan="6">Compound</th><th>IC$_{50}$ [μM]</th></tr>
<tr><td>1.</td><td colspan="6">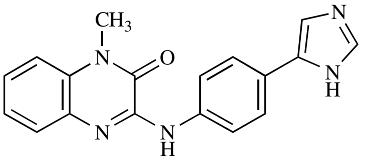</td><td>2.5</td></tr>
<tr><td></td><td colspan="3" rowspan="4">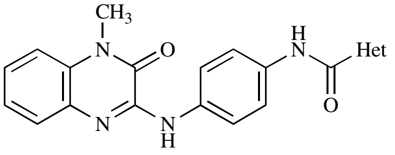</td><td colspan="2">Het</td><td>n</td><td></td></tr>
<tr><td>2.</td><td>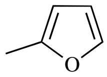</td><td>2-furyl</td><td>-</td><td>2.5</td></tr>
<tr><td>3.</td><td>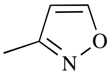</td><td>3-isoxazolyl</td><td>-</td><td>0.73</td></tr>
<tr><td>4.</td><td>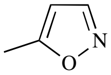</td><td>5-isoxazolyl</td><td>-</td><td>0.71</td></tr>
<tr><td>5.</td><td colspan="3" rowspan="5">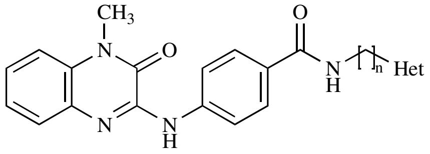</td><td></td><td>3-isoxazolyl</td><td>0</td><td>0.11</td></tr>
<tr><td>6.</td><td>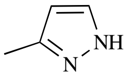</td><td>3-pyrazolyl</td><td>0</td><td>0.2</td></tr>
<tr><td>7.</td><td></td><td>2-furyl</td><td>1</td><td>0.12</td></tr>
<tr><td>8.</td><td>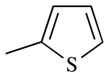</td><td>2-thienyl</td><td>1</td><td>0.11</td></tr>
<tr><td>9.</td><td></td><td>2-thienyl</td><td>2</td><td>>10</td></tr>
<tr><td></td><td colspan="3">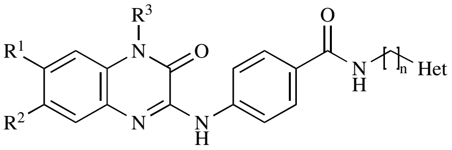</td><td></td><td></td><td></td><td></td></tr>
<tr><td></td><td>R^1</td><td>R^2</td><td>R^3</td><td></td><td></td><td></td><td></td></tr>
<tr><td>10.</td><td>H</td><td>H</td><td>H</td><td rowspan="9"></td><td rowspan="9">2-thienyl</td><td rowspan="9">1</td><td>0.16</td></tr>
<tr><td>11.</td><td>H</td><td>F</td><td>CH_3</td><td>0.14</td></tr>
<tr><td>12.</td><td>CH_3</td><td>H</td><td>CH_3</td><td>0.28</td></tr>
<tr><td>13.</td><td>H</td><td>H</td><td>CH_2CH_3</td><td>0.12</td></tr>
<tr><td>14.</td><td>H</td><td>H</td><td>$CH(CH_3)_2$</td><td>>10</td></tr>
<tr><td>15.</td><td>H</td><td>H</td><td>CH_2CH_2OH</td><td>0.32</td></tr>
<tr><td>16.</td><td>H</td><td>H</td><td>CH_2CO_2H</td><td>5.7</td></tr>
<tr><td>17.</td><td>H</td><td>H</td><td>$CH_2CH_2N(CH_3)_2$</td><td>0.71</td></tr>
<tr><td>18.</td><td colspan="3">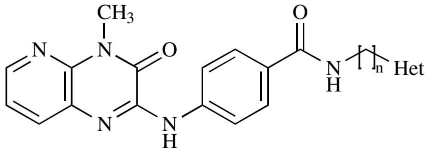</td><td>0.19</td></tr>
</table>

tion of the **C** ring resulted in loss of activity indicating that a completely planar structure is essential for the strong inhibition (compare 1. Quercetin and 3b). For potent inhibition of RMGPa vicinal hydroxyls at least in positions 3' and 4' of ring **B** are essential together with the presence of hydroxyl groups in positions 5 and 7 in ring **A**. Absence of the 3-OH slightly reduces inhibition. However, the considerable effect observed with a total lack of hydroxyls in ring **B** and the presence of three OH groups in ring **A** (see 2. Baicalein) may suggest a different binding mode to the enzyme. In the an-

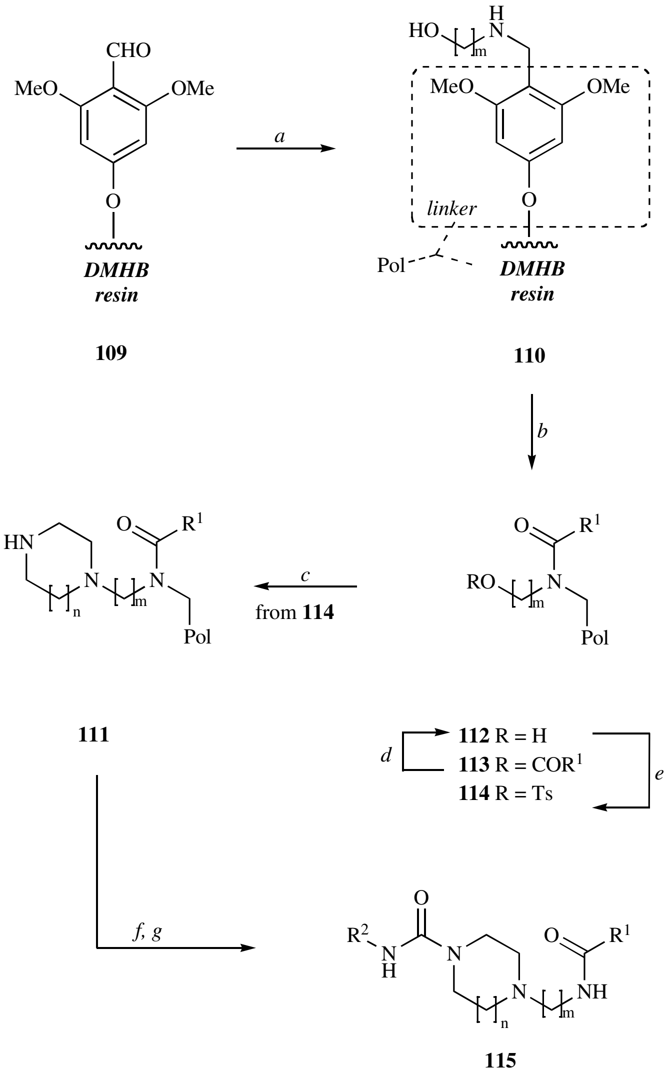
CHO
MeO
OMe
O
DMHB resin
109
a
HO
H
N
m
MeO
OMe
O
linker
Pol
DMHB resin
110
b
O
R1
RO
N
m
Pol
112 R = H
113 R = COR1
114 R = Ts
d
e
c
from 114
HN
O
R1
N
N
n
m
Pol
111
f, g
O
R2
N
H
N
O
R1
N
NH
n
m
115

Scheme 12. *a*) $NH_2(CH_2)_mOH$, 5 eq, $NaBH_3CN$, 10 eq, DCM, r. t.; *b*) 0.33 M R^1CO_2H, 0.4 M 1,3-diisopropylcarbodiimide, NMP, r. t.; *c*) piperazine (n = 1), 35 eq, satd solution in NMP, 80 ºC; *d*) base treatment; *e*) 0.33 M p-toluenesulfonyl chloride, 0.43 M pyridine, DCM, r. t.; *f*) 0.4 M R^2NCO, NMP, r. t.; *g*) 50% TFA/DCM, r. t.

Table 24. 3-Phenyl-2-propenamides as Inhibitors of HLGPa [158]

Compound	Entry	R^1	R^2	IC_{50} [μM]
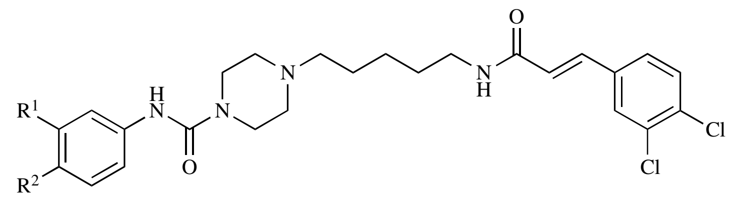 O N N H R1 H N N Cl O Cl R2	1.	Cl	Cl	0.94 (+glu) >20 (–glu)
	2.	Cl	F	0.98
	3.	Cl	H	51
	4.	H	Cl	100
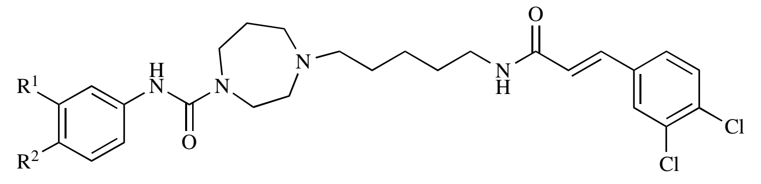 O N N H R1 H N N Cl O Cl R2	5.	Cl	Cl	0.47
	6.	Cl	F	0.72
	7.	Cl	H	1.3
	8.	H	Cl	51

(Table 24). Contd…..

Compound	Entry	n	m	IC$_{50}$ [μM]
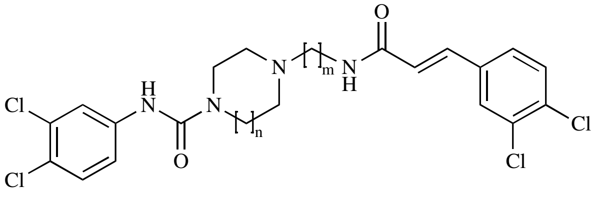 Cl Cl H N O N n N m N H O Cl Cl	9.	1	2	90
	10.	1	3	0.32
	11.	1	4	0.71
	12.	1	5	0.94
	13.	1	6	0.44
	14.	2	2	100
	15.	2	4	0.17
	16.	2	5	0.47
	17.	2	6	24

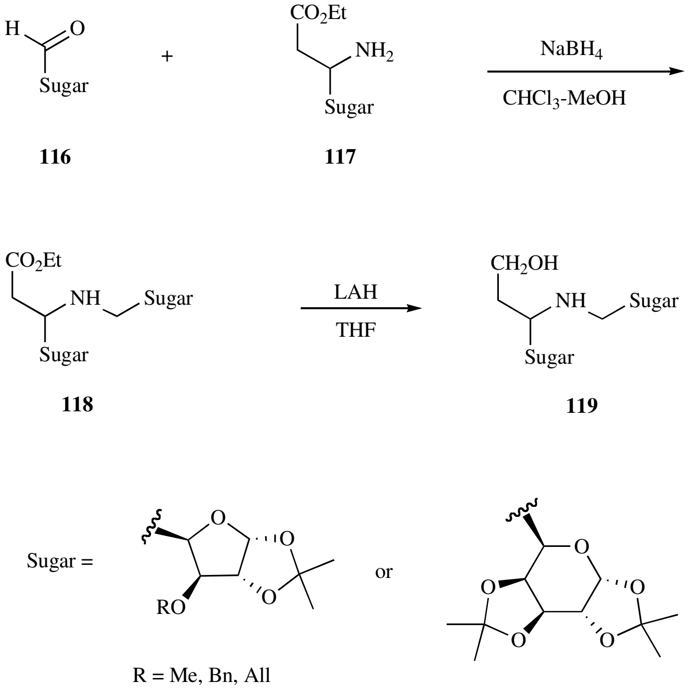

Scheme 13.

thocyanidine series similar effects of vicinal hydroxyls can be observed: 4. Cyanidin and 6. Delphinidin are effective but 5. Pelargonidin is a much weaker inhibitor. A 3'-OMe instead of OH results in significant weakening or loss of inhibitory activity in both series. Although the non-planar catechins are inactive (3b) the presence of a galloyl residue on the 3-OH makes a good inhibitor (3a). While gallic acid itself has no effect its formal dimer (7. Ellagic acid) is rather efficient. No information is available about the binding mode of these derivatives to the enzyme, however, because of the similarity to flavopiridol (cf. Table **12**, Entry 1) it might be possible that they bind to the purine inhibitor site.

A series of thiazolidine-2,4-diones attached to 2,3-dihydrobenzo[1,4]dioxin ring systems was prepared [161] (Scheme **14**) from hydroxyacetophenon derivatives **120** by allylation followed by oxidation of **122** to give the epoxidized Bayer-Villiger product **124**. Intramolecular nucleophilic attack on the epoxide by the phenolate liberated by basic treatment of **124** gave benzodioxins **125**. The corresponding methylenedioxy derivative **125** was obtained from **121** by formylation to **123**, and subsequent oxidation, ring closure, and reduction of the ester. Tosylation gave compounds **126** which were coupled to a phenolic aldehyde to furnish **127**. Final basic condensation to thiazolidine-2,4-dione produced test compounds **128**. Because of solubility problems only a few of the final series and the intermediates could be assayed with GP to show micromolar inhibitory potency (Table **27**).

Based on screening a larger collection of benzamide and related derivatives aminobenzamide (Table **28**, Entry 1), terephthalamide (Entry 6), and *N*-(thiazol-2-yl)acetamide (Entry 8) were selected as leads [162]. The first structure was modified by introducing substituents into the *N*-phenyl ring. To this end, 4,5-difluoro-2-nitrobenzoic acid (**129**) was transformed by standard methods to amides **130** which on coupling with 1-methyl-1H-imidazole-2-thiol to **131** and

Table 25. Sugar-derived β-amino esters and γ-amino alcohols as inhibitors of rat liver GP [159]

Entry	Compound	R^1	R^2	R^3	Inhibition (%) at 100 µg/mL
1.	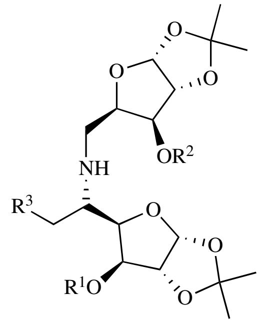	Bn	Me	CO_2Et	46
2.		Bn	All	CO_2Et	none
3.		All	Bn	CO_2Et	30
4.		Bn	All	CH_2OH	41
5.		All	Bn	CH_2OH	73
6.		All	Me	CH_2OH	5
7.	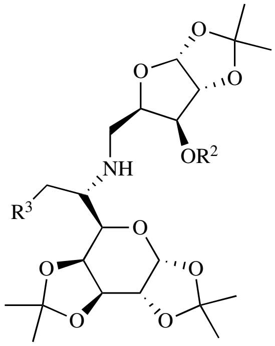	-	Me	CO_2Et	16
8.		-	All	CH_2OH	95
9.	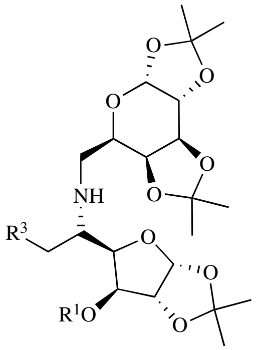	Bn	-	CH_2OH	19

Table 26. Natural Flavonoids as Inhibitiors of GP [160] (IC_{50} [µM])

Flavones, flavonols, and catechins	RMGPa	RMGPb	Anthocyanidines	RMGPa	RMGPb
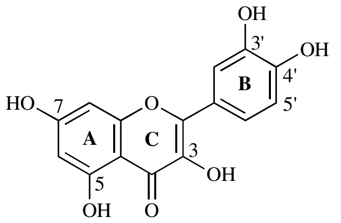 1. Quercetin	4.8	20.9	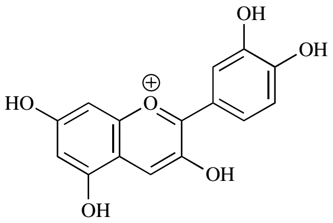 4. Cyanidin	3.0	9.0
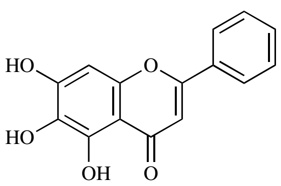 2. Baicalein	11.2	10.2	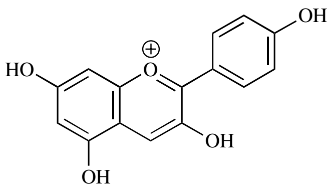 5. Pelargonidin	43.6	6.2

(Table 26). Contd…..

Flavones, flavonols, and catechins	RMGPa	RMGPb	Anthocyanidines	RMGPa	RMGPb
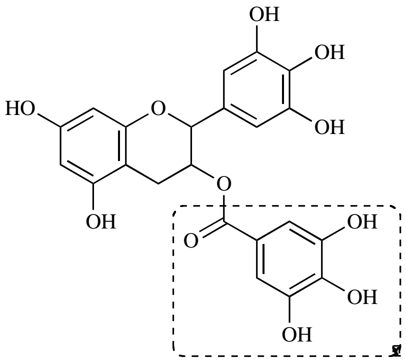 3a. Epigallocatechin-3-gallate 3b. No effect without the gallic acid moiety (highlighted)	7.7	33.9	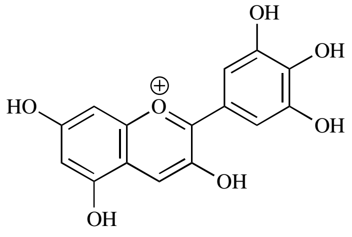 6. Delphinidin	3.1	10.7
			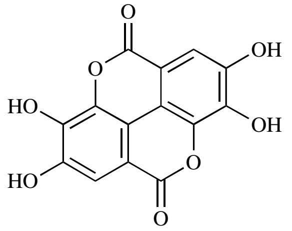 7. Ellagic acid	3.2	12.1

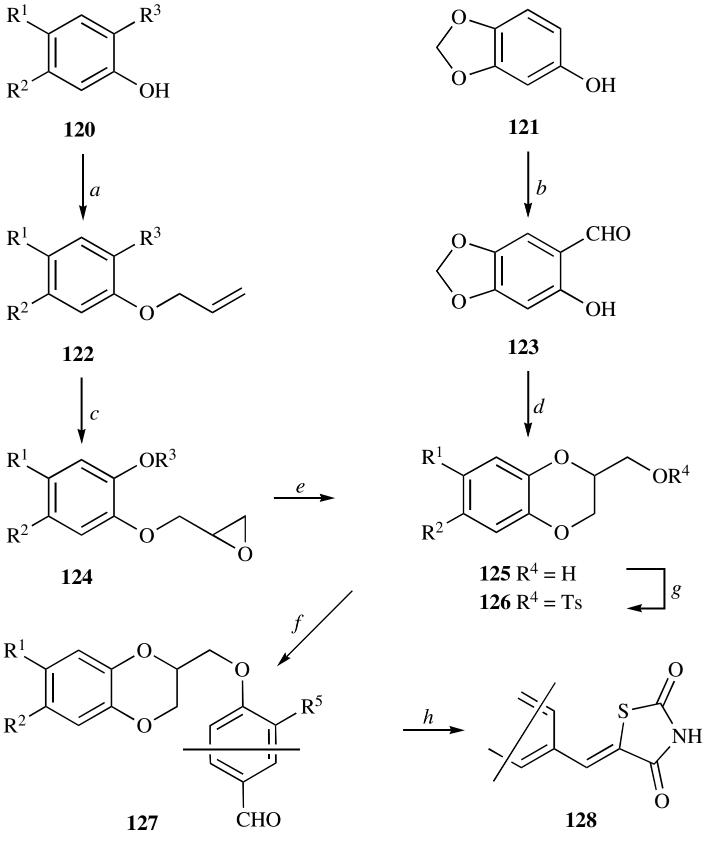

R^1 and/or R^2 = H, Br, OCH_2O; R^3 = $COCH_3$; R^5 = H, OMe.

Scheme 14. *a*) allyl bromide/K_2CO_3/DMF, 80 ºC; *b*) $(CHO)_n$, $MgCl_2/Et_3N$, THF, reflux; *c*) MCPBA/$CHCl_3$, reflux; ; *d*) (i) H_2O_2/Et_3N, 5 ºC; (ii) ethyl dibromopropionate, K_2CO_3/acetone, reflux; (iii) $LiAlH_4$/dry ether; *e*) NaOMe/MeOH, r. t.; *f*) 4-hydroxybenzaldehyde or vanillin or phenol/K_2CO_3/DMF, 80 ºC; *g*) 50 % TFA/CH_2Cl_2, r. t.; *g*) TsCl/pyridine, r. t.; *h*) thiazolidine-2,4-dione, NaOAc, 140 ºC.

subsequent reduction of the nitro group furnished test compounds **132** (Scheme **15**). From a collection of 15 compounds the 3-substituted derivatives (Table **28**, Entries 2-5) showed significantly stronger inhibition than the parent structure.

The terephthalamide modifications were made in the *N*-heterocyclic moieties, and these and analogous isophthalamides **134** were made from the corresponding acid chlorides **133** (Scheme **16**). Only a few variants of the *N*-(thiazol-2-yl)acetamide were made by reacting *N*-aryl-chloroacet-

Table 27. Inhibition of GP by 2,3-dihydrobenzo[1,4]dioxin Derivatives [161]

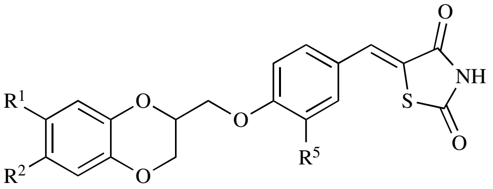

				K_i [μM]	
Entry	**R^1**	**R^2**	**R^5**	**RMGPb**	**RMGPa**
1.	Br	H	H	80	-
2.	Br	Br	H	12	10
3.	Br	Br	OMe	30	9

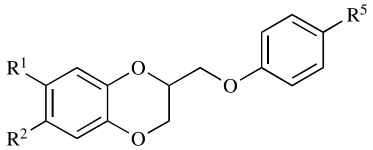

				IC_{50} [μM]	
4.	Br	Br	CHO	550	
5.	Br	Br	H	560	

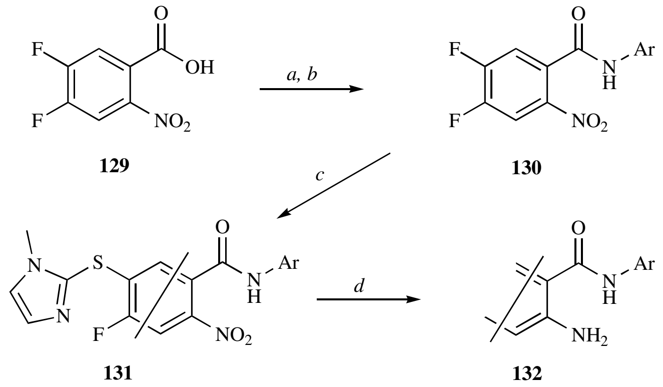

Ar = C_6H_5, 4-Me-C_6H_4, 2- or 3- or 4-MeO-C_6H_4, 2- or 3- or 4-CN-C_6H_4, 2- or 3- or 4-NH_2-C_6H_4, 3-F-C_6H_4, 3-CF_3-C_6H_4, 2,6-di-F-C_6H_3, $C_6H_5CH_2$.

Scheme 15. *a*) $(COCl)_2$ (1.2 eq), DMF (two drops), CH_2Cl_2, r. t., 2 h; *b*) Ar-NH_2 (1 equiv), pyridine (2 eq), CH_2Cl_2, r. t.; *c*) 1-methyl-1H-imidazole-2-thiol (1 eq), Et_3N (3 eq), CH_3CN, refl.; *d*) Fe powder (10 eq), *i*PrOH, satd aq NH_4Cl, refl., 0.5 h.

amides **135** with *N*-aryl-piperazines to give test compounds **136** (Scheme **16**). None of these changes brought about important improvements of the inhibition as shown by Entries 6 and 7 as well as 8 and 9 in Table **28** presenting the most efficient compounds of the respective series.

The authors suggested these compounds to bind at the new allosteric site based on pharmacophore mapping and molecular docking simulations. Co-crystallisation trials of RMGPb with compound in Entry 5 of Table **28** failed[#].

CONCLUSION

Inhibition of glycogen phosphorylase, the rate limiting enzyme of glycogen degradation in the liver, has been the subject of much investigation for lowering blood sugar levels in type 2 diabetes. The catalytic site of the enzyme accommodates analogs of D-glucose. New, efficient inhibitors include β-D-glucopyranosylamines acylated with substituted acetic acids, aliphatic carboxylic acids with bulky appendages, dicarboxylic acids, oxamic acids, and phosphoric acid, *N*-acyl-*N'*-β-D-glucopyranosyl ureas, and *N*- and *C*-β-D-glucopyranosyl heterocycles have also been developed. Most important is the finding that large hydrophobic groups interacting with the side chains of the β-channel next to the catalytic site are essential for tight binding. Attached to a glucopyranosyl urea scaffold such derivatives are nanomolar inhibitors. Binding of DAB to the catalytic site showed this derivative to be an oxocarbenium ion transition-state analog. Other iminosugars were less efficient inhibitors. Indirubin derivatives and analogs of flavopiridol investigated as inhibi-

---

[#] Oikonomakos, N.G. *unpublished observations.*

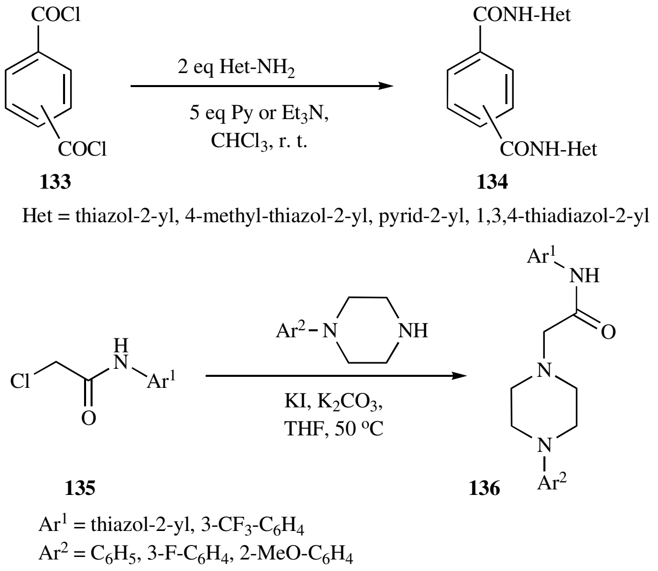
COCl
COCl
2 eq Het-NH2
5 eq Py or Et3N,
CHCl3, r. t.
CONH-Het
CONH-Het
Cl
H
N
Ar1
O
Ar2-N
NH
KI, K2CO3,
THF, 50 °C
Ar1
NH
O
N
N
Ar2

133 **134**

Het = thiazol-2-yl, 4-methyl-thiazol-2-yl, pyrid-2-yl, 1,3,4-thiadiazol-2-yl

135 **136**

Ar^1 = thiazol-2-yl, 3-CF_3-C_6H_4
Ar^2 = C_6H_5, 3-F-C_6H_4, 2-MeO-C_6H_4

Scheme 16.

Table 28. Inhibition of RMGPa by Benzamide and Related Derivatives [162]

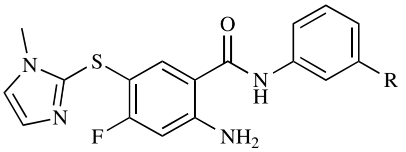
N
S
N
F
O
N
H
NH2
R

Entry	R		IC_{50} [μM]
1.	H		215
2.	CN		9.9
3.	F		31
4.	CF_3		8.9
5.	NH_2		2.7
6.	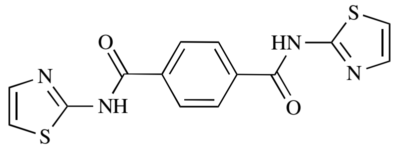		337
7.	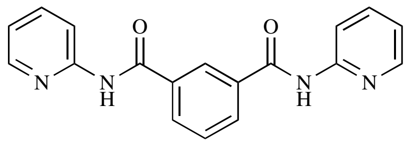		58
	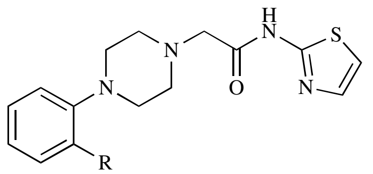		
8.	H		97
9.	F		36

tors of the purine site were not more efficient than earlier compounds. Cyclodextrins bind at the storage site. Inhibitors of the AMP-site include acyl ureas, phthalic acid and dihydropyridine diacid derivatives, pentacyclic triterpenes, and a dicinnamoyl dihydroxy pentanedioic acid. Some phthalic acid derivatives exhibited ~10-fold selectivity towards the liver enzyme. Novel compounds binding to the new allosteric site were found by replacing the 5-chloroindol moiety by chlorinated thienopyrroles, and appending these to quinolone derivatives. 5-Chloroindoloyl glycinamides appeared as simplified structures with affinity to the same site. Several new compound classes emerged as inhibitory structures: anilino-quinoxalines, 3,4-dichloro-cinnamides, bicyclic sugar derivatives, natural flavonoids, 2,3-dihydrobenzo[1,4] dioxin as well as benzamide derivatives which bind with an unknown mechanism. Extensive application of diverse computational methods together with X-ray crystallographic investigation of enzyme-inhibitor complexes is becoming a very useful aid in designing new inhibitory stuctures for GP. Provided sufficient tissue selectivity can be achieved, inhibition of GP can be expected to become a powerful therapy for type 2 diabetes.

NOTE ADDED IN PROOF

Several new structures investigated as inhibitors of GP were published after completion and submission of the manuscript. 2-Naphthyl-substituted glucopyranosylidene-spiro-oxathiazole was reported to be the best known glucose analogue inhibitor of RMGPb (K_i = 160 nM) [163]. A *C*-β-D-glucopyranosyl cyclopropylamide inhibited RMGPb weakly (16 % inhibition at 2.5 mM) [164]. Analogs of DAB such as its enantiomer, C-2 and C-3 epimers, C-1 and *N*-substituted derivatives, and compounds with a sulfur instead of the ring nitrogen displayed significantly weaker or no binding to GPb [165]. Several six-membered iminosugars and analogs proved practically inactive against RMGPb [166]. Further studies and thermodynamic characterization of acylurea type compounds (cf Table **13**) as well as a new inhibitor with a quinolone scaffold (IC_{50} = 44 nM with RMGPb) were reported [167]. A new series of 5-chloro-*N*-aryl- and -heteroaryl-1H-indole-2-carboxamide derivatives proved low micromolar inhibitors of HLGPa, and the best compound (IC_{50} = 0.25 μM) had a 26 % glucose lowering effect in db/db mice [168]. A study on hyphodermins and their synthetic analogs revealed that 2-oxo-hexahydro- and -tetrahydrobenzo[*cd*]indole carboxylic acids (IC_{50} = 0.8-1.2 mM against GPa) can be a potential new class of molecules for inhibitor design [169]. Bis-3-(3,4-dichlorophenyl) acrylamide derivatives showed synergy with glucose in inhibiting HLGPa and the best compound had IC_{50} = 12 nM in the presence of glucose [170]. Amino acid anthranilamide derivatives were identified as glucose sensitive inhibitors of HLGPa with an example showing remarkable in vivo activity [171]. A new study appeared on the inhibition of GPb by flavonoids reporting in some cases contradictory results to those published previously (cf Table **26**) [172]. Several pyrazolo[4,3-b]oleanane derivatives were shown to inhibit RMGPa in the low micromolar range [173]. New pentacyclic triterpenes were isolated from *Gypsophila oldhamiana* and evaluated for their GP inhibitory activity [174]. A survey on GP inhibitor design appeared presenting selected inhibitory structures [175].

ACKNOWLEDGEMENT

Original research work was supported by the Hungarian Scientific Research Fund (OTKA 45927, 46081, 61336, 68578), the Greek-Hungarian Intergovernmental R&D Program (GR 4/03) financed by the Research and Technology Innovation Fund (Hungary) and Greek General Secretariat for Research and Technology (GSRT), GSRT ENTEP04-EP70, EU Marie Curie Early Stage Training (EST) contract No MEST-CT-020575, and a Marie Curie Host Fellowships for the Transfer of Knowledge (ToK) contract No MTKD-CT-2006-042776. We wish to thank our academic colleagues L. N. Johnson, A. Vasella, G. W. J. Fleet, K. E. Tsitsanou, V. Skamnaki, M. N. Kosmopoulou, G. Archontis, V. Nagy, Zs. Hadady, N. Felföldi, J.-P. Praly, T. Docsa, P. Gergely, T. Hadjiloi, T. Gimisis, D. Loganathan, H. Sun, Y. Blériot, colleagues from pharmaceutical industry M. Kristiansen, L. Nørskov-Lauritsen (Novo Nordisk), K. U. Wendt, E. Defossa, D. Schmoll (Sanofi-Aventis), R. Pauptit, A. M. Birch (AstraZeneca), and J. Treadway (Pfizer), and MSc students C. Kyritsi, D. Papageorgiou, D. Sovantzis, K. Telepó, B. Kónya, and Cs. Hüse for their outstanding contributions to the research work on the discovery of glycogen phosphorylase inhibitors.

REFERENCES

[1] Moller, D.E. *Nature,* **2001**, *414*, 821-827.

[2] Zimmet, P.; Alberti, K.G.M.M.; Shaw, J. *Nature,* **2001**, *414*, 782-861.

[3] Green, A.; Hirsch, N.C.; Pramming, S.K. *Diabetes-Metab. Res. Rev.,* **2003**, *19*, 3-7.

[4] Diamond, J. *Nature,* **2003**, *423*, 599-602.

[5] Hengesh, E.J. In *Principles of Medicinal Chemistry*. Foye, W.O.; Lemke, T.L.; Williams, D.A., Eds.; Williams & Wilkins: Baltimore, **1995**, pp 581-600.

[6] Martin, J.L.; Veluraja, K.; Ross, K.; Johnson, L.N.; Fleet, G.W.J.; Ramsden, N.G.; Bruce, I.; Orchard, M.G.; Oikonomakos, N.G.; Papageorgiou, A.C.; Leonidas, D.D.; Tsitoura, H.S. *Biochemistry,* **1991**, *30*, 10101-10116.

[7] Toye, A.; Gauguier, D. *Genome Biol.,* **2003**, *4*, 241.

[8] Barroso, I. *Diabetic Med.,* **2005**, *22*, 517-535.

[9] Ehtisham, S.; Barrett, T.G. *Ann. Clin. Biochem.,* **2004**, *41*, 10-16.

[10] Bloomgarden, Z.T. *Diabetes Care,* **2004**, *27*, 998-1010.

[11] Alberti, G.; Zimmet, P.; Shaw, J.; Bloomgarden, Z.; Kaufman, F.; Silink, M. *Diabetes Care,* **2004**, *27*, 1798-1811.

[12] Panunti, B.; Jawa, A.A.; Fonseca, V.A. *Drug Discov. Today: Disease Mech.,* **2004**, *1*, 151-157.

[13] Stumvoll, M.; Goldstein, B.J.; van Haeften, T.W. *Lancet,* **2005**, *365*, 1333-1346.

[14] Lowell, B.B.; Shulman, G.I. *Science,* **2005**, *307*, 384-387.

[15] Cobb, J.; Dukes, I. In *Annual Reports in Medicinal Chemistry*. Bristol, J.A., Ed.; Academic Press: San Diego, **1998**; Vol. *33*, pp 213-222.

[16] Perfetti, R.; Barnett, P.S.; Mathur, R.; Egan, J.M. *Diabetes Metab. Rev.,* **1998**, *14*, 207-225.

[17] Rose, M.L.; Paulik, M.A.; Lenhard, J.M. *Expert Opin. Ther. Patents,* **1999**, *9*, 1-14.

[18] Zhang, B.B.; Moller, D.E. *Curr. Opin. Chem. Biol.,* **2000**, *4*, 461-467.

[19] Rendell, M. *Drugs,* **2004**, *64*, 1339-1358.

[20] Cheng, A.Y.Y.; Fantus, I.G. *Can. Med. Assoc. J.,* **2005**, *172*, 213-226.

[21] Padwal, R.; Majumdar, S.R.; Johnson, J.A.; Varney, J.; McAlister, F.A. *Diabetes Care,* **2005**, *28*, 736-744.

[22] Krentz, A.J.; Bailey, C.J. *Drugs,* **2005**, *65*, 385-411.

[23] van de Laar, F.A.; Lucassen, P.L.; Akkermans, R.P.; van de Lisdonk, F.H.; Rutten, G.E.; van Weel, C. *Diabetes Care,* **2005**, *28*, 154-163.

[24] Murata, G.H.; Duckworth, W.C.; Hoffman, R.M.; Wendel, C.S.; Mohler, M.J.; Shah, J.H. *Biomed. Pharmacother.,* **2004**, *58*, 551-559.

[25] Wagman, A.S.; Nuss, J.M. *Curr. Pharm. Design,* **2001**, *7*, 417-450.

[26] Cohen, P. *Phil. Trans. R. Soc. Lond. B,* **1999**, *354*, 485-495.

[27] Treadway, J.L.; Mendys, P.; Hoover, D.J. *Expert Opin. Invest. Drugs,* **2001**, *10*, 439-454.

[28] Saltiel, A.R.; Kahn, C.R. *Nature,* **2001**, *414*, 799-806.

[29] Staehr, P.; Hother-Nielsen, O.; Beck-Nielsen, H. *Diabetes Obes. Metab.,* **2002**, *4*, 215-223.

[30] Morral, N. *Trends Endocrin. Metab.,* **2003**, *14*, 169-175.

[31] Nourparvar, A.; Bulotta, A.; Di Mario, U.; Perfetti, R. *Trends Pharmacol. Sci.,* **2004**, *25*, 86-91.

[32] Agius, L. *Best Pract. Res. Clin. Endocrin. Metab.,* **2007**, *21*, 587-605.

[33] McCarty, M.F. *Med. Hypoth.,* **2000**, *54*, 483-487.

[34] Bollen, M.; Keppens, S.; Stalmans, W. *Biochem. J.,* **1998**, *336*, 19-31.

[35] Radziuk, J.; Pye, S. *Diabetes Metab. Res. Rev.,* **2001**, *17*, 250-272.

[36] Roden, M.; Bernroider, E. *Best Pract. Res. Clin. Endocrin. Metab.,* **2003**, *17*, 365-383.

[37] Andersen, B.; Rassov, A.; Westergaard, N.; Lundgren, K. *Biochem. J.,* **1999**, *342*, 545-550.

[38] Oikonomakos, N.G. *Curr. Protein Pept. Sci.,* **2002**, *3*, 561-586.

[39] McCormack, J.G.; Westergaard, N.; Kristiansen, M.; Brand, C.L.; Lau, J. *Curr. Pharm. Design,* **2001**, *7*, 1451-1474.

[40] Lerin, C.; Montell, E.; Nolasco, T.; Garcia-Rocha, M.; Guinovart, J.J.; Gomez-Foix, A.M. *Biochem. J.,* **2004**, *378*, 1073-1077.

[41] Baker, D.J.; Timmons, J.A.; Greenhaff, P.L. *Diabetes,* **2005**, *54*, 2453-2459.

[42] Baker, D.J.; Greenhaff, P.L.; MacInnes, A.; Timmons, J.A. *Diabetes,* **2006**, *55*, 1855-1861.

[43] Freeman, S.; Bartlett, J.B.; Convey, G.; Hardern, I.; Teague, J.L.; Loxham, S.J.G.; Allen, J.M.; Poucher, S.M.; Charles, A.D. *Br. J. Pharmacol.,* **2006**, *149*, 775-785.

[44] Baker, D.J.; Greenhaff, P.L.; Timmons, J.A. *Expert Opin. Ther. Patents,* **2006**, *16*, 459-466.

[45] Somsák, L.; Nagy, V.; Hadady, Z.; Docsa, T.; Gergely, P. *Curr. Pharm. Design,* **2003**, *9*, 1177-1189.

[46] Barf, T. *Mini-Rev. Med. Chem.,* **2004**, *4*, 897-908.

[47] Henke, B.R.; Sparks, S.M. *Mini-Rev. Med. Chem.,* **2006**, *6*, 845-857.

[48] Acharya, K.R.; Stuart, D.I.; Varvill, K.M.; Johnson, L.N. *Glycogen phosphorylase b. Description of the protein structure*. World Scientific: Singapore **1991**.

[49] Johnson, L.N. *FASEB J.,* **1992**, *6*, 2274-2282.

[50] Oikonomakos, N.G.; Acharya, K.R.; Johnson, L.N. In *Post-Translational Modification of Proteins*. Harding, J.J.; Crabbe, M.J.C., Eds.; CRC Press: Boca Raton, **1992**, pp 81-151.

[51] Barford, D.; Johnson, L.N. *Nature,* **1989**, *340*, 609-616.

[52] Johnson, L.N.; Acharya, K.R.; Jordan, M.D.; McLaughlin, P.J. *J. Mol. Biol.,* **1990**, *211*, 645-661.

[53] Barford, D.; Hu, S.H.; Johnson, L.N. *J. Mol. Biol.,* **1991**, *218*, 233-260.

[54] Oikonomakos, N.G.; Tiraidis, C.; Leonidas, D.D.; Zographos, S.E.; Kristiansen, M.; Jessen, C.U.; Norskov-Lauritsen, L.; Agius, L. *J. Med. Chem.,* **2006**, *49*, 5687-5701.

[55] Watson, K.A.; McCleverty, C.; Geremia, S.; Cottaz, S.; Driguez, H.; Johnson, L.N. *EMBO J,* **1999**, *18*, 4619-4632.

[56] Watson, K.A.; Mitchell, E.P.; Johnson, L.N.; Cruciani, G.; Son, J.C.; Bichard, C.J.F.; Fleet, G.W.J.; Oikonomakos, N.G.; Kontou, M.; Zographos, S.E. *Acta Cryst.,* **1995**, *D51*, 458-472.

[57] Györgydeák, Z.; Thiem, J. *Adv. Carbohydr. Chem. Biochem.,* **2006**, *60*, 103-182.

[58] Kovács, L.; Ősz, E.; Domokos, V.; Holzer, W.; Györgydeák, Z. *Tetrahedron,* **2001**, *57*, 4609-4621.

[59] Anagnostou, E.; Kosmopoulou, M.N.; Chrysina, E.D.; Leonidas, D.D.; Hadjiloi, T.; Tiraidis, C.; Zographos, S.E.; Györgydeák, Z.; Somsák, L.; Docsa, T.; Gergely, P.; Kolisis, F.N.; Oikonomakos, N.G. *Bioorg. Med. Chem.,* **2006**, *14*, 181-189.

[60] Kannan, T.; Vinodhkumar, S.; Varghese, B.; Loganathan, D. *Bioorg. Med. Chem. Lett.,* **2001**, *11*, 2433-2435.

[61] Chrysina, E.D.; Kosmopoulou, M.N.; Kardakaris, R.; Bischler, N.; Leonidas, D.D.; Kannan, T.; Loganathan, D.; Oikonomakos, N.G. *Bioorg. Med. Chem.,* **2005**, *13*, 765-772.

[62] Alexacou, K.M.; Hayes, J.M.; Tiraidis, C.; Zographos, S.E.; Leonidas, D.D.; Chrysina, E.D.; Archontis, G.; Oikonomakos, N.G.; Paul, J.V.; Varghese, B.; Loganathan, D. *Proteins: Struct. Funct. Bioinf.,* **2008**, *71*, 1307-1323.

[63] Györgydeák, Z.; Hadady, Z.; Felföldi, N.; Krakomperger, A.; Nagy, V.; Tóth, M.; Brunyánszky, A.; Docsa, T.; Gergely, P.; Somsák, L. *Bioorg. Med. Chem.,* **2004**, *12*, 4861-4870.

[64] Somsák, L.; Kovács, L.; Tóth, M.; Ősz, E.; Szilágyi, L.; Györgydeák, Z.; Dinya, Z.; Docsa, T.; Tóth, B.; Gergely, P. *J. Med. Chem.,* **2001**, *44*, 2843-2848.

[65] Petsalakis, E.I.; Chrysina, E.D.; Tiraidis, C.; Hadjiloi, T.; Leonidas, D.D.; Oikonomakos, N.G.; Aich, U.; Varghese, B.; Loganathan, D. *Bioorg. Med. Chem.,* **2006**, *14*, 5316-5324.

[66] Czifrák, K.; Hadady, Z.; Docsa, T.; Gergely, P.; Schmidt, J.; Wessjohann, L.A.; Somsák, L. *Carbohydr. Res.,* **2006**, *341*, 947-956.

[67] Hadjiloi, T.; Tiraidis, C.; Chrysina, E.D.; Leonidas, D.D.; Oikonomakos, N.G.; Tsipos, P.; Gimisis, T. *Bioorg. Med. Chem.,* **2006**, *14*, 3872-3882.

[68] Oikonomakos, N.G.; Kosmopolou, M.; Zographos, S.E.; Leonidas, D.D.; Somsák, L.; Nagy, V.; Praly, J.-P.; Docsa, T.; Tóth, B.; Gergely, P. *Eur. J. Biochem.,* **2002**, *269*, 1684-1696.

[69] Pintér, I.; Kovács, J.; Tóth, G. *Carbohydr. Res.,* **1995**, *273*, 99-108.

[70] Somsák, L.; Felföldi, N.; Kónya, B.; Hüse, C.; Telepó, K.; Bokor, É.; Czifrák, K. *Carbohydr. Res.,* **2008**, *343*, 2083-2093.

[71] Krülle, T.M.; Fuente, C.; Watson, K.A.; Gregoriou, M.; Johnson, L.N.; Tsitsanou, K.E.; Zographos, S.E.; Oikonomakos, N.G.; Fleet, G.W.J. *Synletter,* **1997**, 211-213.

[72] Watson, K.A.; Chrysina, E.D.; Tsitsanou, K.E.; Zographos, S.E.; Archontis, G.; Fleet, G.W.J.; Oikonomakos, N.G. *Proteins: Struct. Funct. Bioinf.,* **2005**, *61*, 966-983.

[73] Czifrák, K.; Kovács, L.; Kövér, K.E.; Somsák, L. *Carbohydr. Res.,* **2005**, *340*, 2328-2334.

[74] Hopfinger, A.J.; Reaka, A.; Venkatarangan, P.; Duca, J.S.; Wang, S. *J. Chem. Inf. Comp. Sci.,* **1999**, *39*, 1151-1160.

[75] So, S.-S.; Karplus, M. *J. Comp.-Aid. Mol. Design,* **2001**, *15*, 613-647.

[76] Watson, K.A.; Mitchell, E.P.; Johnson, L.N.; Son, J.C.; Bichard, C.J.F.; Orchard, M.G.; Fleet, G.W.J.; Oikonomakos, N.G.; Leonidas, D.D.; Kontou, M.; Papageorgiou, A. *Biochemistry,* **1994**, *33*, 5745-5758.

[77] Chrysina, E.D.; Oikonomakos, N.G.; Zographos, S.E.; Kosmopoulou, M.N.; Bischler, N.; Leonidas, D.D.; Kovács, L.; Docsa, T.; Gergely, P.; Somsák, L. *Biocatal. Biotransform.,* **2003**, *21*, 233-242.

[78] Cismaş, C.; Sovantzis, D.; Hadjiloi, T.; Stathis, D.; Gimisis, T.; Hayes, J.M.; Zographos, S.E.; Leonidas, D.D.; Chrysina, E.D.; Oikonomakos, N.G. *submitted.*

[79] Somsák, L.; Nagy, V.; Hadady, Z.; Felföldi, N.; Docsa, T.; Gergely, P. In *Frontiers in Medicinal Chemistry*. Reitz, A.B.; Kordik, C.P.; Choudhary, M.I.; Rahman, A.u., Eds.; Bentham, **2005**; Vol. *2*, pp 253-272.

[80] Archontis, G.; Watson, K.A.; Xie, Q.; Andreou, G.; Chrysina, E.D.; Zographos, S.E.; Oikonomakos, N.G.; Karplus, M. *Proteins: Struct. Funct. Bioinf.,* **2005**, *61*, 984-998.

[81] Gregoriou, M.; Noble, M.E.M.; Watson, K.A.; Garman, E.F.; Krülle, T.M.; Fuente, C.; Fleet, G.W.J.; Oikonomakos, N.G.; Johnson, L.N. *Protein Sci.,* **1998**, *7*, 915-927.

[82] Pan, D.H.; Liu, J.Z.; Senese, C.; Hopfinger, A.J.; Tseng, Y. *J. Med. Chem.,* **2004**, *47*, 3075-3088.

[83] Oikonomakos, N.G.; Skamnaki, V.T.; Ősz, E.; Szilágyi, L.; Somsák, L.; Docsa, T.; Tóth, B.; Gergely, P. *Bioorg. Med. Chem.,* **2002**, *10*, 261-268.

[84] Cruciani, C.; Crivori, P.; Carrupt, P.A.; Testa, B. *J. Mol. Struct. (THEOCHEM),* **2000**, *503*, 17-30.

[85] *VolSurf* 2.0; Molecular Discovery Ltd.: Oxford, UK.

[86] Goodford, P.J. *J. Med. Chem.,* **1985**, *28*, 849-857.

[87] *GRID*, Molecular Discovery Ltd.: Oxford, UK.

[88] Zamora, I.; Oprea, T.; Cruciani, G.; Pastor, M.; Ungell, A.L. *J. Med. Chem.,* **2003**, *46*, 25-33.

[89] Zhou, P.; Li, Z.L. *Sci. China Ser. B-Chem.,* **2007**, *50*, 568-573.

[90] Pan, D.H.; Tseng, Y.F.; Hopfinger, A.J. *J. Chem. Inf. Comp. Sci.,* **2003**, *43*, 1591-1607.

[91] Venkatarangan, P.; Hopfinger, A.J. *J. Chem. Inf. Comp. Sci.,* **1999**, *39*, 1141-1150.

[92] Venkatarangan, P.; Hopfinger, A.J. *J. Med. Chem.,* **1999**, *42*, 2169-2179.

[93] *GOLD*, Cambridge Crystallographic Data Centre: Cambridge, UK.

[94] *GLIDE*, Schrodinger, LLC: New York, NY, 2008.

[95] Hadady, Z.; Tóth, M.; Somsák, L. *Arkivoc,* **2004**, *(vii)*, 140-149.

[96] Chrysina, E.D.; Kosmopolou, M.N.; Tiraidis, C.; Kardarakis, R.; Bischler, N.; Leonidas, D.D.; Hadady, Z.; Somsák, L.; Docsa, T.; Gergely, P.; Oikonomakos, N.G. *Protein Sci.,* **2005**, *14*, 873-888.

[97] Benltifa, M.; Vidal, S.; Gueyrard, D.; Goekjian, P.G.; Msaddek, M.; Praly, J.-P. *Tetrahedron Lett.,* **2006**, *47*, 6143-6147.

[98] Benltifa, M.; Vidal, S.; Fenet, B.; Msaddek, M.; Goekjian, P.G.; Praly, J.-P.; Brunyánszki, A.; Docsa, T.; Gergely, P. *Eur. J. Org. Chem.,* **2006**, 4242-4256.

[99] He, L.; Zhang, Y.Z.; Tanoh, M.; Chen, G.R.; Praly, J.P.; Chrysina, E.D.; Tiraidis, C.; Kosmopoulou, M.; Leonidas, D.D.; Oikonomakos, N.G. *Eur. J. Org. Chem.,* **2007**, 596-606.

[100] Ayad, T.; Genisson, Y.; Broussy, S.; Baltas, M.; Gorrichon, L. *Eur. J. Org. Chem.,* **2003**, 2903-2910.

[101] Lauritsen, A.; Madsen, R. *Org. Biomol. Chem.,* **2006**, *4*, 2898-2905.

[102] Hulme, A.N.; Montgomery, C.H.; Henderson, D.K. *J. Chem. Soc.-Perkin Trans. 1,* **2000**, 1837-1841.

[103] Kim, I.S.; Zee, O.P.; Jung, Y.H. *Org. Lett.,* **2006**, *8*, 4101-4104.

[104] Espelt, L.; Parella, T.; Bujons, J.; Solans, C.; Joglar, J.; Delgado, A.; Clapes, P. *Chem.-Eur. J.,* **2003**, *9*, 4887-4899.

[105] Lombardo, M.; Fabbroni, S.; Trombini, C. *J. Org. Chem.,* **2001**, *66*, 1264-1268.

[106] Huang, Y.F.; Dalton, D.R.; Carroll, P.J. *J. Org. Chem.,* **1997**, *62*, 372-376.

[107] Goujon, J.-Y.; Gueyrard, D.; Compain, P.; Martin, O.R.; Ikeda, K.; Kato, A.; Asano, N. *Bioorg. Med. Chem.,* **2005**, *13*, 2313-2324.

[108] Li, H.Q.; Liu, T.; Zhang, Y.M.; Favre, S.; Bello, C.; Vogel, P.; Butters, T.D.; Oikonomakos, N.G.; Marrot, J.; Bleriot, Y. *Chembiochem,* **2008**, *9*, 253-260.

[109] Johnson, L.N.; Cheetham, J.; McLaughlin, P.J.; Acharya, K.R.; Barford, D.; Phillips, D.C. *Curr. Top Microbiol. Immunol.,* **1988**, *139*, 81-134.

[110] Pinotsis, N.; Leonidas, D.D.; Chrysina, E.D.; Oikonomakos, N.G.; Mavridis, I.M. *Protein Sci.,* **2003**, *12*, 1914-1924.

[111] Oikonomakos, N.G.; Schnier, J.B.; Zographos, S.E.; Skamnaki, V.T.; Tsitsanou, K.E.; Johnson, L.N. *J. Biol. Chem.,* **2000**, *275*, 34566-34573.

[112] Kosmopoulou, M.N.; Leonidas, D.D.; Chrysina, E.D.; Bischler, N.; Eisenbrand, G.; Sakarellos, C.E.; Pauptit, R.; Oikonomakos, N.G. *Eur. J. Biochem.,* **2004**, *271*, 2280-2290.

[113] Kosmopoulou, M.N.; Leonidas, D.D.; Chrysina, E.D.; Oikonomakos, N.G.; Eisenbrand, G. *Lett. Drug Design Discov.,* **2005**, *2*, 377-390.

[114] Kaiser, A.; Nishi, K.; Gorin, F.A.; Walsh, D.A.; Bradbury, E.M.; Schnier, J.B. *Arch. Biochem. Biophys.,* **2001**, *386*, 179-187.

[115] Hampson, L.J.; Arden, C.; Agius, L.; Ganotidis, M.; Kosmopoulou, M.N.; Tiraidis, C.; Elemes, Y.; Sakarellos, C.; Leonidas, D.D.; Oikonomakos, N.G. *Bioorg. Med. Chem.,* **2006**, *14*, 7835-7845.

[116] Ekstrom, J.L.; Pauly, T.A.; Carty, M.D.; Soeller, W.C.; Culp, J.; Danley, D.E.; Hoover, D.J.; Treadway, J.L.; Gibbs, E.M.; Fletterick, R.J.; Day, Y.S.N.; Myszka, D.G.; Rath, V.L. *Chem. Biol.,* **2002**, *9*, 915-924.

[117] Zographos, S.E.; Oikonomakos, N.G.; Tsitsanou, K.E.; Leonidas, D.D.; Chrysina, E.D.; Skamnaki, V.T.; Bischoff, H.; Goldmann, S.; Watson, K.A.; Johnson, L.N. *Structure,* **1997**, *5*, 1413-1425.

[118] Oikonomakos, N.G.; Tsitsanou, K.E.; Zographos, S.E.; Skamnaki, V.T.; Goldmann, S.; Bischoff, H. *Protein Sci.,* **1999**, *8*, 1930-1945.

[119] Tsitsanou, K.E.; Skamnaki, V.T.; Oikonomakos, N.G. *Arch. Biochem. Biophys.,* **2000**, *384*, 245-254.

[120] Klabunde, T.; Wendt, K.U.; Kadereit, D.; Brachvogel, V.; Burger, H.J.; Herling, A.W.; Oikonomakos, N.G.; Kosmopoulou, M.N.; Schmoll, D.; Sarubbi, E.; von Roedern, E.; Schonafinger, K.; Defossa, E. *J. Med. Chem.,* **2005**, *48*, 6178-6193.

[121] Oikonomakos, N.G.; Kosmopoulou, M.N.; Chrysina, E.D.; Leonidas, D.D.; Kostas, I.D.; Wendt, K.U.; Klabunde, T.; Defossa, E. *Protein Sci.,* **2005**, *14*, 1760-1771.

[122] Li, J.; Liu, H.; Yao, X.; Liu, M.; Hu, Z.; Fan, B. *Chemometr. Intell. Lab. Syst.,* **2007**, *87*, 139-146.

[123] Kristiansen, M.; Andersen, B.; Iversen, L.F.; Westergaard, N. *J. Med. Chem.,* **2004**, *47*, 3537-3545.

[124] Deng, Q.; Lu, Z.; Bohn, J.; Ellsworth, K.P.; Myers, R.W.; Geissler, W.M.; Harris, G.; Willoughby, C.A.; Chapman, K.; McKeever, B.; Mosley, R. *J. Mol. Graph. Model.,* **2005**, *23*, 457-464.

[125] Miller, M.D.; Sheridan, R.P.; Kearsley, S.K. *J. Med. Chem.,* **1999**, *42*, 1505-1514.

[126] Oikonomakos, N.G.; Skamnaki, V.T.; Tsitsanou, K.E.; Gavalas, N.G.; Johnson, L.N. *Structure,* **2000**, *8*, 575-584.

[127] Lu, Z.; Bohn, J.; Bergeron, R.; Deng, Q.; Ellsworth, K.P.; Geissler, W.M.; Harris, G.; McCann, P.E.; McKeever, B.; Myers, R.W. *Bioorg. Med. Chem. Lett.,* **2003**, *13*, 4125-4128.

[128] *ICM-pro*, 2.8; Molsoft LLC: San Diego, 2001.

[129] Ogawa, A.K.; Willoughby, C.A.; Bergeron, R.; Ellsworth, K.P.; Geissler, W.M.; Myers, R.W.; Yao, J.; Harris, G.; Chapman, K.T. *Bioorg. Med. Chem. Lett.,* **2003**, *13*, 3405-3408.

[130] Wen, X.; Sun, H.; Liu, J.; Wu, G.; Zhang, L.; Wu, X.; Ni, P. *Bioorg. Med. Chem. Lett.,* **2005**, *15*, 4944-4948.

[131] Wen, X.; Xia, J.; Cheng, K.; Zhang, L.; Zhang, P.; Liu, J.; Zhang, L.; Ni, P.; Sun, H. *Bioorg. Med. Chem. Lett.,* **2007**, *17*, 5777-5782.

[132] Wen, X.; Zhang, P.; Liu, J.; Zhang, L.; Wu, X.; Ni, P.; Sun, H. *Bioorg. Med. Chem. Lett.,* **2006**, *16*, 722-726.

[133] Chen, J.; Liu, J.; Zhang, L.Y.; Wu, G.Z.; Hua, W.Y.; Wu, X.M.; Sun, H.B. *Bioorg. Med. Chem. Lett.,* **2006**, *16*, 2915-2919.

[134] Chen, J.; Liu, J.; Gong, Y.C.; Zhang, L.Y.; Hua, W.Y.; Sun, H.B. *J. China Pharm. Univ.,* **2006**, *37*, 397-402.

[135] Wen, X.; Sun, H.; Liu, J.; Cheng, K.; Zhang, P.; Zhang, L.; Hao, J.; Zhang, L.; Ni, P.; Zographos, S.E.; Leonidas, D.D.; Alexacou, K.M.; Gimisis, T.; Hayes, J.M.; Oikonomakos, N.G. *J. Med. Chem.,* **2008**, *51*, 3540-3550.

[136] Furukawa, S.; Tsurumi, Y.; Murakami, K.; Nakanishi, T.; Ohsumi, K.; Hashimoto, M.; Nishikawa, M.; Takase, S.; Nakayama, O.; Hino, M. *J. Antibiot.,* **2005**, *58*, 497-502.

[137] Furukawa, S.; Murakami, K.; Nishikawa, M.; Nakayama, O.; Hino, M. *J. Antibiot.,* **2005**, *58*, 503-506.

[138] Tiraidis, C.; Alexacou, K.M.; Zographos, S.E.; Leonidas, D.D.; Gimisis, T.; Oikonomakos, N.G. *Protein Sci.,* **2007**, *16*, 1773-1782.

[139] Rath, V.L.; Ammirati, M.; Danley, D.E.; Ekstrom, J.L.; Gibbs, E.M.; Hynes, T.R.; Mathiowetz, A.M.; McPherson, R.K.; Olson, T.V.; Treadway, J.L.; Hoover, D.J. *Chem. Biol.,* **2000**, *7*, 677-682.

[140] Hudson, J.W.; Golding, G.B.; Crerar, M.M. *J. Mol. Biol.,* **1993**, *234*, 700-721.

[141] Martin, W.H.; Hoover, D.J.; Armento, S.J.; Stock, I.A.; McPherson, R.K.; Danley, D.E.; Stevenson, R.W.; Barrett, E.J.; Treadway, J.L. *Proc. Natl. Acad. Sci. USA,* **1998**, *95*, 1776-1781.

[142] Hoover, D.J.; Lefkowitz-Snow, S.; Burgess-Henry, J.L.; Martin, W.H.; Armento, S.J.; Stock, I.A.; McPherson, R.K.; Genereux, P.E.; Gibbs, E.M.; Treadway, J.L. *J. Med. Chem.,* **1998**, *41*, 2934-2938.

[143] Rosauer, K.G.; Ogawa, A.K.; Willoughby, C.A.; Ellsworth, K.P.; Geissler, W.M.; Myers, R.W.; Deng, Q.L.; Chapman, K.T.; Harris, G.; Moller, D.E. *Bioorg. Med. Chem. Lett.,* **2003**, *13*, 4385-4388.

[144] Oikonomakos, N.G.; Zographos, S.E.; Skamnaki, V.T.; Archontis, G. *Bioorg. Med. Chem.,* **2002**, *10*, 1313-1319.

[145] Birch, A.M.; Kenny, P.W.; Oikonomakos, N.G.; Otterbein, L.; Schofield, P.; Whittamore, P.R.O.; Whalley, D.P. *Bioorg. Med. Chem. Lett.,* **2007**, *17*, 394-399.

[146] Whittamore, P.R.O.; Addie, M.S.; Bennett, S.N.L.; Birch, A.M.; Butters, M.; Godfrey, L.; Kenny, P.W.; Morley, A.D.; Murray, P.M.; Oikonomakos, N.G.; Otterbein, L.R.; Pannifer, A.D.; Parker, J.S.; Readman, K.; Siedlecki, P.S.; Schofield, P.; Stocker, A.; Taylor, M.J.; Townsend, L.A.; Whalley, D.P.; Whitehouse, J. *Bioorg. Med. Chem. Lett.,* **2006**, *16*, 5567-5571.

[147] Wright, S.W.; Rath, V.L.; Genereux, P.E.; Hageman, D.L.; Levy, C.B.; McClure, L.D.; McCoid, S.C.; McPherson, R.K.; Schelhorn, T.M.; Wilder, D.E. *Bioorg. Med. Chem. Lett.,* **2005**, *15*, 459-465.

[148] Liu, G.X.; Zhang, Z.S.; Luo, X.M.; Shen, J.H.; Liu, H.; Shen, X.; Chen, K.X.; Jiang, H.L. *Bioorg. Med. Chem.,* **2004**, *12*, 4147-4157.

[149] Morris, G.M.; Goodsell, D.S.; Halliday, R.S.; Huey, R.; Hart, W.E.; Belew, R.K.; Olson, A.J. *J. Comput. Chem.,* **1998**, *19*, 1639-1662.

[150] Morris, G.M.; Goodsell, D.S.; Huey, R.; Hart, W.E.; Halliday, S.; Belew, R.; Olson, A.J. *Autodock* 3.0.3; The Scripps Research Institute, Molecular Graphics Laboratory, Department of Molecular Biology: La Jolla CA, 1999.

[151] Prathipati, P.; Pandey, G.; Saxena, A.K. *J. Chem. Inf. Model.,* **2005**, *45*, 136-145.

[152] *Catalyst*, 4.5; Accelrys Inc.: San Diego, 2008.

[153] Oikonomakos, N.G.; Chrysina, E.D.; Kosmopoulou, M.N.; Leonidas, D.D. *Biochim. Biophys. Acta-Proteins and Proteomics,* **2003**, *1647*, 325-332.

[154] *InsightII*, Accelrys Inc.: San Diego, 2008.

[155] Bohm, H.J. *J. Comp.-Aid. Mol. Design,* **1992**, *6*, 61-78.

[156] Bohm, H.J. *J. Comp.-Aid. Mol. Design,* **1992**, *6*, 593-606.

[157] Dudash, J., Joseph; Zhang, Y.; Moore, J.B.; Look, R.; Liang, Y.; Beavers, M.P.; Conway, B.R.; Rybczynski, P.J.; Demarest, K.T. *Bioorg. Med. Chem. Lett.,* **2005**, *15*, 4790-4793.

[158] Li, Y.H.; Coppo, F.T.; Evans, K.A.; Graybill, T.L.; Patel, M.; Gale, J.; Li, H.; Tavares, F.; Thomson, S.A. *Bioorg. Med. Chem. Lett.,* **2006**, *16*, 5892-5896.

[159] Verma, S.S.; Mishra, R.C.; Tamarakar, A.K.; Tripathi, B.K.; Srivastava, A.K.; Tripathi, R.P. *J. Carbohydr. Chem.,* **2004**, *23*, 493-511.

[160] Jakobs, S.; Fridrich, D.; Hofem, S.; Pahlke, G.; Eisenbrand, G. *Mol. Nutr. Food Res.,* **2006**, *50*, 52-57.

[161] Juhász, L.; Docsa, T.; Brunyánszki, A.; Gergely, P.; Antus, S. *Bioorg. Med. Chem.,* **2007**, *15*, 4048-4056.

[162] Chen, L.; Li, H.L.; Liu, J.; Zhang, L.Y.; Liu, H.; Jiang, H.L. *Bioorg. Med. Chem.,* **2007**, *15*, 6763-6774.

[163] Somsák, L.; Nagy, V.; Vidal, S.; Czifrák, K.; Berzsényi, E.; Praly, J.-P., *Bioorg. Med. Chem. Lett.,* **2008**, *18*, 5680-5683.

[164] Bertus, P.; Szymoniak, J.; Jeanneau, E.; Docsa, T.; Gergely, P.; Praly, J.-P.; Vidal, S. *Bioorg. Med. Chem. Lett.,* **2008**, *18*, 4774-4778.

[165] Minami, Y.; Kurlyarna, C.; Ikeda, K.; Kato, A.; Takebayashi, K.; Adachi, I.; Fleet, G.W.J.; Kettawan, A.; Karnoto, T.; Asano, N., *Bioorg. Med. Chem.,* **2008**, *16*, 2734-2740.

[166] Kuriyama, C.; Kamiyama, O.; Ikeda, K.; Sanae, F.; Kato, A.; Adachi, I.; Imahori, T.; Takahata, H.; Okamoto, T.; Asano, N. *Bioorg. Med. Chem.,* **2008**, *16*, 7330-7336.

[167] Anderka, O.; Loenze, P.; Klabunde, T.; Dreyer, M.K.; Defossa, E.; Wendt, K.U.; Schmoll, D. *Biochemistry,* **2008**, *47*, 4683-4691.

[168] Onda, K.; Suzuki, T.; Shiraki, R.; Yonetoku, Y.; Negoro, K.; Momose, K.; Katayama, N.; Orita, M.; Yamaguchi, T.; Ohta, M.; Tsukamoto, S. *Bioorg. Med. Chem.,* **2008**, *16*, 5452-5464.

[169] Loughlin, W.A.; Pierens, G.K.; Petersson, M.J.; Henderson, L.C.; Healy, P.C. *Bioorg. Med. Chem.,* **2008**, *16*, 6172-6178.

[170] Onda, K.; Shiraki, R.; Yonetoku, Y.; Momose, K.; Katayama, N.; Orita, M.; Yamaguchi, T.; Ohta, M.; Tsukamoto, S.-I. *Bioorg. Med. Chem.,* **2008**, *16*, 8627-8634.

[171] Evans, K.A.; Li, Y.H.; Coppo, F.T.; Graybill, T.L.; Cichy-Knight, M.; Patel, M.; Gale, J.; Li, H.; Thrall, S.H.; Tew, D.; Tavares, F.; Thomson, S.A.; Weiel, J.E.; Boucheron, J.A.; Clancy, D.C.; Epperly, A.H.; Golden, P.L. *Bioorg. Med. Chem. Lett.,* **2008**, *18*, 4068-4071.

[172] Kato, A.; Nasu, N.; Takebayashi, K.; Adachi, I.; Minami, Y.; Sanae, F.; Asano, N.; Watson, A.A.; Nash, R.J. *J. Agric. Food Chem.,* **2008**, *56*, 4469-4473.

[173] Chen, J.; Gong, Y.C.; Liu, J.; Hua, W.Y.; Zhang, L.Y.; Sun, H.B. *Chem. Biodivers.,* **2008**, *5*, 1304-1312.

[174] Luo, J.G.; Liu, J.; Kong, L.Y. *Chem. Biodivers.,* **2008**, *5*, 751-757.

[175] Oikonomakos, N.G.; Somsák, L. *Curr. Opin. Invest. Drugs,* **2008**, *9*, 379-395.

Received: August 01, 2008 Revised: September 30, 2008 Accepted: October 05, 2008